

**INVESTIGATION OF SEISMIC ISOLATION EFFICIENCY FOR
BUILDING STRUCTURES**

A THESIS SUBMITTED TO
THE GRADUATE SCHOOL OF NATURAL AND APPLIED SCIENCES
OF
MIDDLE EAST TECHNICAL UNIVERSITY

SEDA ÖZDEMİR

IN PARTIAL FULFILLMENT OF THE REQUIREMENTS
FOR
THE DEGREE OF MASTER OF SCIENCE
IN
EARTHQUAKE STUDIES

DECEMBER 2016

Approval of the thesis:

**INVESTIGATION OF SEISMIC ISOLATION EFFICIENCY FOR BUILDING
STRUCTURES**

submitted by **SEDA ÖZDEMİR** in partial fulfillment of the requirements for the degree of **Master of Science in Earthquake Studies Department, Middle East Technical University** by,

Prof. Dr. Gülbin Dural Ünver
Dean, Graduate School of **Natural and Applied Sciences**

Assoc. Prof. Dr. Ayşegül Askan Gündoğan
Head of Department, **Earthquake Studies**

Prof. Dr. Ahmet Yakut
Supervisor, **Civil Engineering Department, METU**

Assist. Prof. Dr. Bekir Özer Ay
Co-supervisor, **Department of Architecture, METU**

Examining Committee Members:

Prof. Dr. Uğurhan Akyüz, Head of the Examining Committee,
Civil Engineering Department, METU

Prof. Dr. Ahmet Yakut
Civil Engineering Department, METU

Assist. Prof. Dr. Bekir Özer Ay
Department of Architecture, METU

Assoc. Prof. Dr. Ayşegül Askan Gündoğan
Civil Engineering Department, METU

Assist. Prof. Dr. Abdullah Dilsiz
Civil Engineering Department, YBU

Date:

I hereby declare that all information in this document has been obtained and presented in accordance with academic rules and ethical conduct. I also declare that, as required by these rules and conduct, I have fully cited and referenced all material and results that are not original to this work.

Name, Last Name: SEDA ÖZDEMİR

Signature :

ABSTRACT

INVESTIGATION OF SEISMIC ISOLATION EFFICIENCY FOR BUILDING STRUCTURES

Özdemir, Seda

M.S., Department of Earthquake Studies

Supervisor : Prof. Dr. Ahmet Yakut

Co-Supervisor : Assist. Prof. Dr. Bekir Özer Ay

December 2016, 118 pages

The main goal of this study is to assess the efficacy of seismic isolation for building type of structures with different structural systems, namely, dual systems and moment frame systems having also different number of floors. Specific to this study, the main parameters employed for efficacy assessment will be the interstorey drift ratio and floor acceleration since both structural and non-structural damage to be occurred in a system are directly related to these two parameters. To assess the variations in interstorey drift ratio and floor accelerations between different structural systems, linear elastic response spectrum analysis procedures are followed for two different site-specific seismicity levels representing two site regions from Izmir and Isparta, respectively. To enhance the accuracy of the response, seismically isolated dual systems having different number of floors are analyzed non-linearly in modal space under the seismicity level of Izmir, since for non-structural content, floor acceleration value that the structure undergoes has a special importance when the content of a building constitutes of valuable acceleration-sensitive equipments. The analyses performed in

this thesis work indicated that for both type of structural systems, by the application of seismic isolation design method, the efficiency of reduction in interstorey drift and floor acceleration decreases as the number of floor increases. In addition, the amount of efficiency differ from each other between dual systems and moment frame systems. Another major conclusion is that linear elastic analysis procedures may underestimate both floor acceleration and interstorey drift responses.

Keywords: seismic isolation efficiency, multi-storey buildings, interstorey drift, floor acceleration, high structural performance level

ÖZ

BİNA TİPİ YAPILARDA SİSMİK İZOLASYON ETKİNLİĞİNİN İNCELENMESİ

Özdemir, Seda

Yüksek Lisans, Deprem Çalışmaları Bölümü

Tez Yöneticisi : Prof. Dr. Ahmet Yakut

Ortak Tez Yöneticisi : Yrd. Doç. Dr. Bekir Özer Ay

Aralık 2016 , 118 sayfa

Bu tez çalışmasında, farklı kat adedine sahip perdeli çerçeve ve çerçeve sistemli bina türü yapıların sismik izolasyon verimliliği araştırılmıştır. Bu çalışma özelinde verimlilik değerlendirmesine esas alınan başlıca parametreler, görelî kat ötelenmeleri ve kat ivmeleri olacaktır. Bu parametrelerin tercih edilme sebebi olarak, binalarda yapısal ve yapısal olmayan hasarların bu iki parametreye doğrudan bağlı olması söylenebilir. Çalışmada esas alınan bu iki parametre, farklı yapısal sistemler üzerinde, İzmir ve Isparta bölgelerinden iki farklı sahaya özel depremselliği temsil eden tepki spektrumlarının kullanılmasıyla doğrusal elastik analiz yöntemleri izlenerek incelenmiştir. Doğrusal elastik tepki spektrumu analizi yaklaşımındaki hassasiyeti arttırmak amacıyla, farklı kat adedine sahip sismik izolatörlü perdeli çerçeve sistemler modsal uzay alanında doğrusal olmayan analiz, İzmir depremselliği için tekrarlanmıştır. Analiz yöntemindeki hassasiyeti arttırmak, özellikle kat ivmelerinden etkilenebilecek, yapısal olmayan, ivme hassasiyeti içeren, yüksek maliyetli ekipmanlara sahip binalar için

oldukça önemlidir. Bu çalışmada elde edilen sonuçlara göre bina kat sayısı arttıkça, sismik izolasyon verimliliği hem perdeli çerçeve hem de çerçeve sistemler için azalmaktadır. Ayrıca verimlilikteki değişimin miktarı perdeli çerçeve ve çerçeve sistem için farklılık göstermektedir. Bu çalışmada elde edilen başlıca sonuçlardan bir diğeri ise doğrusal elastik analiz yöntemleri ile hesaplanan kat ivmelerinin ve görelî kat ötelenmelerinin doğrusal olmayan analiz yöntemleri ile hesaplanan değerlerden önemli ölçüde farklılık gösterebileceğidir.

Anahtar Kelimeler: sismik izolasyon verimliliği, çok katlı binalar, görelî kat ötelenmesi, kat ivmesi, yüksek yapısal performans seviyesi

To my parents...

ACKNOWLEDGMENTS

I would like to express my sincere thanks to my thesis supervisor Prof. Dr. Ahmet Yakut for providing me his further experience and guidance during my study. I would also like to express my deep thankfulness to my thesis co-supervisor Assist. Prof. Dr. Bekir Özer Ay for motivating me since the beginning of my thesis work, and supporting my earthquake engineering knowledge with his area of specialization. I would like to thank my thesis committee, Prof. Dr. Uğurhan Akyüz, Assoc. Prof. Dr. Ayşegül Askan Gündoğan and Assist. Prof. Dr. Abdullah Dilsiz for their valuable comments and suggestions for this thesis work, also which I will make use of in my future research career. I owe thanks to Alp Caner, PhD, P.E. for trusting and supporting me during my thesis work and my whole engineering career, as well as for providing me the opportunity to work on my thesis along with my job. I am also grateful to Naz Topkara Özcan for her seismic hazard studies that I adopt in this thesis work. I must also thank to my officemates Arzu İpek Yılmaz and Ezgi Karakaya for their kind help, moral support, and favor. I am also thankful to Uğurcan Özçamur for sharing his experience in seismic isolation design considerations. I would also like to thank Mustafa Burçin Gövsulu and Kaan Kaatsız for their sincere guidance in structural analysis, modeling and design issues. I would like to thank my dearest friend Başar Özbilen for his amity, cheerfulness and good memories that we shared for about 10 years. Thank to my late grandfather Abdurrahman Özdemir for believing in my virtuousness since I was a child. I must also thank to my grandmother Nezahat Özen for her prayers that have always been with me. My deepest thanks belong to my family; my parents Zeynep Özen Özdemir and Ersin Özdemir, my sisters Seren Özdemir and Ecem Özdemir. I am indebted to their unconditional love and self-sacrifice, as well as for the inspiration of being enlightened, versatile and ethical through my whole life.

TABLE OF CONTENTS

ABSTRACT	v
ÖZ	vii
ACKNOWLEDGMENTS	x
TABLE OF CONTENTS	xi
LIST OF TABLES	xv
LIST OF FIGURES	xviii
LIST OF ABBREVIATIONS	xxvi
CHAPTERS	
1 INTRODUCTION	1
1.0.1 Philosophy of Seismic Isolation	6
1.1 Concepts of Seismic Isolation	8
1.1.1 Equivalent Lateral Force Procedure [5]	10
1.2 Literature Review	12
1.3 Motivation to this Thesis Work	14
1.4 Scope of the Work	15
2 STRUCTURAL MODELING AND ANALYSIS	17

2.1	Architectural Considerations	18
2.2	Structural Modeling	21
2.3	Seismicity	24
2.3.1	Ground Motion Selection and Scaling for the Targeted DBE Site Specific Response Spectrum for Izmir	27
2.4	Analysis and Design of Structural Systems	36
2.4.1	Method of Analyses	37
2.4.1.1	Structural Design	38
2.4.2	Conventional Design Approach	39
2.4.2.1	Fixed Base Dual Systems (SWFB15, SWFB10, SWFB5)	39
2.4.2.2	Fixed Base Moment Frame Systems (FB15, FB10, FB5)	42
2.4.2.3	Seismic Isolation Design Approach	43
3	ANALYSIS RESULTS	57
3.1	RSA Results for Izmir	58
3.1.1	IDR(%) and PFA (g) Results of ISOSW15, ISO15, SWFB15, FB15 for Izmir	58
3.1.2	PFA (g) Results of ISOSW15, ISO15, SWFB15, FB15 for Izmir	63
3.1.3	IDR(%) Results of ISOSW10, ISO10, SWFB10, FB10 for Izmir	66
3.1.4	PFA(g) Results of ISOSW10, ISO10, SWFB10, FB10 for Izmir	69

3.1.5	IDR(%) Results of ISOSW5, ISO5, SWFB5, FB5 for Izmir	71
3.1.6	PFA(g) Results of ISOSW5, ISO5, SWFB5, FB5 for Izmir	75
3.2	FNA Results of ISOSW15, ISOSW10 and ISOSW5 for Izmir	77
3.2.1	PFA(g) Results of ISOSW15 for Izmir from FNA .	78
3.2.2	PFA(g) Results of ISOSW10 for Izmir from FNA .	81
3.2.3	PFA(g) Results of ISOSW5 for Izmir from FNA . .	82
3.2.4	IDR(%) Results of ISOSW15 for Izmir from FNA	84
3.2.5	IDR(%) Results of ISOSW10 for Izmir from FNA	87
3.2.6	IDR(%) Results of ISOSW5 for Izmir from FNA .	89
3.3	Summary and Discussion of Analysis Results	91
4	SUMMARY AND CONCLUSIONS	95
4.1	Summary	95
4.2	Conclusion	95
4.3	Recommendation for Future Work	96
	REFERENCES	97
APPENDICES		
A	SEISMIC PARAMETERS OF PSHA FOR IZMIR	101
B	SEISMIC PARAMETERS OF PSHA FOR ISPARTA	105
C	RSA RESULTS FOR ISPARTA	107

C.1	IDR(%) Results of ISOSW15, ISO15, SWFB15, FB15 for Isparta	107
C.2	PFA(g) Results of ISOSW15, ISO15, SWFB15, FB15 for Isparta	108
C.3	IDR(%) Results of ISOSW10, ISO10, SWFB10, FB10 for Isparta	108
C.4	PFA(g) Results of ISOSW10, ISO10, SWFB10, FB10 for Isparta	109
C.5	IDR(%) Results of ISOSW5, ISO5, SWFB5, FB5 for Isparta	110
C.6	PFA(g) Results of ISOSW5, ISO5, SWFB5, FB5 for Isparta	110
CURRICULUM VITAE		117

LIST OF TABLES

TABLES

Table 1.1	Damage Control and Building Performance Levels [3]	4
Table 2.1	Structural System Definitions for 15-Storey Models	17
Table 2.2	Structural System Definitions for 10-Storey Models	17
Table 2.3	Structural System Definitions for 5-Storey Models	18
Table 2.4	Architectural Details	18
Table 2.5	5% Damped SRSS Spectral Acceleration Values from Site Specific PSHA for Izmir	26
Table 2.6	5% Damped SRSS Spectral Acceleration Values from Site Specific PSHA for Isparta	26
Table 2.7	Selected Ground Motion Records for Time History Analysis Proce- dure	27
Table 2.8	Methods of Analyses	38
Table 2.9	Structural Member Sizes in SWFB15, ISOSW15, ISO15 and FB15 .	39
Table 2.10	Fixed Base Period (T_{fix}) of the Conventional Systems	44
Table 2.11	Target Isolator Performance for Izmir (UB)	45
Table 2.12	Target Isolator Performance for Isparta (UB)	45
Table 2.13	Linear Isolator Parameters for ISOSW15, Izmir & Isparta	47

Table 2.14 Linear Isolator Parameters for ISOSW10, Izmir & Isparta	49
Table 2.15 Linear Isolator Parameters for ISOSW5, Izmir & Isparta	50
Table 2.16 Linear Isolator Parameters for ISO15, Izmir & Isparta	52
Table 2.17 Linear Isolator Parameters for ISO10, Izmir & Isparta	54
Table 2.18 Linear Isolator Parameters for ISO5, Izmir & Isparta	56
Table 3.1 Limitations on the Maximum Interstorey Drifts	58
Table 3.2 Modal Participating Mass Ratios, ISOSW15	61
Table 3.3 Modal Participating Mass Ratios, ISO15	62
Table 3.4 Modal Participating Mass Ratios, SWFB15	63
Table 3.5 Modal Participating Mass Ratios, FB15	64
Table 3.6 Modal Participating Mass Ratios, ISOSW10	67
Table 3.7 Modal Participating Mass Ratios, ISO10	67
Table 3.8 Modal Participating Mass Ratios, SWFB10	68
Table 3.9 Modal Participating Mass Ratios, FB10	68
Table 3.10 Modal Participating Mass Ratios, ISOSW5	72
Table 3.11 Modal Participating Mass Ratios, ISO5	73
Table 3.12 Modal Participating Mass Ratios, SWFB5	74
Table 3.13 Modal Participating Mass Ratios, FB5	74
Table 3.14 PFA (g) of the Top Floor under GM:0015 Excitation in x-direction .	78
Table 3.15 Mean PFA (g) of ISOSW15 from the 7 GM Records in x-direction .	79
Table 3.16 Mean PFA (g) of ISOSW15 from the 7 GM Records in y-direction .	80
Table 3.17 Mean PFA (g) of ISOSW10 from the 7 GM Records in x-direction .	81

Table 3.18 Mean PFA (g) of ISOSW10 from the 7 GM Records in y-direction . . .	82
Table 3.19 Mean PFA (g) of ISOSW5 from the 7 GM Records in x-direction . . .	83
Table 3.20 Mean PFA (g) of ISOSW5 from the 7 GM Records in y-direction . . .	84
Table 3.21 Mean IDR(%) of 7 GM Records in x-direction for ISOSW15	85
Table 3.22 Mean IDR(%) of 7 GM Records in y-direction for ISOSW15	86
Table 3.23 Mean IDR(%) of 7 GM Records in x-direction for ISOSW10	87
Table 3.24 Mean IDR(%) of 7 GM Records in y-direction for ISOSW10	88
Table 3.25 Mean IDR(%) of 7 GM Records in x-direction for ISOSW5	89
Table 3.26 Mean IDR(%) of 7 GM Records in y-direction for ISOSW5	90
Table A.1 Seismic sources defined for Izmir site	101
Table A.2 Standard Least Square Regression, All Earthquakes	101
Table A.3 Maximum Likelihood Method, All Earthquakes	102
Table A.4 Standard Least Square Regression, Main Shocks Only	103
Table A.5 Maximum Likelihood Method, Main Shocks Only	103
Table A.6 Subjective Probabilities of Alternative Assumptions (Logic Tree Method)	103
Table A.7	104
Table A.8	104
Table B.1 Seismic Source Zones for Isparta	105
Table B.2 Parameters for seismic source zones	105
Table B.3	106
Table B.4	106

LIST OF FIGURES

FIGURES

Figure 1.1 Change of Deflection Pattern, Conventionally Designed (on the left) and Seismically Isolated Building (on the right)[2]	3
Figure 1.2 General Structural Performance Levels	5
Figure 1.3 Transmission of Ground Motions [30]	6
Figure 1.4 Elastomeric Bearings: a)Natural Rubber Bearing (NRB) b) elastomeric bearing device c)Lead Rubber Bearing (LRB) [16]	7
Figure 1.5 Friction Pendulum System (FPS) [16]	8
Figure 1.6 Some of the Energy Dissipation Devices [28]	8
Figure 1.7 Effects of base isolation: a) on spectral acceleration, b) on lateral displacement [16]	9
Figure 1.8 Idealized Bilinear Force-Displacement Relation of an Isolator [33] .	9
Figure 1.9 Damping Coefficients [5]	11
Figure 1.10 Upper Bound (UB) Nominal (N) Lower Bound (LB) Characteristics of a Typical Isolation Unit [33]	12
Figure 2.1 Key Plan of the Hospital Blocks	19
Figure 2.2 Typical Architectural Plan of the Hospital Block	20
Figure 2.3 Typical 3D SAP2000 Model from a Seismically Isolated Dual System with 15 floors	23

Figure 2.4 Typical 3D SAP2000 Model from a Seismically Isolated Moment Frame System with 15 floors	24
Figure 2.5 5% Damped SRSS Site Specific Response Spectra (DBE) for Izmir and Isparta	25
Figure 2.7 GM: 0015 in x direction	28
Figure 2.8 GM: 0015 in y direction	28
Figure 2.6 Izmir SRSS Target Design Spectrum vs 5% Damped SRSS Spec- trum of GM: 0015	28
Figure 2.9 GM: 0762 in x direction	29
Figure 2.10 GM: 0762 in y direction	29
Figure 2.11 Izmir SRSS Target Design Spectrum vs 5% Damped SRSS Spec- trum of GM: 0762	29
Figure 2.12 GM: 0807 in x direction	30
Figure 2.13 GM: 0807 in y direction	30
Figure 2.14 Izmir SRSS Target Design Spectrum vs 5% Damped SRSS Spec- trum of GM: 0807	30
Figure 2.15 GM: 1015 in x direction	31
Figure 2.16 GM: 1015 in y direction	31
Figure 2.17 Izmir SRSS Target Design Spectrum vs 5% Damped SRSS Spec- trum of GM: 1015	31
Figure 2.18 GM: 1633 in x direction	32
Figure 2.19 GM: 1633 in y direction	32
Figure 2.20 Izmir SRSS Target Design Spectrum vs 5% Damped SRSS Spec- trum of GM: 1633	32

Figure 2.21 GM: 2714 in x direction	33
Figure 2.22 GM: 2714 in y direction	33
Figure 2.23 Izmir SRSS Target Design Spectrum vs 5% Damped SRSS Spectrum of GM: 2714	33
Figure 2.24 GM: 3503 in x direction	34
Figure 2.25 GM: 3503 in y direction	34
Figure 2.26 Izmir SRSS Target Design Spectrum vs 5% Damped SRSS Spectrum of GM: 3503	34
Figure 2.27 Izmir SRSS Target Design Spectrum vs 5% Damped SRSS Spectrum of all GMs	35
Figure 2.28 Izmir 5% Damped SRSS Target Spectrum vs 5% Damped SRSS Mean Spectrum of 7 GMs	36
Figure 2.29 Typical Formwork Plan for SWFB15	41
Figure 2.30 Behaviour of Moment Frame Systems and Shear Walled Frame Systems[20]	42
Figure 2.31 Typical Formwork Plan for FB15	43
Figure 2.32 ISOSW15-Nonlinear UB Isolation Characteristics of Type 1: L800, Izmir	46
Figure 2.33 ISOSW15-Nonlinear UB Isolation Characteristics of Type 2: L900, Izmir	46
Figure 2.34 ISOSW15-Nonlinear UB Isolation Characteristics of Type 3: L1000, Izmir	47
Figure 2.35 ISOSW10-Nonlinear UB Isolation Characteristics of Type 1: L500, Izmir	48

Figure 2.36 ISOSW10-Nonlinear UB Isolation Characteristics of Type 2: L600, Izmir	48
Figure 2.37 ISOSW10-Nonlinear UB Isolation Characteristics of Type 3: L800, Izmir	49
Figure 2.38 ISOSW5-Nonlinear UB Isolation Characteristics of Type 1: L280, Izmir	50
Figure 2.39 ISOSW5-Nonlinear UB Isolation Characteristics of Type 2: L400, Izmir	50
Figure 2.40 ISO15-Nonlinear UB Isolation Characteristics of Type 1: L600, Izmir	51
Figure 2.41 ISO15-Nonlinear UB Isolation Characteristics of Type 2: L700, Izmir	51
Figure 2.42 ISO15-Nonlinear UB Isolation Characteristics of Type 3: L900, Izmir	52
Figure 2.43 ISO10-Nonlinear UB Isolation Characteristics of Type 1: L400, Izmir	53
Figure 2.44 ISO10-Nonlinear UB Isolation Characteristics of Type 2: L500, Izmir	53
Figure 2.45 ISO10-Nonlinear UB Isolation Characteristics of Type 3: L600, Izmir	54
Figure 2.46 ISO5-Nonlinear UB Isolation Characteristics of Type 1: L240, Izmir	55
Figure 2.47 ISO5-Nonlinear UB Isolation Characteristics of Type 2: L300, Izmir	55
Figure 3.1 IDR(%) (in x direction) through Floors of 15 Storey Systems for Izmir DBE Level from RSA	59
Figure 3.2 IDR(%) (in y direction) through Floors of 15 Storey Systems for Izmir DBE Level from RSA	60

Figure 3.3 PFA(g) (in x direction) through Floors of 15 Storey Systems for Izmir DBE Level from RSA	64
Figure 3.4 PFA(g) (in y direction) through Floors of 15 Storey Systems for Izmir DBE Level from RSA	65
Figure 3.5 IDR(%) (in x direction) through Floors of 10 Storey Systems for Izmir DBE Level from RSA	66
Figure 3.6 IDR(%) (in y direction) through Floors of 10 Storey Systems for Izmir DBE Level from RSA	69
Figure 3.7 PFA(g) (in x direction) through Floors of 10 Storey Systems for Izmir DBE Level from RSA	70
Figure 3.8 PFA(g) (in y direction) through Floors of 10 Storey Systems for Izmir DBE Level from RSA	70
Figure 3.9 IDR(%) (in x direction) through Floors of 5 Storey Systems for Izmir DBE Level from RSA	71
Figure 3.10 IDR(%) (in y direction) through Floors of 5 Storey Systems for Izmir DBE Level from RSA	72
Figure 3.11 PFA(g) (in x direction) through Floors of 5 Storey Systems for Izmir DBE Level from RSA	75
Figure 3.12 PFA(g) (in y direction) through Floors of 5 Storey Systems for Izmir DBE Level from RSA	76
Figure 3.13 Acceleration of CoR of each Floor under GM:0015 Excitation in x-direction	78
Figure 3.14 PFA(g) (in x direction) through Floors of ISOSW15 for Izmir DBE Level from FNA	79
Figure 3.15 PFA(g) (in y direction) through Floors of ISOSW15 for Izmir DBE Level from FNA	80

Figure 3.16 PFA(g) (in x direction) through Floors of ISOSW10 for Izmir DBE Level from FNA	81
Figure 3.17 PFA(g) (in y direction) through Floors of ISOSW10 for Izmir DBE Level from FNA	82
Figure 3.18 PFA(g) (in x direction) through Floors of ISOSW5 for Izmir DBE Level from FNA	83
Figure 3.19 PFA(g) (in y direction) through Floors of ISOSW5 for Izmir DBE Level from FNA	84
Figure 3.20 IDR(%) (in x direction) through Floors of ISOSW15 for Izmir DBE Level from FNA	85
Figure 3.21 IDR(%) (in y direction) through Floors of ISOSW15 for Izmir DBE Level from FNA	86
Figure 3.22 IDR(%) (in x direction) through Floors of ISOSW10 for Izmir DBE Level from FNA	87
Figure 3.23 IDR(%) (in y direction) through Floors of ISOSW10 for Izmir DBE Level from FNA	88
Figure 3.24 IDR(%) (in x direction) through Floors of ISOSW5 for Izmir DBE Level from FNA	89
Figure 3.25 IDR(%) (in y direction) through Floors of ISOSW5 for Izmir DBE Level from FNA	90
Figure 3.26 (%) Reduction in Interstorey Drift Ratio (%) for Dual Systems Izmir & Isparta	91
Figure 3.27 (%) Reduction in Interstorey Drift Ratio (%) for Moment Frame Systems Izmir & Isparta	92
Figure 3.28 (%) Reduction in Top Floor Accelerations (g) for Dual Systems Izmir & Isparta	93

Figure 3.29 (%) Reduction in Top Floor Accelerations (g) for Moment Frame Systems Izmir & Isparta	94
Figure A.1 Dominant seismic sources for Izmir site	102
Figure B.1 Seismic Source Zones Defined for Europe and Eastern Mediterian Regions	106
Figure C.1 IDR(%) (in x direction) through Floors of 15 Storey Systems for Isparta DBE Level from RSA	108
Figure C.2 IDR(%) (in y direction) through Floors of 15 Storey Systems for Isparta DBE Level from RSA	109
Figure C.3 PFA(g) (in x direction) through Floors of 15 Storey Systems for Isparta DBE Level from RSA	110
Figure C.4 PFA(g) (in y direction) through Floors of 15 Storey Systems for Isparta DBE Level from RSA	111
Figure C.5 IDR(%) (in x direction) through Floors of 10 Storey Systems for Isparta DBE Level from RSA	111
Figure C.6 IDR(%) (in y direction) through Floors of 10 Storey Systems for Isparta DBE Level from RSA	112
Figure C.7 PFA(g) (in x direction) through Floors of 10 Storey Systems for Isparta DBE Level from RSA	112
Figure C.8 PFA(g) (in y direction) through Floors of 10 Storey Systems for Isparta DBE Level from RSA	113
Figure C.9 IDR(%) (in x direction) through Floors of 5 Storey Systems for Isparta DBE Level from RSA	113
Figure C.10 IDR(%) (in y direction) through Floors of 5 Storey Systems for Isparta DBE Level from RSA	114

Figure C.11 PFA(g) (in x direction) through Floors of 5 Storey Systems for Isparta DBE Level from RSA	114
Figure C.12 PFA(g) (in y direction) through Floors of 5 Storey Systems for Isparta DBE Level from RSA	115

LIST OF ABBREVIATIONS

2013 TMMH	2013 Technical Memorandum of the Ministry of Health
ASCE 7-10	American Society of Civil Engineers, Minimum Design Loads for Buildings and Other Structures, 2010
CoR	Center of Rigidity
DBE	Design Basis Earthquake
FB15	Fixed Base Moment Frame System with 15 Floors
FEMA	Federal Emergency Management Agency
FNA	Fast Nonlinear Analysis
g	Gravitational Acceleration
GM	Ground Motion
IDR	Interstorey Drift Ratio
ISOSW15	Seismically Isolated Dual System with 15 Floors
ISO15	Seismically Isolated Moment Frame System with 15 Floors
MCE	Maximum Credible Earthquake
PFA	Peak Floor Acceleration
PSHA	Probabilistic Seismic Hazard Assessment
RSA	Linear Response Spectrum Analysis
SWFB15	Fixed Base Dual System with 15 Floors
TEC 2007	Turkish Earthquake Code 2007
TS 498	Design Loads for Buildings
TS 500	Turkish Reinforced Concrete Building Code 2007
UB	Upper Bound

CHAPTER 1

INTRODUCTION

Seismic activities resulting in strong ground motion may have catastrophic consequences like loss of life and property. After major earthquakes, many people loss their lives not due to earthquake itself but due to poorly designed man made structures. The outcome of a major or moderate earthquake may often be economic loss as well. In this manner, structural engineers are responsible for designing earthquake resistant structures to prevent the structure from collapsing, or damaging of structural and non structural elements in it. Designing of a structure by taking earthquake into account falls into the framework of Earthquake Design.

Earthquake Engineering is a multidisciplinary branch that deals with seismic analysis, design and assessment of structures. Day by day, this field of study is evolving to develop different structural performance criteria for structures undergoing seismic action. Recently, these criteria are mostly based on economical considerations. In our global world, the economy is the governing parameter for any kind of investment. Regarding the functional importance of the structure to the investor, the seismic performance level of the structure is assigned and the structural design is performed accordingly.

To explain the seismic performance levels, some concepts of structural mechanics could be employed as fundamentals. In the definition of force versus displacement curves from structural mechanics, the force represents the loads that are supposed to be resisted by the structure and the displacement is indication of the damage to the structure. In that manner, designing a structure such that the structural members remain in their elastic range of force versus displacement relation is quite safe pro-

vided that the members have sufficient strength to resist the loads. However, this approach is not economical in engineering point of view. Therefore; an energy dissipation concept needed to be introduced, meaning that the structural members under consideration go beyond their inelastic range on the force versus displacement behavior by exposing some permanent deformation under the condition that ductility is ensured. Forming energy dissipation mechanisms within the structural system is admitting some damage to the structure without life loss, or total collapse.

In seismic codes currently in use, some predefined and controllable damage to the structure is allowed with regard to the expected seismic performance of the structure for a defined earthquake level. In controlled damage approach, ductility of the system has to be ensured. Ductility can be simply defined as the deformability through inelastic range of a structural member without significant reduction in the capacity leading to failure. Since inelastic design approach means some controlled damage to both structural and non-structural elements, cost of the damage allowed has to be evaluated considering also the probability of that level of damage to occur. After evaluating costs and probability of damage, design force levels are to be decided on and the structure is designed accordingly. Considering and including the consequences of the damage can be named as Performance Based Earthquake Engineering. In engineering point of view, focus for structural design is mainly based on this approach.

In some cases, cost evaluation of the damage is not acceptable depending on the type of the structure. If the consequences of the damage level are not acceptable, earthquake demand can be decreased by seismic isolation and energy dissipation devices by modifying building response characteristics. Conceptually, seismic isolation diminishes the high frequency oscillation of the superstructure by simply "decoupling" the structure from the ground. Being one of the passive seismic control systems, seismic isolation reduces forces transmitted to the superstructure by elongating the period of the structure and adding some amount of damping. Added damping is an inherent property of most passive control systems. On the other hand, there are also active seismic control systems solely dissipating seismic energy like dampers. Eventually, the main purpose is to utilize active and/or passive seismic control systems to decrease interstorey drift and floor accelerations to prevent structural and non-structural damage. In that case, ductility of the system is not necessarily to be satisfied since

the structure is simply separated from earthquake excitation to perform rather a calm oscillation as a rigid body.

In Figure 1.1, a simple sketch of conventionally designed and seismically isolated buildings are illustrated.

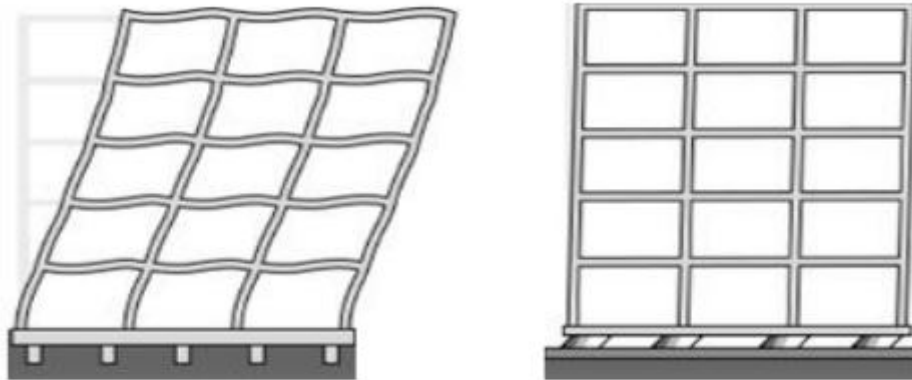


Figure 1.1: Change of Deflection Pattern, Conventionally Designed (on the left) and Seismically Isolated Building (on the right)[2]

In subsection 1.0.1, philosophy of seismic base isolation is explained. Typical devices used for seismic isolation are also mentioned briefly.

According to function of the building to be designed, the buildings may be supposed to ensure high level of seismic performance to protect the property in buildings. According to FEMA 356¹ [3], this seismic performance level corresponds to "Operational Level (1-A)". In Table 1.1, building performance levels are defined based on FEMA 356.

¹ Note that FEMA 356 has been superseded by American Society of Civil Engineers [ASCE] 41[4], Seismic Rehabilitation of Buildings.

Table 1.1: Damage Control and Building Performance Levels [3]

	Target Building Performance Levels			
	Collapse Prevention	Life Safety	Immediate Occupancy	Operational
	Level (5-E)	Level (3-C)	Level (1-B)	Level (1-A)
Overall Damage	Severe	Moderate	Light	Very Light
General	Little residual stiffness and strength, but load-bearing columns and walls function. Large permanent drifts. Some exits blocked. Infills and unbraced parapets failed or at incipient failure. Building is near collapse.	Some residual strength and stiffness left in all stories. Gravity-load-bearing elements function. No out-of-plane failure of walls or tipping of parapets. Some permanent drift. Damage to partitions. Building may be beyond economical repair.	No permanent drift. Structure substantially retains original strength and stiffness. Minor cracking of facades, partitions, and ceilings as well as structural elements. Elevators can be restarted. Fire protection operable.	No permanent drift. Structure substantially retains original strength and stiffness. Minor cracking of facades, partitions, and ceilings as well as structural elements. All systems important to normal operation are functional.
Nonstructural components	Extensive damage.	Falling hazards mitigated but many architectural, mechanical, and electrical systems are damaged.	Equipment and contents are generally secure, but may not operate due to mechanical failure or lack of utilities.	Negligible damage occurs. Power and other utilities are available, possibly from standby sources.
Comparison with performance intended for buildings designed under the <i>NEHRP Provisions</i> , for the Design Earthquake	Significantly more damage and greater risk.	Somewhat more damage and slightly higher risk.	Less damage and lower risk.	Much less damage and lower risk.

Regarding force-displacement relation, general structural performance levels are illustrated in Figure 1.2.

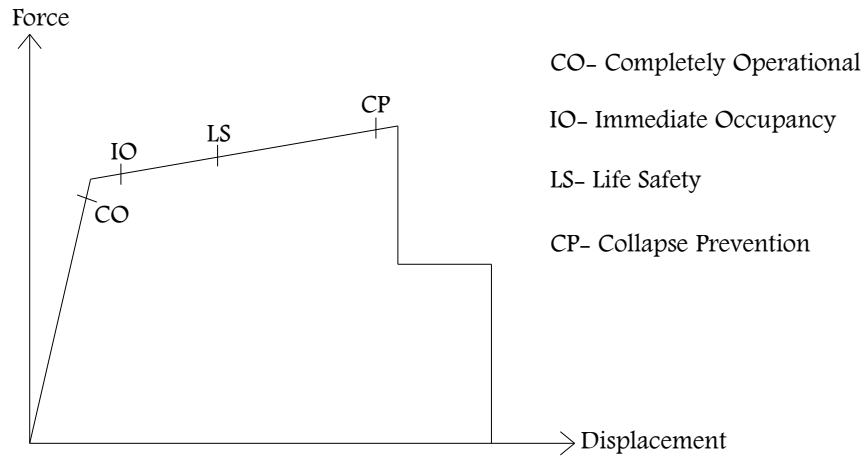


Figure 1.2: General Structural Performance Levels

As it can be seen from Figure 1.2, at high performance levels, namely, "Completely Operational" and "Immediate Occupancy", structural deformations remain within elastic, or almost elastic range, respectively. When the structure undergoes plastic deformations, the damage is controlled by ensuring "Life Safety" and "Collapse Prevention".

In recent years, seismic isolation became a popular concept in earthquake design practice since it is one of the most feasible solutions to achieve high seismic performance levels. In seismic isolation approach, earthquake demand is diminished rather than increasing the force capacity of the structural members to resist seismic action by achieving a high level of seismic performance. Since increase in force capacity of the structural members means also increase in rigidity of the structural system, earthquake demand response of the structure simply increases as well, which is dynamically an undesired situation. As the rigidity of the structural system becomes high, dynamic characteristics of the structure make the overall system suffer from high frequency ground motion. Therefore, increasing the rigidity of the structural system to resist lateral earthquake loads is the simplest but at the same time a paradoxical approach in earthquake resistant design. In that sense, instead of increasing force capacity of the structural system, decreasing the earthquake demand is more reasonable.

1.0.1 Philosophy of Seismic Isolation

The fundamental principle of seismic isolation is to alter the response of the structure such that strong and destructive effect of earthquake excitation will not be transmitted to the superstructure [30].

Being specific for building structures, a building which is perfectly rigid will have a period equal to zero. As the ground disturbed by earthquake excitation, accelerations due to inertial forces in the building will be the same as the acceleration value of the ground moving [30]. The amount of drift will be identical for the ground and the building. On the other hand, a building which is perfectly flexible will have a period equal to infinity. In this case, there will be no inertia induced acceleration in the building, and the building will stay as stationary, yet the ground will be displaced. Relative displacement between the building and the ground will exactly be equal to the amount of ground displacement. This phenomena is visualized in Figure 1.3.

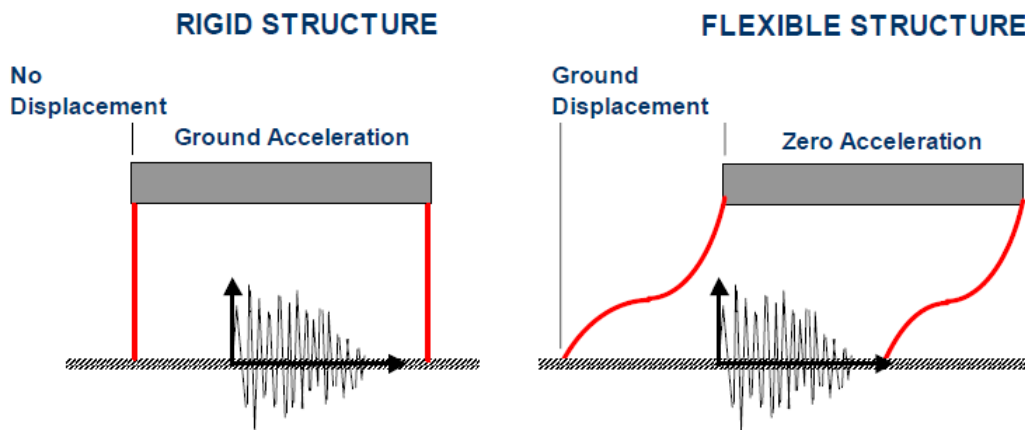


Figure 1.3: Transmission of Ground Motions [30]

In reality, typical structural behavior is in between these two extreme cases. By implementing seismic isolation, flexibility of the structure is further increased with respect to its original stiffness. By increasing the flexibility, fundamental period of vibration increases. Increment in natural period results in large displacements. Large displacements are controlled by damping of the seismic isolation device itself, and/or by the

contribution of additional dampers.

A seismic isolation device, or seismic isolator is a member having a very low lateral stiffness compared to superstructure, and a vertical stiffness high enough to sustain vertical loads from the superstructure. The main idea to make use of the low lateral rigidity in one of the bottom layers of the superstructure (most of the time at the foundation level) is to concentrate the lateral deformation due to earthquake into one layer of the structure. In this way, structure above the isolation level experiences almost a rigid body motion, meaning that structural and non-structural damages are mostly eliminated and the functionality of the seismically isolated structure is aimed to be remained as fully operational immediately after a major or moderate earthquake.

After a major earthquake, structures like hospitals and bridges are expected to serve immediately after the disaster. Museums, data centers, military and governmental buildings,... etc. are also strategic buildings regarding their valuable content. Seismic isolation technique is common mostly in these kind of structures. When a special focus is given on hospitals, they include medical equipments constituting a very large part of the total investment due to their high costs. Based on the total costs of both structural and non-structural elements including contents, seismic demand of the buildings having valuable content like hospitals could be diminished by seismic isolation and energy dissipation methods.

Typical seismic protection devices are as follows:

- Elastomeric Bearings

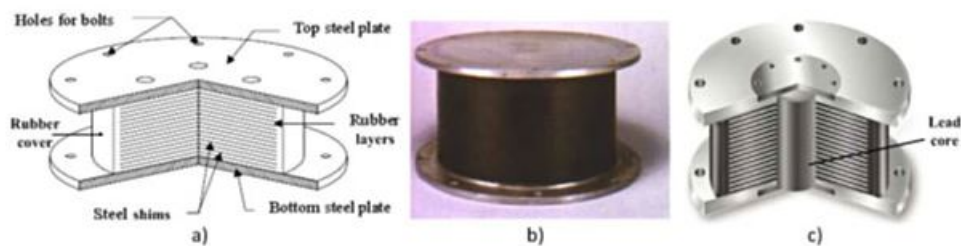


Figure 1.4: Elastomeric Bearings: a) Natural Rubber Bearing (NRB) b) elastomeric bearing device c) Lead Rubber Bearing (LRB) [16]

- Friction Pendulum Bearings

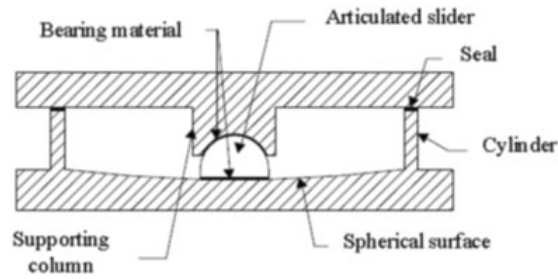


Figure 1.5: Friction Pendulum System (FPS) [16]

- Damping Devices

	Metallic damper	Friction damper	Viscous damper	Semi-active damper
Basic construction				
Idealised Hysteric behaviour				

Figure 1.6: Some of the Energy Dissipation Devices [28]

1.1 Concepts of Seismic Isolation

The main idea of seismic isolation is to increase the fundamental period of the structure. In this way, corresponding spectral acceleration value of which structure undergoes will decrease. Obviously, in a structural system with elongated fundamental period, lateral displacement will increase. This effect can be seen in Figure 1.7.

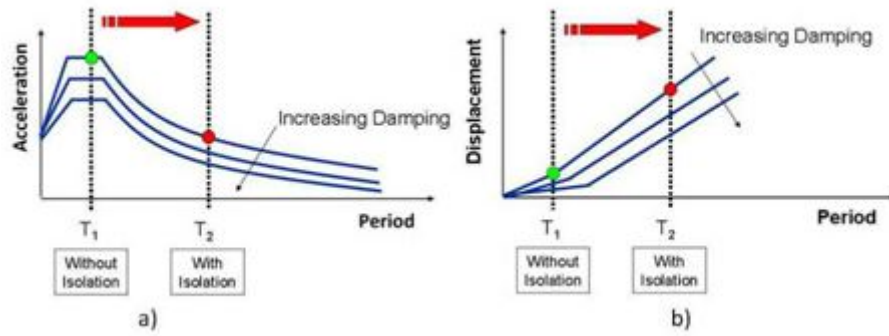


Figure 1.7: Effects of base isolation: a) on spectral acceleration, b) on lateral displacement [16]

In seismically isolated systems, increased displacement concentrated at the isolation level is controlled by inherent damping provided by the device itself. Damping mechanisms for various types of isolators are different.

Regarding engineering parameters of seismic isolation units, they can be mathematically modeled as a bilinear force-displacement relation as in Figure 1.8.

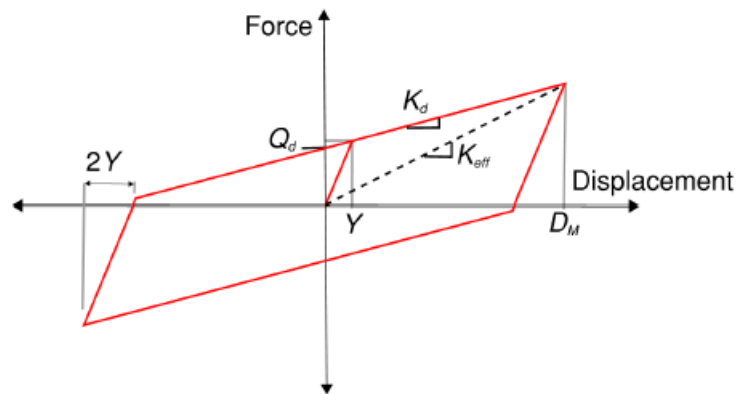


Figure 1.8: Idealized Bilinear Force-Displacement Relation of an Isolator [33]

In Figure 1.8, K_{eff} stands for the effective stiffness of the isolation unit, Q_d is the characteristic strength, Y is the yield displacement and K_d is the post yield stiffness.

1.1.1 Equivalent Lateral Force Procedure [5]

In this subsection, basic isolation design parameters will be presented based on [5].

In equations (1.1) to (1.4), basic parameters to calculate linear effective parameters of isolation units are presented.

In equation (1.1), D_D is the isolator design displacement, at the center of rigidity of the isolation system, which is excluding additional displacement due to actual and accidental torsion [5].

$$D_D = \left(\frac{g}{4\pi^2} \right) \frac{S_{D1} T_D}{B_D} \quad (1.1)$$

where

g : acceleration due to gravity

S_{D1} : design 5 percent damped spectral acceleration parameter at 1-s period

B_D : numerical coefficient related to the effective damping of the isolation system at the design displacement, β_D , as set forth in Table 17.5.1 [5]

T_D : effective period of the seismically isolated structure in seconds, at the design displacement

Effecting damping, β_D of the system is as in the equation (1.2):

$$\beta_D = \frac{1}{2\pi} \left(\frac{\text{total area of hysteresis loop}}{K_{D_{max}} D_D^2} \right) \quad (1.2)$$

Damping coefficient, B_D is related to the effective damping calculated from the equation (1.2). Corresponding damping coefficient values are presented in Table 1.9 [5].

Effective period of the system, T_D is presented in the equation (1.3)

$$T_D = 2\pi \sqrt{\frac{W}{K_{D_{min}} g}} \quad (1.3)$$

Table 17.5-1 Damping Coefficient, B_D or B_M

Effective Damping, β_D or β_M (percentage of critical) ^{a,b}	B_D or B_M Factor
≤ 2	0.8
5	1.0
10	1.2
20	1.5
30	1.7
40	1.9
≥ 50	2.0

^aThe damping coefficient shall be based on the effective damping of the isolation system determined in accordance with the requirements of Section 17.8.5.2.

^bThe damping coefficient shall be based on linear interpolation for effective damping values other than those given.

Figure 1.9: Damping Coefficients [5]

where

W : effective seismic weight of the structure above the isolation interface

$K_{D_{min}}$: minimum effective stiffness of the isolation system at the design displacement

To calculate seismic force, V_b , at the structure above the isolation system, equation (1.4) gives the relation as:

$$V_b = K_{D_{max}} D_D \quad (1.4)$$

In equations (1.3) and (1.4), the minimum and maximum effective stiffness terms will be treated by the lower bound (LB) and upper bound (UB) characteristics of the isolation units, respectively.

In [33], it is stated that the properties of seismic isolation units are subjected to variation over the design life due to the effects of aging and contamination, scragging as

well as due to the effects of heating during an earthquake excitation. Moreover, engineering properties of seismic isolation units may also vary among the manufacturers of seismic isolation devices. Some of these effects will increase the stiffness, on the other hand others will decrease these parameters [33]. Obviously, increased effective stiffness will lead to higher forces in the superstructure. For the sake of conservatism Therefore, in next generation design codes, like ASCE 7-16 [6] it is suggested to use upper bound modification factors to assess superstructure behavior by increased stiffness; while to use lower bound modification factors to determine isolator displacement large enough to be on the safe side by decreased stiffness as compared to nominal design parameters. In Figure 1.10, the changes in isolator parameters by upper bound, nominal and lower bound characteristics are demonstrated.

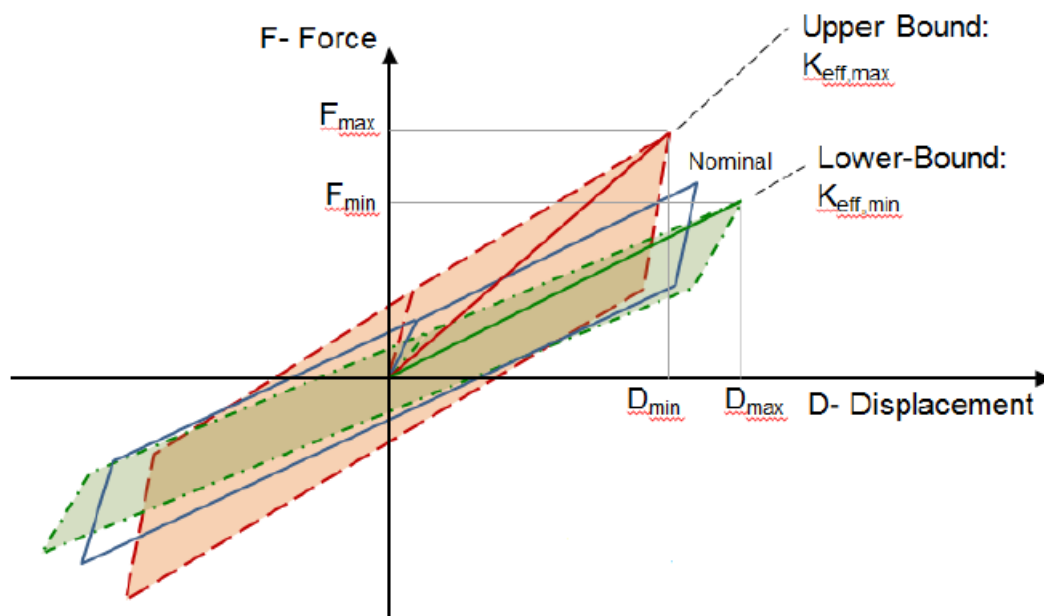


Figure 1.10: Upper Bound (UB) Nominal (N) Lower Bound (LB) Characteristics of a Typical Isolation Unit [33]

1.2 Literature Review

In literature, seismically isolated multi-storey buildings are investigated for various purposes. One of the studies that deals with the height of the structure is carried out

by Islam et al. [15]. In this work [15], the authors investigate the optimal height that wind is not predominant to earthquake action. They state that seismic isolation will not bring advantage to the system where wind is more critical than the earthquake [15]. In addition, according to Islam et al. [15], if the period of a building without seismic isolation is already long, introducing seismic isolation will not bring much difference to the general behavior of the building under seismic action. In that manner, the objective of the study in [15] was to investigate the building structures having dissimilar heights and plan area to determine critical height up to which seismic isolation is efficient. Based on the analyses performed with 108 numbers of models with different configurations of 4 to 30 stories built up, it is revealed that up to 30 to 40 m height, seismic isolation can be competent in medium risk seismicity for reinforced concrete buildings [15]. Regarding structural suitability, it is stated that heavy structures are the most cost effective ones to be designed as seismically isolated [15]. When it comes to the natural period of the structure, the authors of [15] think that the period of a non-isolated structure should be lower than 2 seconds. Since structural configuration is also an essential parameter, aspect ratio of a structure to be evaluated for the suitability of implementing seismic isolation is also mentioned in the paper [15] as the structure with a high aspect ratio may cause overturning problem [15].

Another work [14] focused on the effect of shear walls on seismically isolated buildings by Haider and Fareed. Based on this study, inclusion of shear walls has minor effects on the total base shear, therefore accelerations. On the other hand, it is found that shear walls provide a significant reduction in the interstorey drift values.

In the study of Dimos et al. [12], seismic isolation efficiency is investigated for multi-storey buildings by implementing seismic isolation at various elevations. The results had indicated that seismic isolation only at the base level may not be sufficient. A similar work had been performed in paper [17] published by Phocas and Pamboris, as well to extend the approach of base isolation by investigating the effectiveness of multi-storey structures with multi level isolation application.

In various studies in literature, analysis methods for seismically isolated structures are focused on. For instance, in the work of [19] conducted by Saatcioglu et al, the suitability of equivalent linear elastic analysis of seismically isolated multi-storey

buildings is assessed. In this study, a parametric study on two buildings with 3 floors and 5 floors were analyzed by using strong earthquake excitations. Based on this study, linear analysis procedure is found to be conservative regarding total isolation displacement and interstorey drifts [19]. On the other hand, when the systems are analyzed linearly, absolute peak floor accelerations are obtained as underestimated compared to the cases where nonlinear behavior is included [19]. Therefore, the authors suggest that equivalent linear elastic analysis can be used for preliminary design by conservatively resulted in isolator displacement and interstorey drifts. However, if the building includes acceleration sensitive equipments, more accurate bilinear models should be used as linear approximation underestimates the peak floor accelerations [19].

To optimally design the isolation units, dynamical characteristics of the structure above the isolation and the frequency content of earthquake excitation is also an important parameter. In the work of Baratta and Corbi [8], the researchers proposed counting in soil characteristics as an input in determining overall dynamic behavior. According to the authors, soil structure interaction is important since soil layers above the bedrock work like a filter to the earthquake excitation from deep layers of the Earth. Filtering effect of the soil deposits alter the earthquake frequency.

1.3 Motivation to this Thesis Work

In Turkey, seismic isolation became very popular after the 2013 Technical Memorandum of Ministry of Health, which obliges design of hospitals located in first or second seismic zone and having 100 or more inpatient bed availability as seismically isolated. In recent years, numerous hospital buildings have been started to be planned, designed and constructed as seismically isolated in Turkey. According to the Memorandum, there is no project specific or site specific technical criteria when deciding on the seismic isolation application to the intended hospital buildings. In fact, Turkish Earthquake Code 2007 (TEC 2007) [22] does not cover the design considerations of seismically isolated buildings, yet most of the hospitals and buildings have been designed and constructed based on TEC 2007 [22] for the structure above the isolation level, and on international codes for the seismic isolation units. There-

fore, there seems to be a mixed approach up to now, which is a confounding factor in overall structural design. During structural design stages including design of seismic isolation units, multiple criteria from several codes and specifications, even conflicting one another, may confuse the designer, the manufacturer of the isolation units, the owner and the administrative staff included in the project. In the absence of a national seismic isolation specification, design of the system as a whole may be unsatisfying regarding several aspects. In this study, one of the structural blocks of a real hospital project to be designed as seismically isolated from Turkey is investigated. In this thesis work, main parameters will be interstorey drift ratio and floor acceleration values based on the limitations specified in the 2013 Technical Memorandum of Ministry of Health (2013 TMMH) [21]. Interstorey drift and floor acceleration values will be evaluated with different structural system assumptions and number of floors to assess the benefit by seismic isolation application.

1.4 Scope of the Work

In this study, seismic isolation efficiency of a typical hospital building from a real project in Turkey is investigated. To achieve this goal, several structural system assumptions with different number of floors including the case in the original project is analyzed.

In the original project, number of floors is 15 with different storey heights and architectural plan dimensions. With regard to architectural occupancy, first two basement floors are designed as parking area. The isolation level is above the second basement floor from the foundation level.

Structural system of the original project is to be designed as seismically isolated with shear walls in addition to the moment frame system. In this way, structural system in the original project is a seismically isolated dual system.

In this thesis work, the efficiency of seismic isolation in application of seismic isolation together with shear walls in a moment frame system, which is the original case, is analyzed.

Assessment of efficiency is performed by comparing the seismically isolated dual system with a conventionally designed dual system and seismically isolated moment frame system having the same number of floors. Method of analyses of the structural systems is specified in Table 2.8.

Through the analyses, the controlling parameters will be interstorey drift ratio and floor accelerations. In the 2013 Technical Memorandum of Ministry of Health (2013 TMMH) [21], interstorey drift ratio is limited to be less than %0.5 and maximum floor acceleration is limited up to $0.2g$ in the structural design of seismically isolated hospital buildings. In this study, these limit values for interstorey drift ratio and floor accelerations will also be checked by making use of different structural system assumptions mentioned in Section 2.1 and under the action of two levels of seismicity from Turkey, namely, Izmir and Isparta.

To visualize the flow of the work, studies performed in each chapter are explained briefly:

In Chapter 1, some concepts of structural performance levels are introduced. In the following parts in Chapter 1, being one of the methods for decreasing seismic demand, which is focused on this thesis work, seismic isolation philosophy is presented with also engineering formulations and examples of devices used for this purpose. Literature review to present the state of art, motivation to study on the thesis topic and scope of the work finalized Chapter 1.

In Chapter 2, structural modeling and analysis including architectural considerations are explained in detail.

In Chapter 3, analysis results obtained for the cases investigated are stated in the order of linear and nonlinear analysis.

In Chapter 4, concluding remarks and future research recommendations are briefly presented by providing also a summary of this work.

CHAPTER 2

STRUCTURAL MODELING AND ANALYSIS

In this chapter, the structural modeling and analysis performed for different reinforced concrete structural systems used in this study are explained. In order to compare the seismic performance levels of a typical hospital building block with different structural system assumptions, four separate finite element models of the same hospital block are generated and analyzed for two different seismicity levels. The abbreviations for the models are explained in Table 2.1. To compare the seismic performance levels of these four different structural systems in terms of total building height, structural systems specified in Table 2.1 are analyzed also with different number of floors, in our study, with 10 floors and 5 floors.

Table2.1: Structural System Definitions for 15-Storey Models

SWFB15	Fixed Base Dual System with 15 Floors
ISOSW15	Seismically Isolated Dual System with 15 Floors
ISO15	Seismically Isolated Moment Frame System with 15 Floors
FB15	Fixed Base Moment Frame System with 15 Floors

In Table 2.2 and Table 2.3 notation for the systems having different number of floors are explained.

Table2.2: Structural System Definitions for 10-Storey Models

SWFB10	Fixed Base Dual System with 10 Floors
ISOSW10	Seismically Isolated Dual System with 10 Floors
ISO10	Seismically Isolated Moment Frame System with 10 Floors
FB10	Fixed Base Moment Frame System with 10 Floors

Table2.3: Structural System Definitions for 5-Storey Models

SWFB5	Fixed Base Dual System with 5 Floors
ISOSW5	Seismically Isolated Dual System with 5 Floors
ISO5	Seismically Isolated Moment Frame System with 5 Floors
FB5	Fixed Base Moment Frame System with 5 Floors

In subsection 2.1, architectural considerations are explained in detail.

2.1 Architectural Considerations

Architectural design of the structural system is taken from one of the buildings of a real hospital project to be designed as seismically isolated in Turkey. Key plan of the hospital blocks is demonstrated in Figure 2.1. The block analyzed is marked on the key plan as a shaded region. In the original design, architectural plan dimensions and storey heights are not identical and each floor has been designed for different purposes like surgery rooms, mechanical rooms, bedrooms, common use areas, offices, parking areas... etc. For the architectural design of the structural systems specified in Table 2.1, an ideal architectural floor is selected such that it represents each kind of functionality in the hospital, rather than being specific regarding purpose of utilization. This approach is required since the analyses to be performed in this work need to be independent from the architectural design especially in terms of floor masses. In consideration of this study, all the floor mass and stiffness values are identical.

Basic architectural details are provided in Table 2.4:

Table2.4: Architectural Details

Plan Dimensions	60.3 m (in x direction) 79.2 m (in y direction)
Span Length (in general)	8.5 m
Storey Height	4.6 m
Number of Stories/Total Building Height	15/ 69 m 10 / 46 m 5 / 23 m

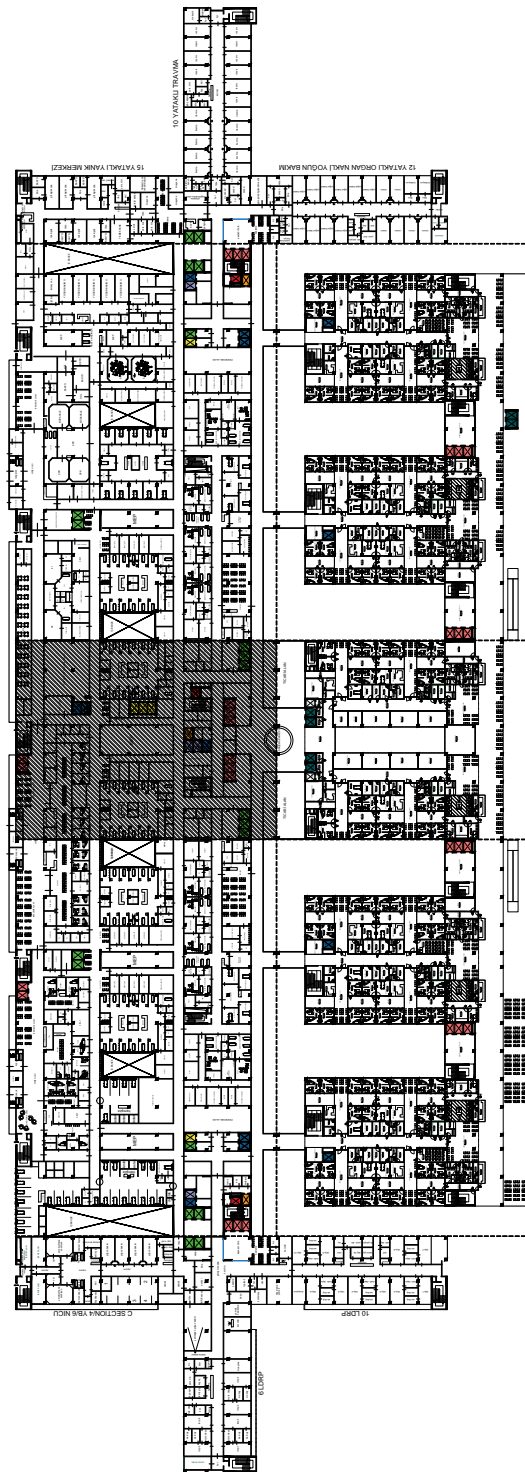


Figure 2.1: Key Plan of the Hospital Blocks

The block in the shaded region demonstrated in Figure 2.1 is used in the analyses. In Figure 2.2, analyzed block is given in detail.



[

Figure 2.2: Typical Architectural Plan of the Hospital Block

2.2 Structural Modeling

In this study, SWFB15 model is used as the basis set and the other three models, FB15, ISOSW15 and ISO15, are generated from SWFB15 model. Geometry of SWFB15 is modeled via Probina Orion 2013[25] packaged software as a fixed base system. Foundation of the building is not modeled since the main purpose of the analyses is to assess the superstructure behavior under seismic loads. Beams and columns are modeled by frame members. Modeling of shear walls are performed by using middle column model approach instead of meshed shell elements to avoid excessive duration of analysis. Due to the same reason, slab members are modeled as rigid diaphragms and the loads distributed on the slabs are uniformly distributed on the beam elements by Probina Orion 2013[25]. Structural design of the fixed base system is based on Turkish Earthquake Code 2007 (TEC 2007)[22] specifications.

Dead load of the members is automatically computed by the Probina Orion 2013[25] by the predefined unit weight of the concrete in the software. Live load arrangement is performed according to the functional utilization of the architectural spaces and in accordance with the regulations specified in Design Loads for Buildings (TS 498)[31] Code. Checkerboard pattern live load arrangement is also considered by the software Probina Orion 2013[25]. Partition walls lying on the beams are considered as dead load and distributed uniformly as line load on the beams. The ones distributed on the slab are considered as live load and added to the system as uniformly distributed to the corresponding slab area. Miscellaneous loading like wind, snow and soil pressure is not considered.

In this study, seismicity used as the input is assumed as being from a first degree seismic zone and site-specific. Requirements for buildings in a first degree seismic zone are satisfied per TEC 2007[22] and Turkish Reinforced Concrete Code (TS 500)[32] to the fixed base dual systems, namely, SWFB15, SWFB10 and SWFB5. Earthquake loading is carried out by both equivalent static lateral force procedures and mode superposition method to obtain dynamic increment coefficient needed to be applied to the analysis results from mode superposition method. In addition, check of high ductile dual system requirements as specified in 2.5.2 through 2.5.4 clauses in TEC 2007 is also satisfied. Based on the received percentage of the earthquake force by shear

walls in each direction, "Structural Behavior Factor", (R) is modified from 7 to 6.29 and 6.34 in two earthquake directions x and y, respectively.

For the moment frame systems FB15, FB10 and FB5, high ductility requirement from[22] is also achieved by a structural behavior factor R of 8 in both earthquake directions.

For the seismically isolated structural systems ISOSW15, ISO15, ISOSW10, ISO10, ISOSW5 and ISO5, isolators are modeled by making use of bilinear modeling. To model isolation units, two joint multi linear plastic link elements are used to represent the nonlinear behavior. For a preliminary assessment and comparison of efficiency between different structural systems having different number of floors, linear elastic response spectrum analysis is performed with upper bound ¹ characteristic values of the isolation units. effective values constituting of main seismic isolation design parameters, namely, effective stiffness (K_{eff}) and effective damping (ζ_{eff}). Design considerations of isolation units are further explained in section 2.4.2.3.

Analysis and assessment of the structural systems specified in 2.1 are performed through SAP2000 18 [9] software. Typical 3-dimensional visual materials from structural computer models are provided in Figure 2.3 and Figure 2.4.

¹ This concept is explained in section 1.1

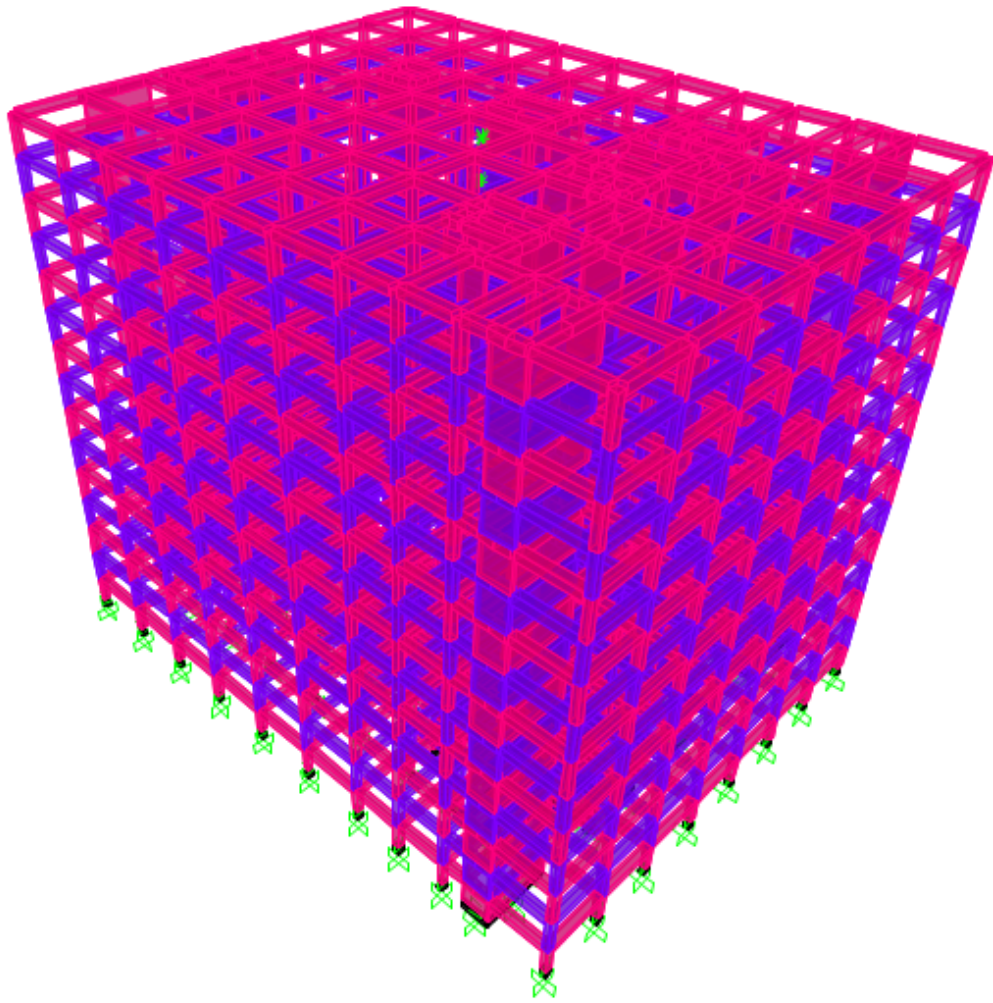


Figure 2.3: Typical 3D SAP2000 Model from a Seismically Isolated Dual System with 15 floors

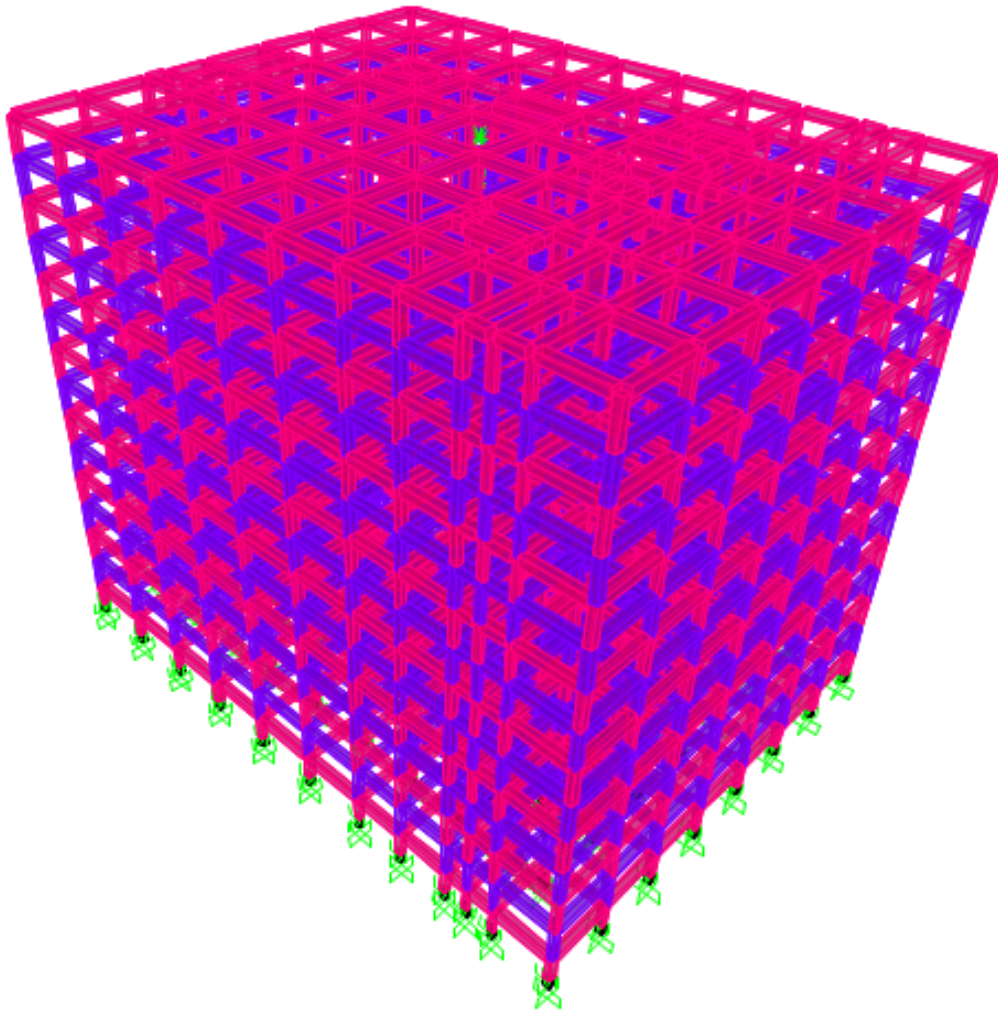


Figure 2.4: Typical 3D SAP2000 Model from a Seismically Isolated Moment Frame System with 15 floors

2.3 Seismicity

In all sets of four models, the seismic demand is adapted from a first degree seismic zone in Turkey. For linear response spectrum analyses, site-specific response spectra curve for Design Basis Earthquake (DBE) obtained for two different regions, namely, Izmir and Isparta to assess the structural behavior under different seismicity levels in similar periods. In both linear and nonlinear analyses procedures, DBE level earthquake is used to evaluate the seismic effects on the superstructure.

Site specific DBE level of response spectrum curve had been previously obtained from Probabilistic Seismic Hazard Assessment (PSHA). For fast nonlinear analysis, appropriate ground motion records are selected and scaled based on the site specific target spectrum. Criteria for ground motion selection and scaling is explained in Section 2.3.1. The site specific response spectra for Izmir and Isparta are given in Figure 2.5.

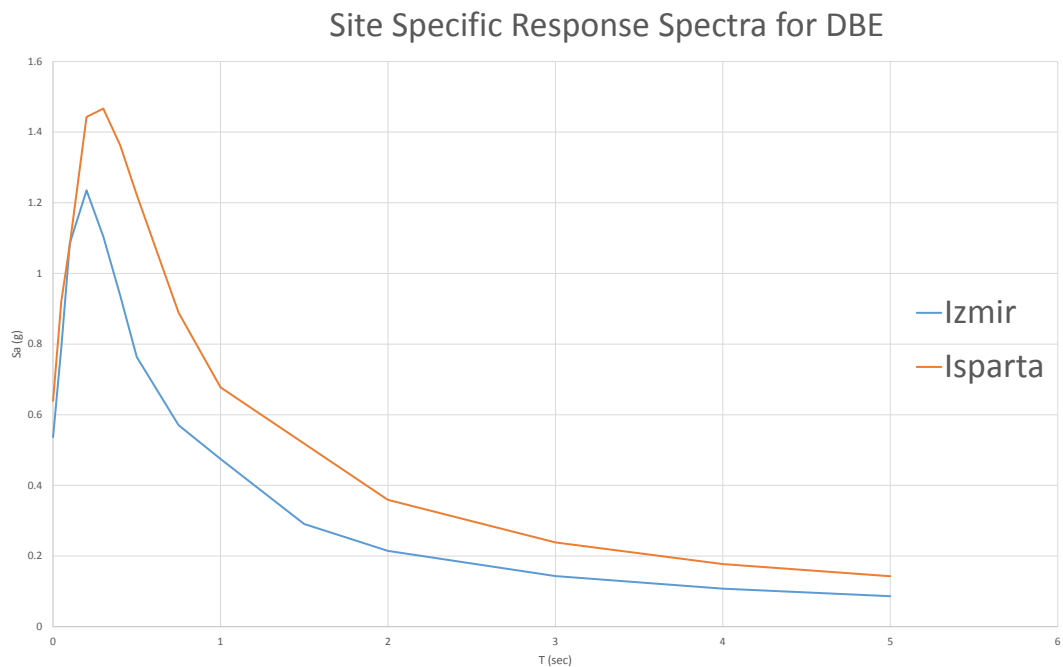


Figure 2.5: 5% Damped SRSS Site Specific Response Spectra (DBE) for Izmir and Isparta

Spectral acceleration values for characteristic periods, T (sec) are provided in Table 2.5 and Table 2.6 in terms of g in (m/s^2)

Table2.5: 5% Damped SRSS Spectral Acceleration Values from Site Specific PSHA for Izmir

T(sec)	Sa (g)
0	0.53651
0.05	0.79144
0.1	1.08498
0.2	1.23526
0.3	1.10448
0.4	0.93886
0.5	0.76297
0.75	0.57031
1	0.47476
1.5	0.29094
2	0.21463
3	0.14339
4	0.10777
5	0.08632

Table2.6: 5% Damped SRSS Spectral Acceleration Values from Site Specific PSHA for Isparta

T(sec)	Sa (g)
0	0.63908
0.05	0.92209
0.1	1.08186
0.2	1.443
0.3	1.4664
0.4	1.3637
0.5	1.22213
0.75	0.88881
1	0.67756
2	0.35906
3	0.23868
4	0.17732
5	0.14287

2.3.1 Ground Motion Selection and Scaling for the Targeted DBE Site Specific Response Spectrum for Izmir

For response history analyses, a total number of 7 real ground motion is selected for the seismicity level of Izmir.

Based on the site specific fault mechanism, earthquake magnitude, shear wave velocity (V_{s30}) tectonic regime and fault distance properties, appropriate real ground motion histories are selected. Site specific seismicity parameters for Izmir are provided in the Appendix A. For Izmir site, majority of the focal mechanism is formed by normal faults and strike-slip faults [11]. During ground motion selection procedure, candidate accelerograms are sought to meet the soil type and fault mechanism criteria. However, in the presence of fewness in available real ground motions, fault mechanism criteria is relaxed [7]. Note also that no records containing pulse are selected as eligible. Selected ground motion records are presented in Table 2.7.

Table 2.7: Selected Ground Motion Records for Time History Analysis Procedure

Record Name	Earthquake Name	Magnitude	Joyner-Boore Distance (km)	V_{s30} (m/s)	Style of Faulting	Scale Factor
0015	Kern County	7.36	38.42	385	Reverse	1.93
0762	Loma Prieta	6.93	39.32	368	Reverse	2.70
0807	Loma Prieta	6.93	47.41	401	Reverse	3.96
1015	Northridge-01	6.69	47.79	405	Reverse	4.32
1633	Manjil,Iran	7.37	12.56	724	Strike-Slip	0.61
2714	Chi-Chi,Taiwan-04	6.2	38.11	442	Strike-Slip	2.71
3503	Chi-Chi,Taiwan-06	6.3	29.64	475	Reverse	2.40

Through Figures 2.6, 2.11, 2.14, 2.17, 2.20, 2.23 and 2.26, scaled SRSS spectra of ground motion records selected obtained via SeismoSignal[27]. Scaling of the ground motions comply with the criteria specified in [5].

Individual time histories used in response history analyses are also provided through Figures 2.7 to 2.25.

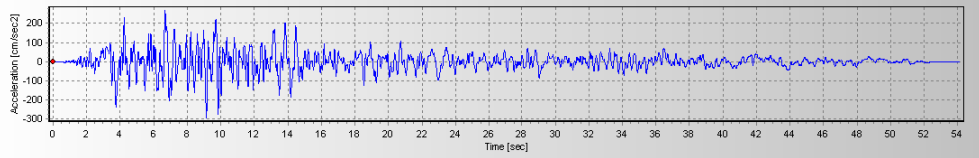


Figure 2.7: GM: 0015 in x direction

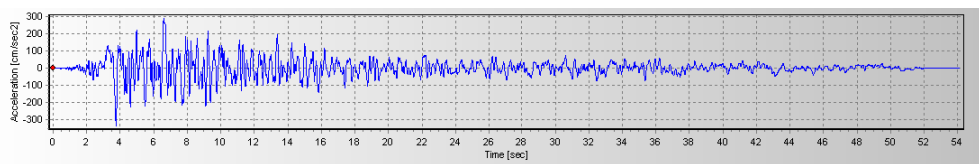


Figure 2.8: GM: 0015 in y direction

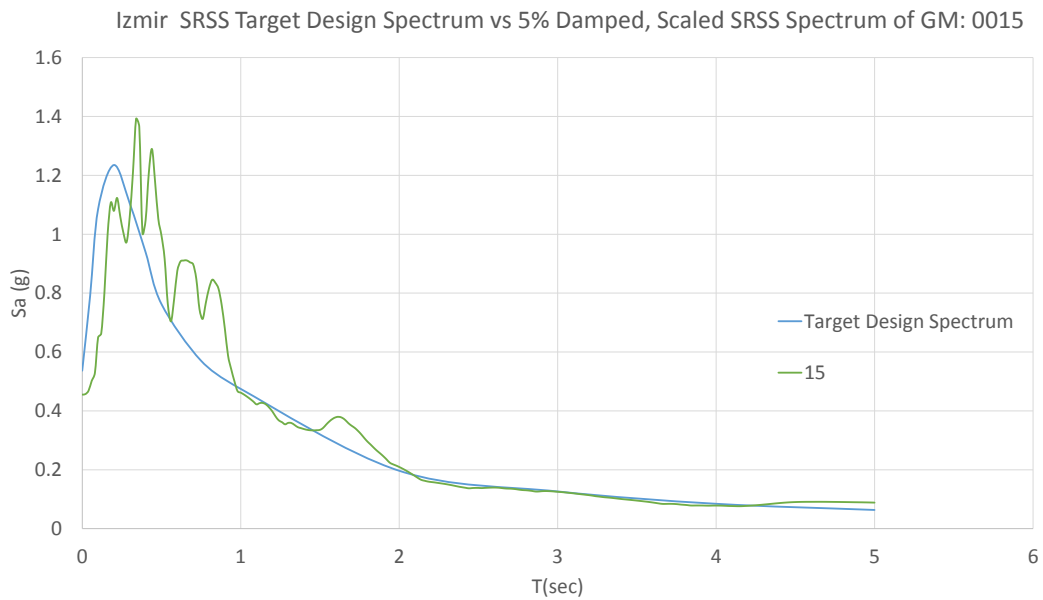


Figure 2.6: Izmir SRSS Target Design Spectrum vs 5% Damped SRSS Spectrum of GM: 0015

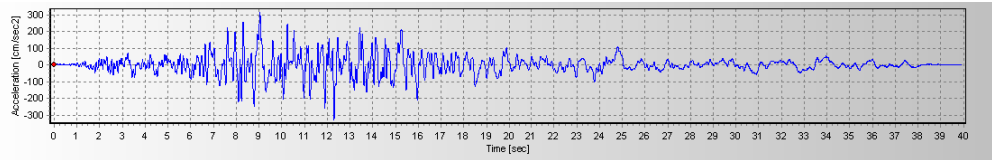


Figure 2.9: GM: 0762 in x direction

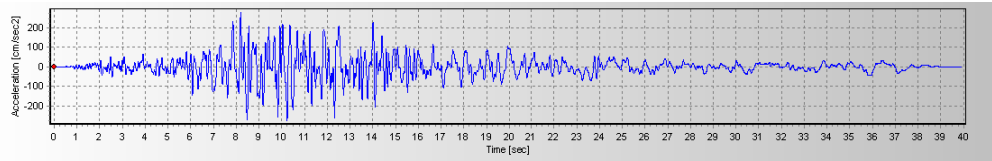


Figure 2.10: GM: 0762 in y direction

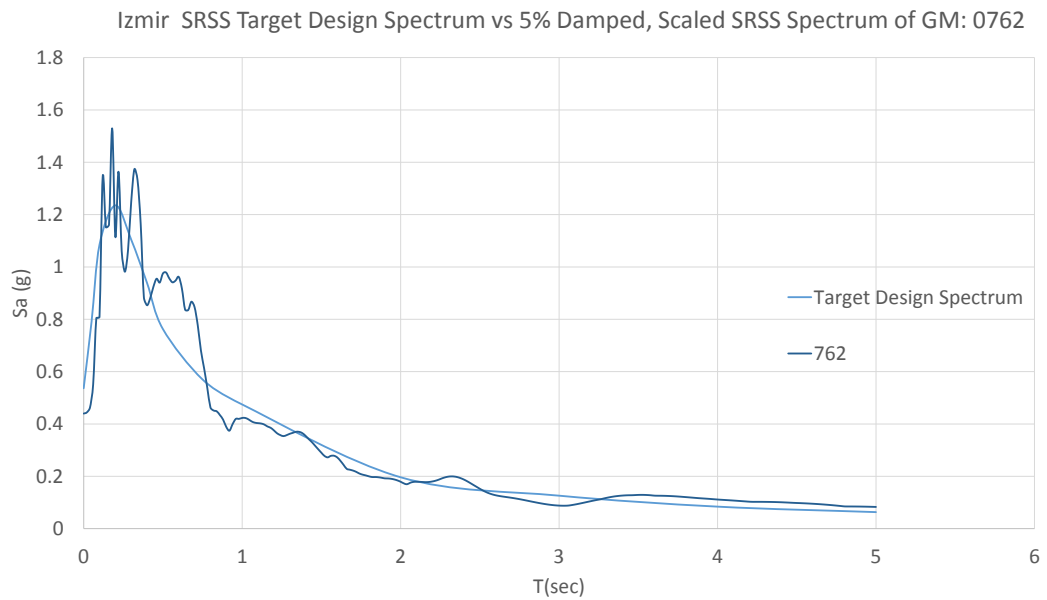


Figure 2.11: Izmir SRSS Target Design Spectrum vs 5% Damped SRSS Spectrum of GM: 0762

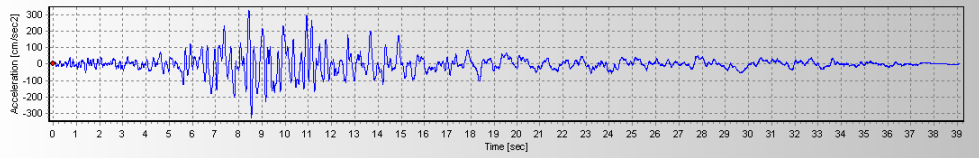


Figure 2.12: GM: 0807 in x direction

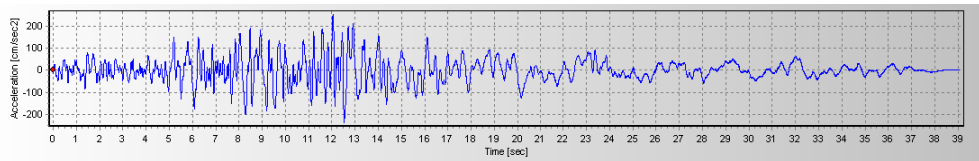


Figure 2.13: GM: 0807 in y direction

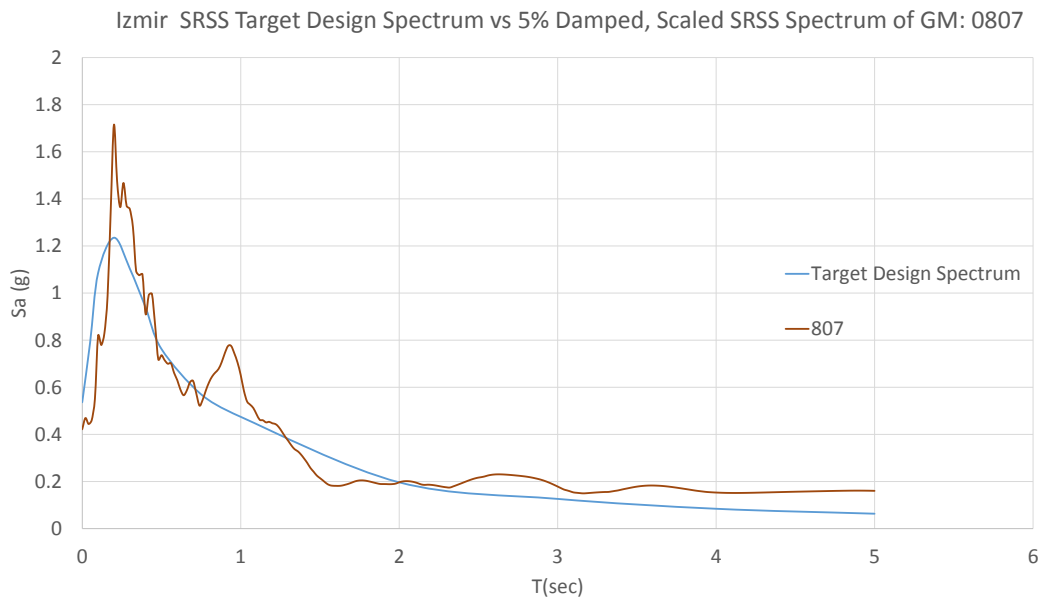


Figure 2.14: Izmir SRSS Target Design Spectrum vs 5% Damped SRSS Spectrum of GM: 0807

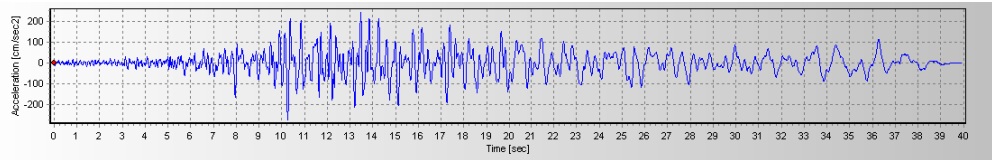


Figure 2.15: GM: 1015 in x direction

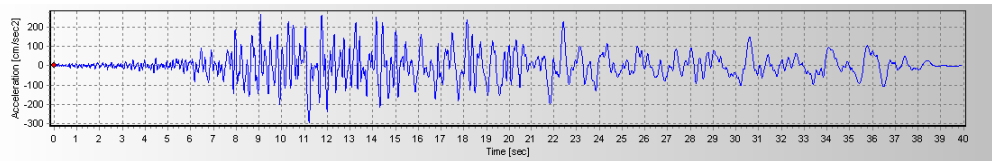


Figure 2.16: GM: 1015 in y direction

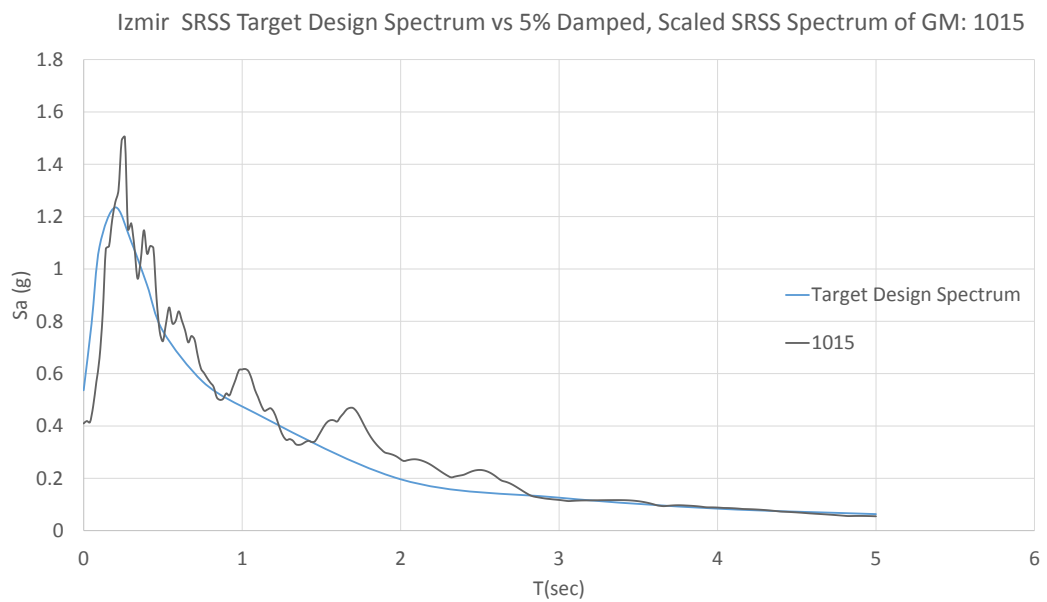


Figure 2.17: Izmir SRSS Target Design Spectrum vs 5% Damped SRSS Spectrum of GM: 1015

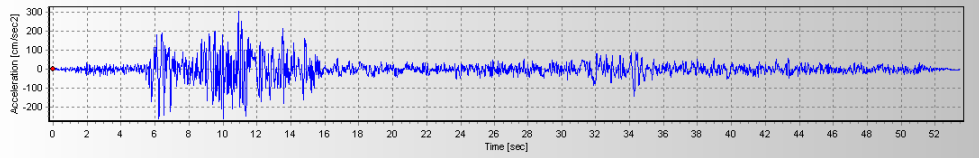


Figure 2.18: GM: 1633 in x direction

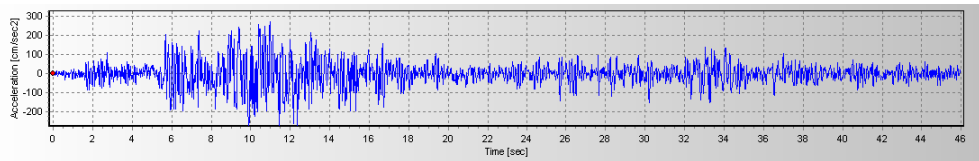


Figure 2.19: GM: 1633 in y direction

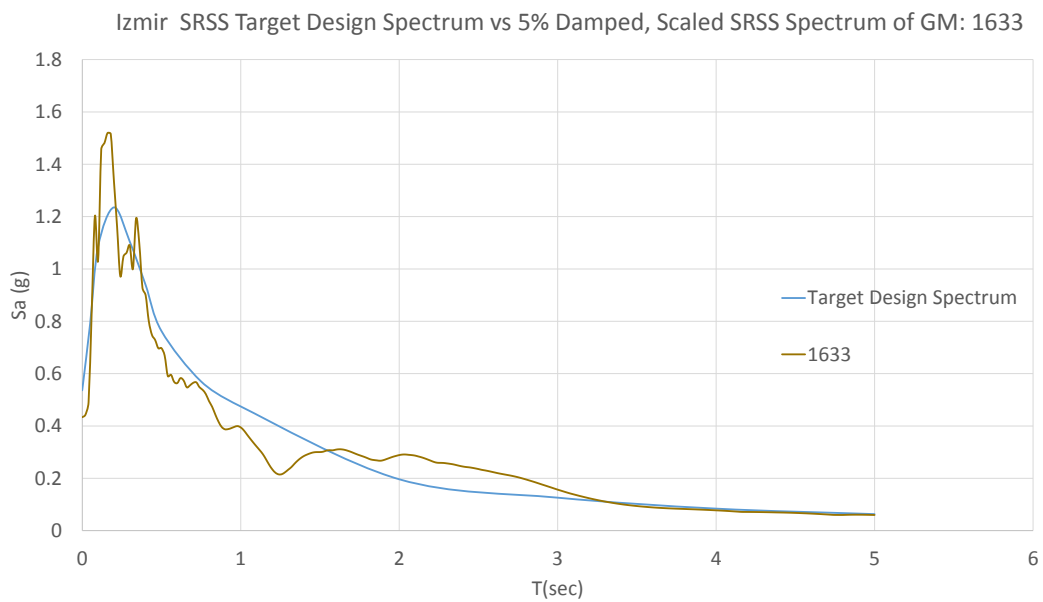


Figure 2.20: Izmir SRSS Target Design Spectrum vs 5% Damped SRSS Spectrum of GM: 1633

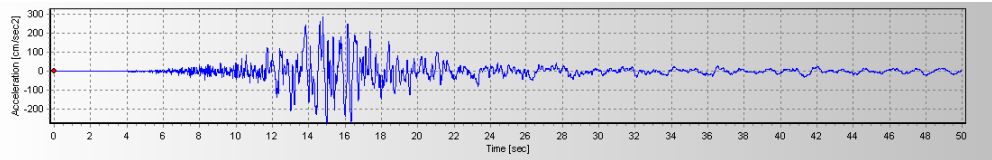


Figure 2.21: GM: 2714 in x direction

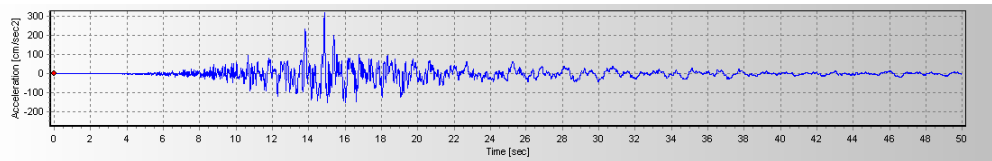


Figure 2.22: GM: 2714 in y direction

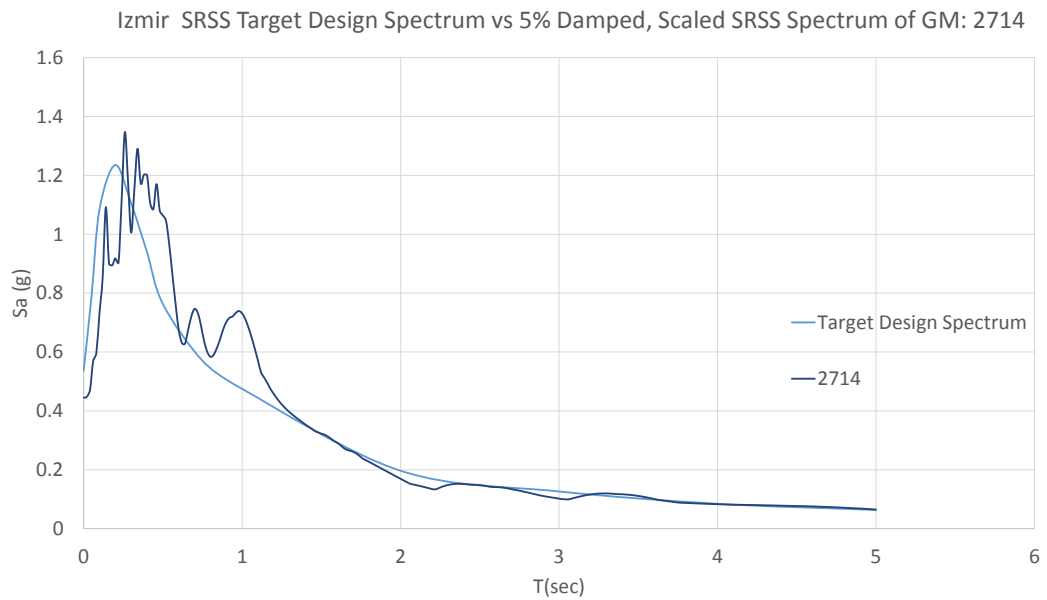


Figure 2.23: Izmir SRSS Target Design Spectrum vs 5% Damped SRSS Spectrum of GM: 2714

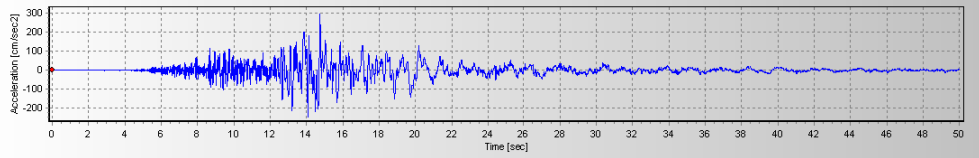


Figure 2.24: GM: 3503 in x direction

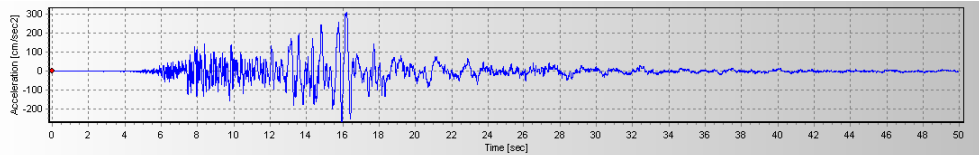


Figure 2.25: GM: 3503 in y direction

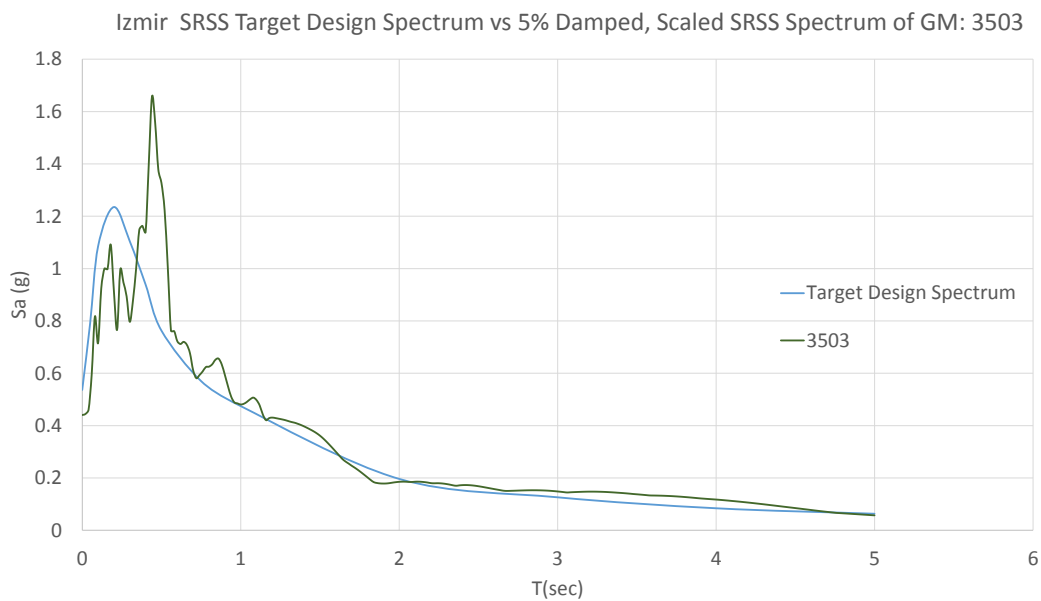


Figure 2.26: Izmir SRSS Target Design Spectrum vs 5% Damped SRSS Spectrum of GM: 3503

5% damped SRSS (scaled) response spectra of all 7 ground motion records are demonstrated in Figure 2.27.

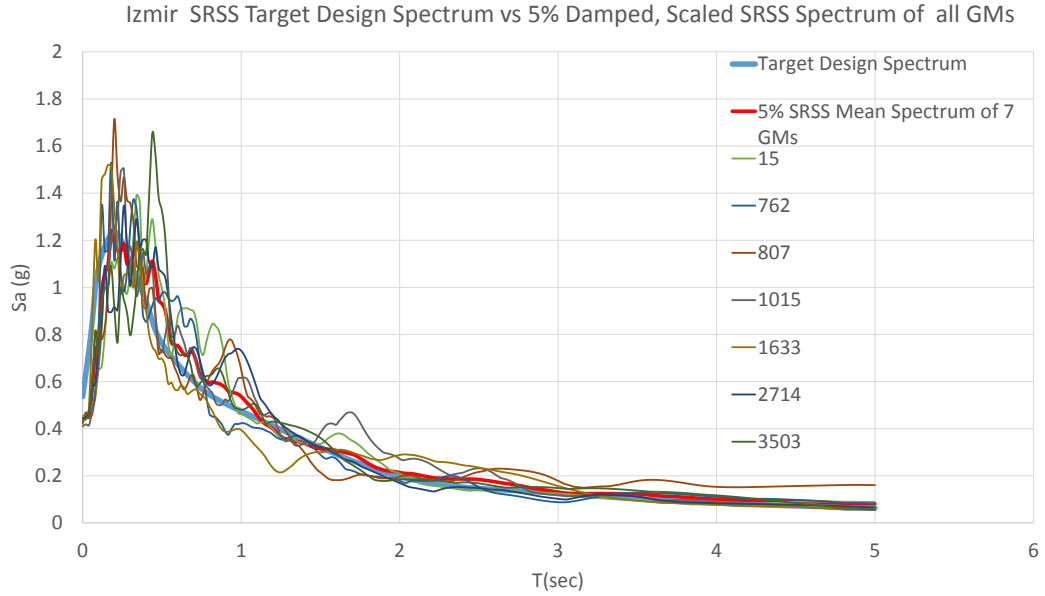


Figure 2.27: Izmir SRSS Target Design Spectrum vs 5% Damped SRSS Spectrum of all GMs

Mean of 5% damped SRSS (Square Root of Sum of Squares) spectra is constructed to fit the targeted site specific spectrum. As it is required in [5], each pair of motions selected were scaled such that in the period range from $0.5T_d$ to $1.25T_m$, mean of the SRSS spectra from all pair of horizontal components did not fall below the corresponding spectral acceleration value of the site specific spectrum to be used in the design.

Based on [5], T_d corresponds to effective period of the seismically isolated structure at the design displacement and T_m is the effective period of the seismically isolated structure at the maximum displacement. Design displacement and maximum displacement are resulted in the action of DBE (Design Basis Earthquake) and MCE (Maximum Considered Earthquake), respectively. DBE is the earthquake level having a probability of occurrence of 10% in 50 years and MCE that of 2% in 50 years. In this study, T_d and T_m are equal to 3sec and 3.68sec, respectively. Based on the scaling criteria specified in [5], starting point of scaling range is 1.5 sec ($0.5T_d$) and ending point of it equals to 4.6 sec ($1.25T_m$).

5% damped SRSS mean spectrum curve of 7 ground motions and interested period range regarding scaling criteria are demonstrated in Figure 2.28:



Figure 2.28: Izmir 5% Damped SRSS Target Spectrum vs 5% Damped SRSS Mean Spectrum of 7 GMs

To evaluate the seismic performance of the superstructure, DBE level is employed. MCE level is used in the capacity design of isolation units. Isolators are designed to withstand a higher seismic demand as compared to the superstructure. The reason is that in the case of an earthquake event exceeding the design basis earthquake level, isolation units should ensure the structural stability and for the superstructure, life safety. In the scope of this thesis work, the main focus is given to superstructure behavior, therefore the seismicity is based on DBE level. MCE level earthquake considerations are out of the scope of this work. In section 2.4.2.3, main seismic isolation design parameters take place based on DBE level earthquake.

2.4 Analysis and Design of Structural Systems

The main goal of the analyses of four different system is to compare the variation of interstorey drift and floor accelerations through each floor. For this purpose, analy-

sis methods mentioned in subsection 2.4.1, Table 2.8 are employed for the different structural systems described in 2.1:

2.4.1 Method of Analyses

The efficiency in reduction of seismic forces via seismic isolation design approach will be assessed by linear elastic response spectrum analysis procedures.

To explore the accuracy of the linear elastic response spectrum analysis method, Fast Nonlinear Analysis (FNA) will also be performed for one of the seismically isolated systems (ISO15) as well as to include nonlinear characteristics of the seismic isolation units.

FNA is selected rather than Nonlinear Time History Analysis (NTHA) due to prolonged computing time resulted in NTHA. In [34], the author states that the computational speed of FNA method as compared to the traditional "brute force"[34] method of nonlinear time history analysis is found as several magnitudes faster in many nonlinearity cases. Interested readers may refer to the fundamental equilibrium equations[34] which provide efficiency in computing time specified. As it is also mentioned in [34], certain types of large strains, as in the case of the seismic isolation modeled by link members, can be assumed as a lumped nonlinear element in the system by applying FNA method. Note that in seismically isolated systems, all the nonlinearity is limited and restraint to the link members such that the superstructure remains elastic, which is the main goal. Therefore, FNA can be an efficient way to assess the superstructure by the only nonlinearity in link members representing isolation units in modal space. For this reason, the analysis can also be named as a nonlinear modal time history analysis. Based on the study of Siller [29], the analysis performed in modal space based on modal parameters, which mainly are eigenvectors and eigenvalues, requires a relatively small number of modes to regenerate the response of the system. In addition, the orthogonality of the eigenvectors allows a given degree of freedom to be fully described by its own eigenvector, which reduces even more algebraic burden. According to Siller, one disadvantage of making use of modal coordinates may be that "the modal responses have little physical meaning in case of an issue during an updating or identification analysis, in which the differences

between an experimental model and its theoretical counterpart must be conciliated" [29]. In this thesis work, FNA is employed to assess the performance difference of seismically isolated systems having different number of floors by including nonlinear characteristics of isolation units, which is not taken into consideration in linear elastic response spectrum analysis assessment.

In Table 2.8, method of analyses used in this study are tabulated.

Table2.8: Methods of Analyses

SWFB15, SWFB10, SWFB5	Linear Response Spectrum Analysis (RSA)
FB15, FB10, FB5	Linear Response Spectrum Analysis (RSA)
ISOSW15, ISOSW10, ISOSW5	Linear Response Spectrum Analysis (RSA)
ISO10, ISO5	Linear Response Spectrum Analysis (RSA)
ISO15	Linear Response Spectrum Analysis (RSA) Fast Nonlinear Analysis (FNA)

2.4.1.1 Structural Design

In fixed base dual system with 15 floors (SWFB15), design of structural members are performed via Probrina Orion 2013 package software. Dimensions of main structural members in SWFB15 is directly adopted to the other models, namely, FB15, ISOSW15, ISO15 with subtle changes in the positioning of beams and columns having smaller dimensions around elevator shafts, staircases and mechanical or electrical shaft regions which previously had shear walls in SWFB15 model. Structural models with 10 and 5 floors are generated from the ones with 15 floors without changing the member dimensions. In the structural systems specified in Table 2.1, structural member dimensioning is performed based on the most critical load combinations based on Turkish Reinforced Concrete Building Code (TS 500)[32].

In Table 2.9, structural member sizes are summarized:

Table2.9: Structural Member Sizes in SWFB15, ISOSW15, ISO15 and FB15

Column Dimensions (in general)	80 cm X 80 cm
Beam Dimensions (in general)	60 cm (width) 70 cm (height)
Slab Thickness	20 cm
Shear wall Thickness	40 cm

Design criteria of each structural system will be explained in Sections 2.4.2.1,2.4.2.2 and 2.4.2.3.

2.4.2 Conventional Design Approach

To investigate the seismic performance levels under the seismicity levels specified in 2.3 for the selected hospital block, conventional design approach is also employed to compare with the original seismically isolated dual system design. Analyzing inter-storey drift ratios and floor accelerations by making use of the analysis methods specified in Table 2.8, results from conventional design approach is obtained. Comparison of conventional design approach and seismically isolated dual system is provided in Chapter 3 in detail.

2.4.2.1 Fixed Base Dual Systems (SWFB15, SWFB10, SWFB5)

In this case, the structural system is selected as dual system considering conventional design approach. Being in the first seismic zone, the structural system is arranged to satisfy high ductility level. Shear walls, which are main lateral load carrying systems, are oriented appropriately based on the architectural allowances. To prevent coupling behavior in x and y direction, an additional shear wall apart from the ones presumed by architectural layout is positioned in the upper left edge of the plan. All the shear walls are 40 cm in width and in various length and configuration based on the architectural layout. Most of the shear walls are positioned around stairs, elevator shafts and mechanical and/or electrical shafts. Typical formwork plan is demonstrated in Figure 2.29. In structural design of fixed base dual systems, targeted seismic perfor-

mance level is selected as high ductility. In that manner, strong beam weak column approach is applied and the system is designed accordingly. Structural design criteria for the reinforced concrete system is based on Turkish Earthquake Code 2007 (TEC 2007)[22] and Turkish Building Code (TS 500)[32]. Building Importance Factor, I is taken as 1.5 since the type of the building is hospital. Since the basic idea in seismic isolation approach is to extend the fixed base fundamental period of the structure to decrease spectral acceleration values received by the structure, first three fundamental period of the fixed base dual system are analyzed meticulously. Due to the fact that the plan dimension of the analyzed block in y direction is longer than in x direction, strong axis of the structural system is y axis. Therefore, first fundamental mode of the system is obtained as being in x-direction. The second fundamental mode is in y direction, and the third fundamental mode behavior occurred as torsional. These fundamental modes are observed to be well separated, ensuring the desired uncoupled behavior in two horizontal directions.

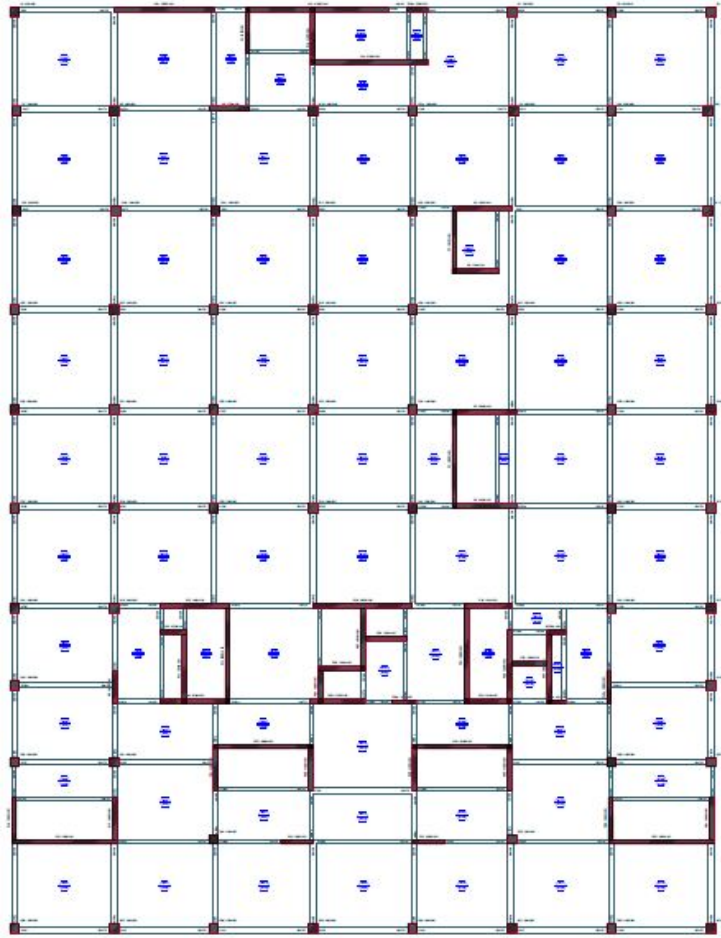


Figure 2.29: Typical Formwork Plan for SWFB15

In Figure 2.30, effect of shear walls to the structural deformation of a moment frame system is illustrated. In a moment frame system, top deflection is not that much of a shear walled frame system under lateral forces. However, most of the deflection is around mid-height. On the other hand, a shear walled system can be regarded as a vertical cantilever without moment framing, and most of the lateral deflection is at the top, whereas there is less deformation around bottom and mid-height compared to moment frame system. Therefore, a fair combination of moment frame and shear walled frame system is mutually beneficial regarding lateral deflections.

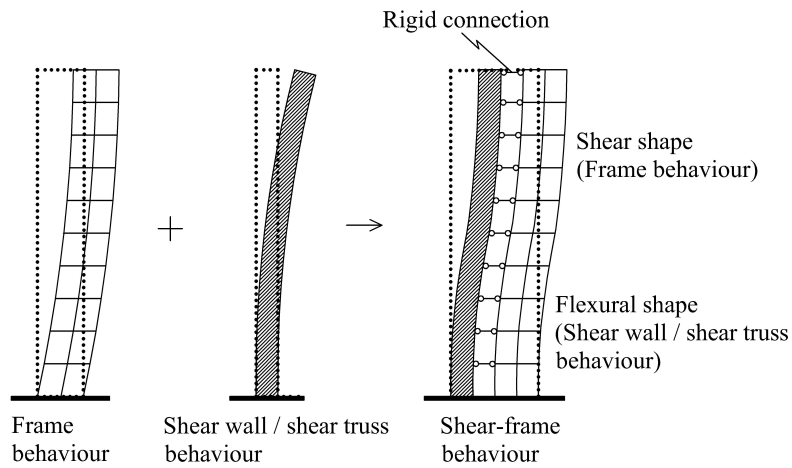


Figure 2.30: Behaviour of Moment Frame Systems and Shear Walled Frame Systems[20]

2.4.2.2 Fixed Base Moment Frame Systems (FB15, FB10, FB5)

Fixed base moment frame systems are also designed as being highly ductile with a structural behavior factor of 8 in both earthquake directions x and y. Ductility requirements by TEC 2007 is also applied to the fixed base moment frame systems as specified in 2.4.2.1. Building Importance Factor, I is also taken as 1.5 for the fixed base moment frame systems. Typical frame plan is given in Figure 2.31:

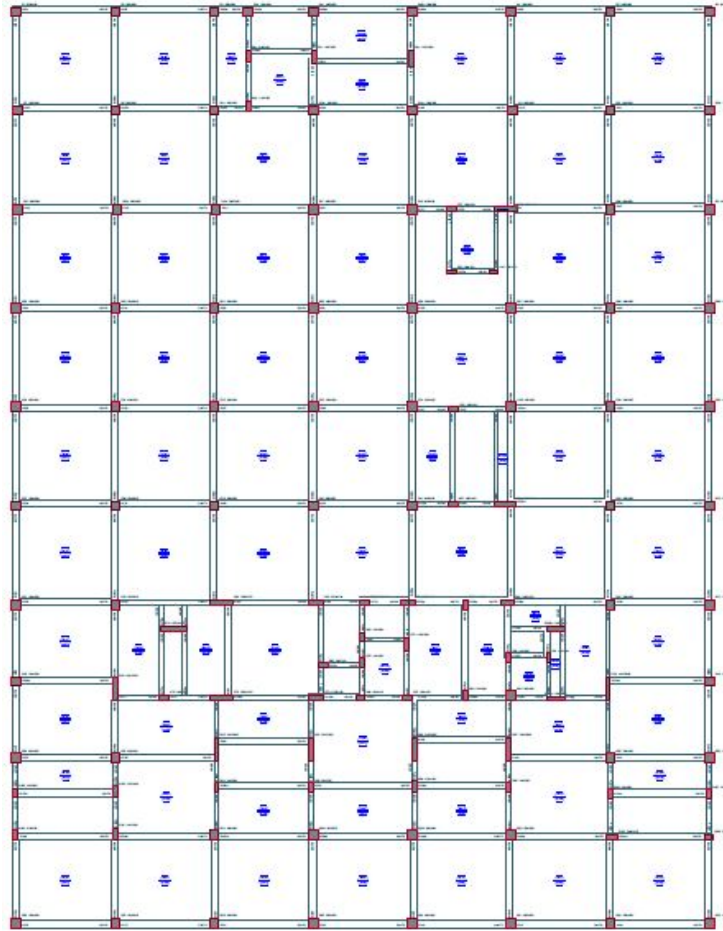


Figure 2.31: Typical Formwork Plan for FB15

2.4.2.3 Seismic Isolation Design Approach

First of all, as it is mentioned in [5], Building Importance Factor, I is taken as 1. In all of the seismically isolated models, the isolation level is formed in foundation level. In real application of seismic isolation, isolation units are linked to each other via a rigid slab/foundation or axially rigid beams ensuring isolation units to move together. Therefore, separation points of seismic isolation units and the superstructure is constrained by "Body" definition of SAP2000[9] for both translational and rotational directions to achieve diaphragm behavior just above the isolators.

For the vertical structural members, type of seismic isolator to be used is based on the

vertical load on the corresponding member. For the seismically isolated dual systems, rigidity of the superstructure played a big role, such that when the system is analyzed for a seismic input, the lateral displacement of the isolators under the shear walls is observed as relatively low compared to the ones of columns.

In linear response spectrum analysis procedures, effective values of the isolation units are used. Basic effective values considered are upper bound (UB) effective stiffness and effective damping values of the targeted seismic isolation design. Although the effective damping is theoretically calculated as 40.43%, effective damping of each system is limited to 30% to exclude higher mode effects in single degree of freedom analysis. For this purpose, maximum allowable effective damping is specified as 30% in [1]. Corresponding damping coefficients for percentage effective damping values are described in Table 1.9 from [5]. Nonlinear behavior of seismic isolation units are also taken into consideration through Fast Nonlinear Analysis (FNA) procedure. Seismic isolator characteristics are specified in Table 2.11 and Table 2.12. The target performance level of each structural system having different number of floors is the same for all systems. This approach is adopted for the sake of comparability of inter-storey drift ratio and peak floor accelerations (among different systems) as being the only changing parameters.

As it is explicitly known, fixed base period of each different system having different number of floors is different.

In Table 2.10, fixed base periods of each conventional system are given.

Table 2.10: Fixed Base Period (T_{fix}) of the Conventional Systems

Fixed Base System	Fixed Base Period (T_{fix}) (sec)
SWFB15	1.47
SWFB10	0.85
SWFB5	0.33
FB15	2.18
FB10	1.43
FB5	0.70

As it is stated in Tables 2.11 and 2.12, isolated period of each system is set to 3sec. For Izmir, undamped spectral acceleration value corresponding to 3 sec is around 0.14g and for Isparta 0.24g. By applying a fair reduction for damping of the device around 30% for upper bound isolator characteristics, the damping coefficient from Table 1.9 [5] corresponds to a value of 1.7. Applying a damping reduction to the spectral acceleration values at 3sec period by the coefficient equal to 1.7 ends up with spectral acceleration values of 0.08g for Izmir and 0.14g for Isparta. In order not to exceed the maximum allowed floor acceleration value of 0.2g, 3 sec target isolation period found to be as appropriate.

Table2.11: Target Isolator Performance for Izmir (UB)

Isolation Period (T_{iso}) (sec)	Calculated UB Isolation Displacement (d_{iso}) (cm)
3.00	18.9

Table2.12: Target Isolator Performance for Isparta (UB)

Isolation Period (T_{iso}) (sec)	Calculated UB Isolation Displacement (d_{iso}) (cm)
3.00	31.4

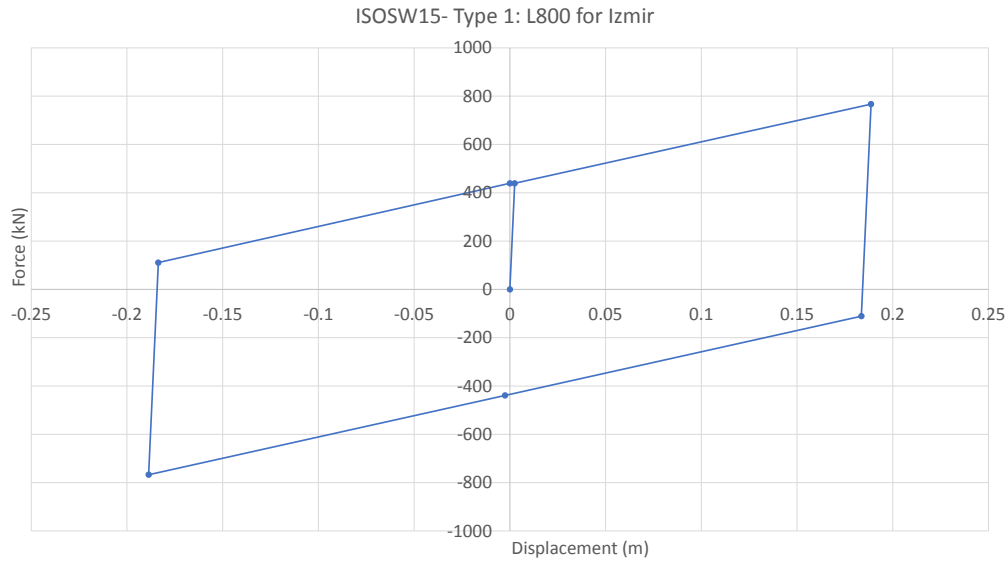


Figure 2.32: ISOSW15-Nonlinear UB Isolation Characteristics of Type 1: L800, Izmir

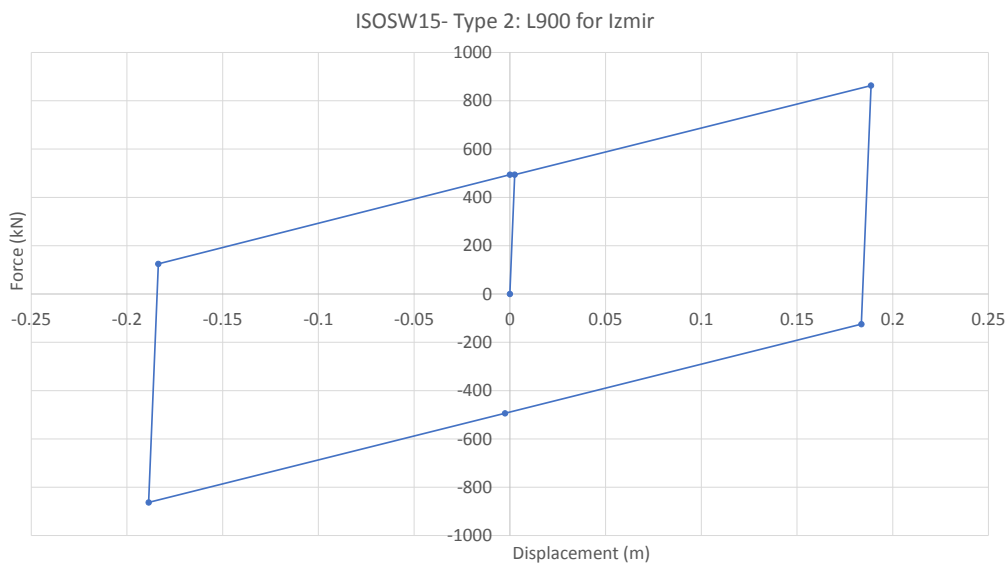


Figure 2.33: ISOSW15-Nonlinear UB Isolation Characteristics of Type 2: L900, Izmir

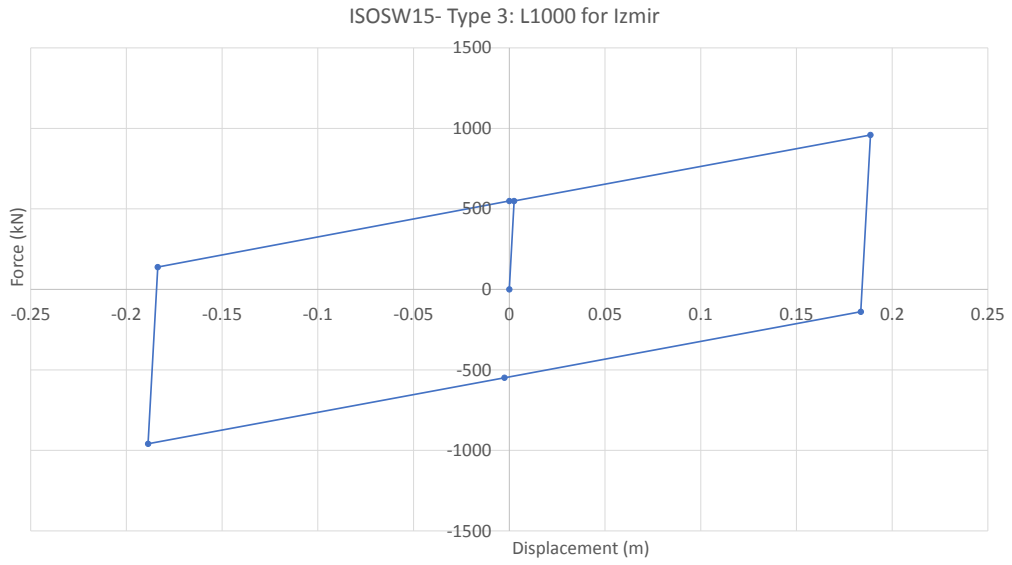


Figure 2.34: ISOSW15-Nonlinear UB Isolation Characteristics of Type 3: L1000, Izmir

Table2.13: Linear Isolator Parameters for ISOSW15, Izmir & Isparta

Isolator Type	Maximum Vertical Load (kN)	Effective Stiffness (K_{eff}) (kN/m)	Effective Damping (ζ_D) (%)	Damping Coefficient B_D [5]
1	8000	3578	40.43	1.7
2	9000	4024	40.43	1.7
3	10000	4471	40.43	1.7

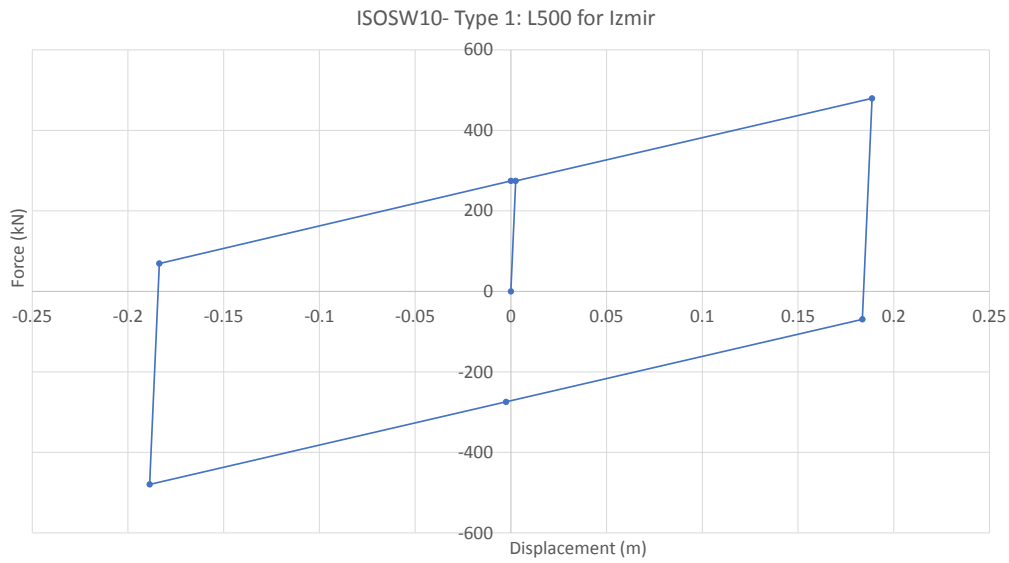


Figure 2.35: ISOSW10-Nonlinear UB Isolation Characteristics of Type 1: L500, Izmir

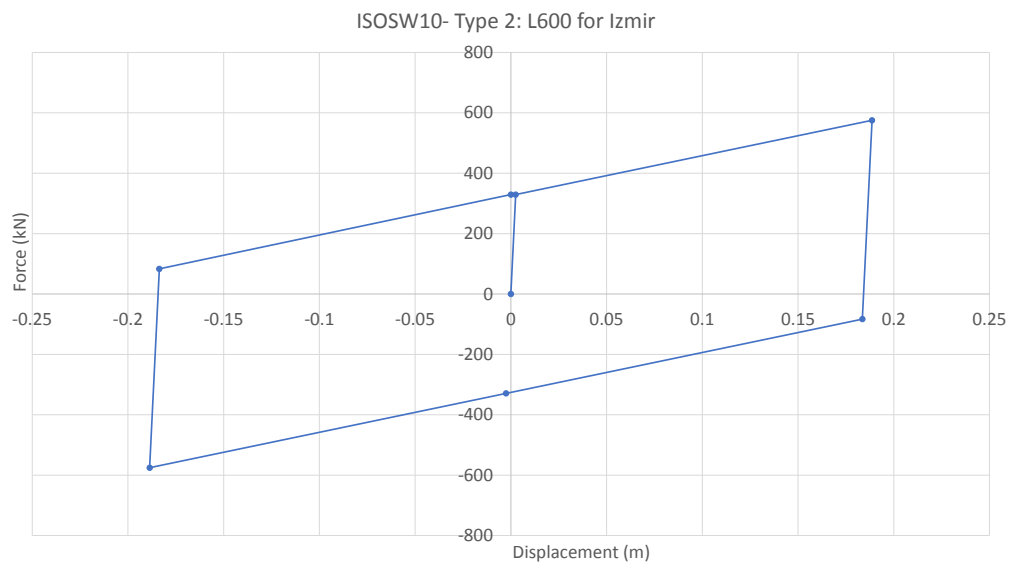


Figure 2.36: ISOSW10-Nonlinear UB Isolation Characteristics of Type 2: L600, Izmir

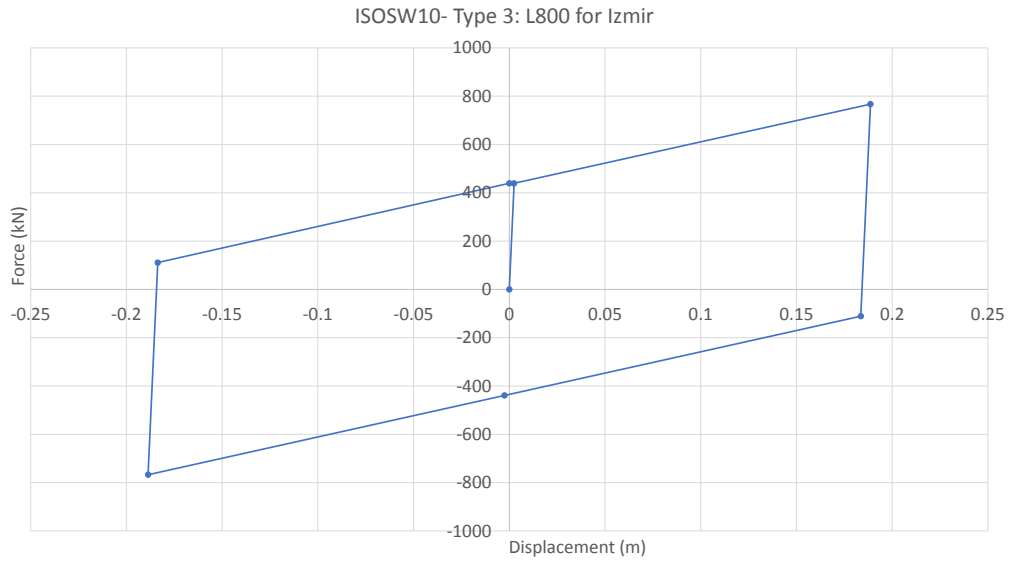


Figure 2.37: ISOSW10-Nonlinear UB Isolation Characteristics of Type 3: L800, Izmir

Table2.14: Linear Isolator Parameters for ISOSW10, Izmir & Isparta

Isolator Type	Maximum Vertical Load (kN)	Effective Stiffness (K_{eff}) (kN/m)	Effective Damping (ζ_D) (%)	Damping Coefficient B_D [5]
1	5000	2235	40.43	1.7
2	6000	2683	40.43	1.7
3	8000	3578	40.43	1.7

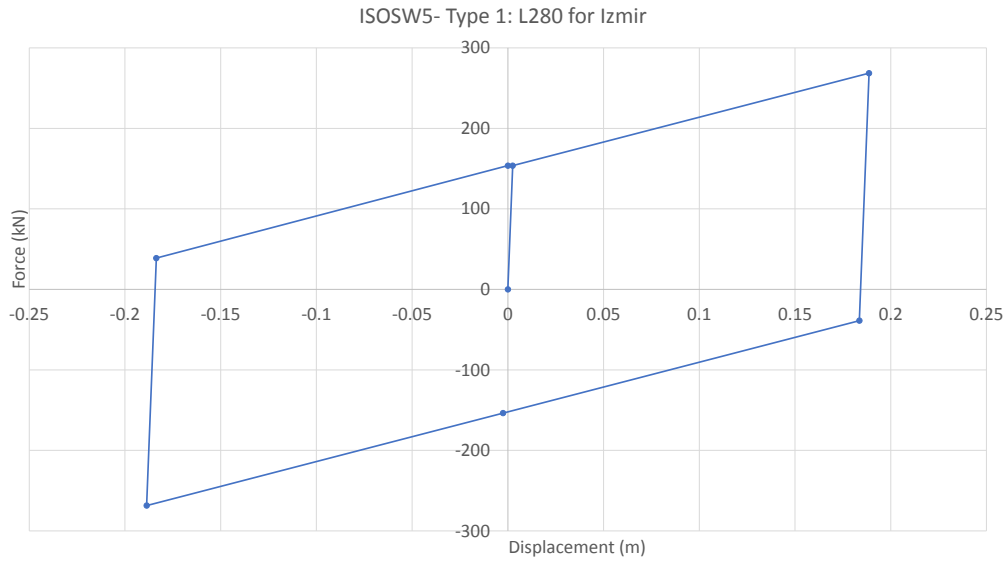


Figure 2.38: ISOSW5-Nonlinear UB Isolation Characteristics of Type 1: L280, Izmir

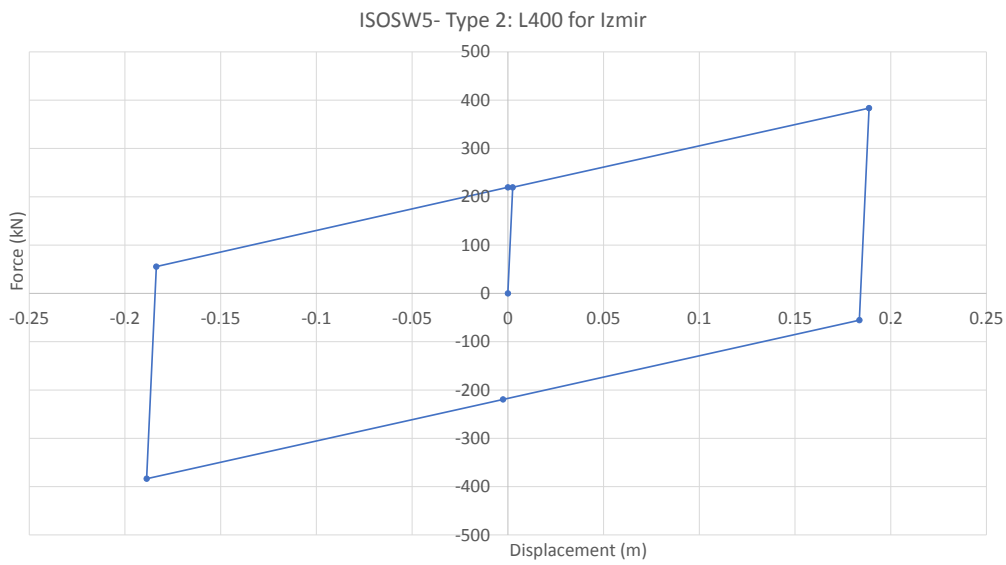


Figure 2.39: ISOSW5-Nonlinear UB Isolation Characteristics of Type 2: L400, Izmir

Table 2.15: Linear Isolator Parameters for ISOSW5, Izmir & Isparta

Isolator Type	Maximum Vertical Load (kN)	Effective Stiffness (K_{eff}) (kN/m)	Effective Damping (ζ_D) (%)	Damping Coefficient B_D [5]
1	2800	1252	40.43	1.7
2	4000	1789	40.43	1.7

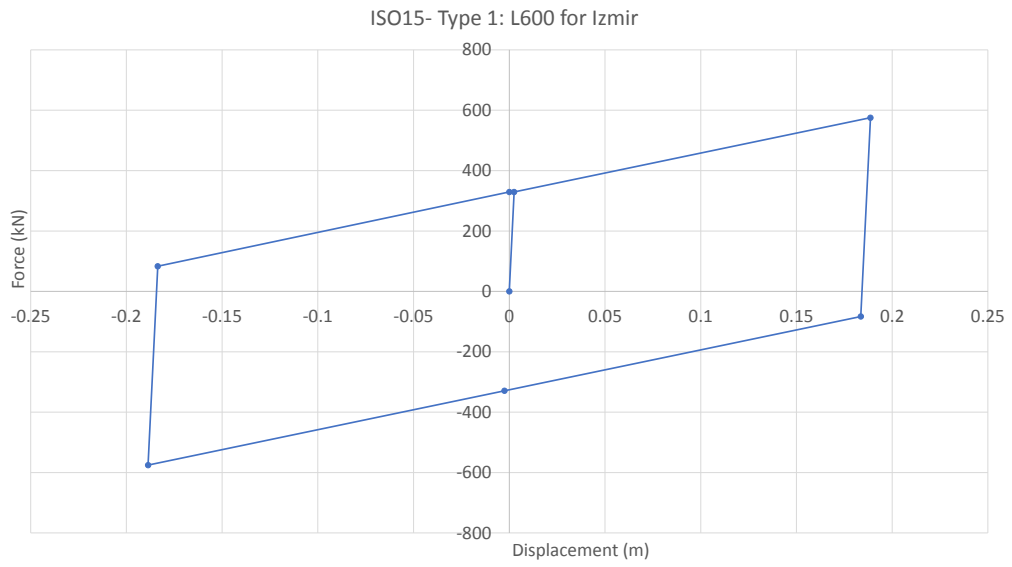


Figure 2.40: ISO15-Nonlinear UB Isolation Characteristics of Type 1: L600, Izmir

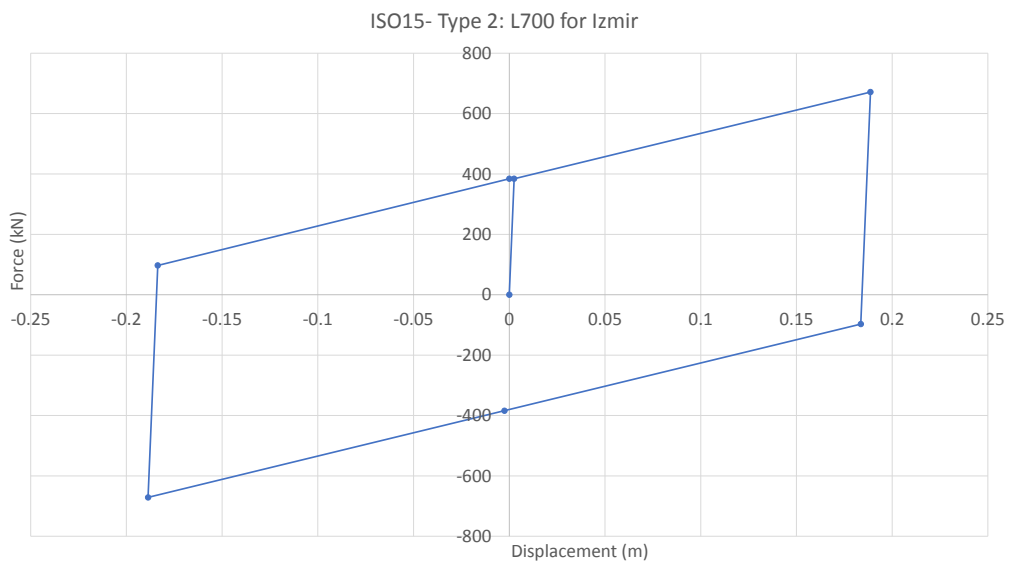


Figure 2.41: ISO15-Nonlinear UB Isolation Characteristics of Type 2: L700, Izmir

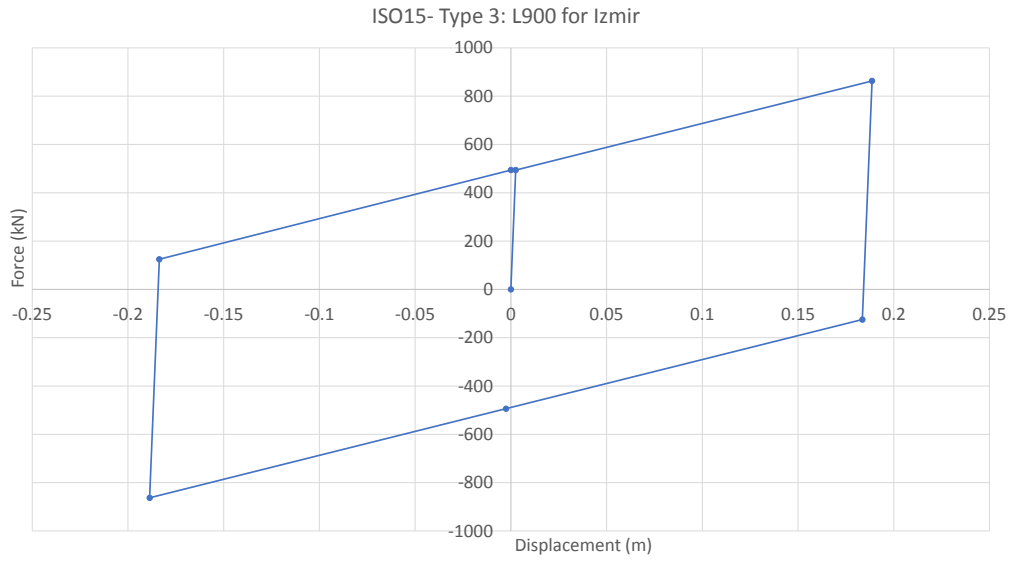


Figure 2.42: ISO15-Nonlinear UB Isolation Characteristics of Type 3: L900, Izmir

Table2.16: Linear Isolator Parameters for ISO15, Izmir & Isparta

Isolator Type	Maximum Vertical Load (kN)	Effective Stiffness (K_{eff}) (kN/m)	Effective Damping (ζ_D) (%)	Damping Coefficient B_D [5]
1	6000	2683	40.43	1.7
2	7000	3130	40.43	1.7
3	9000	4025	40.43	1.7

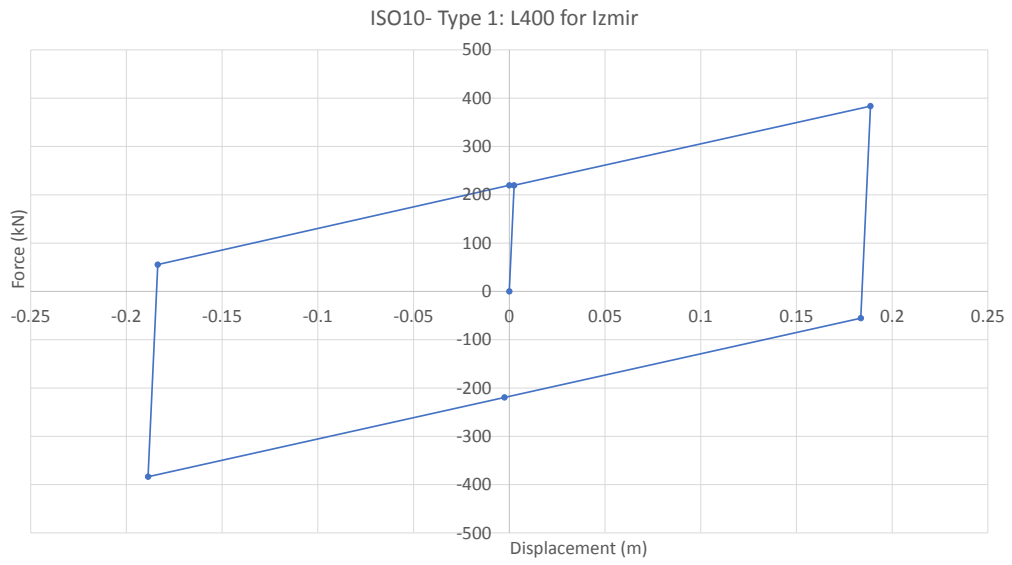


Figure 2.43: ISO10-Nonlinear UB Isolation Characteristics of Type 1: L400, Izmir

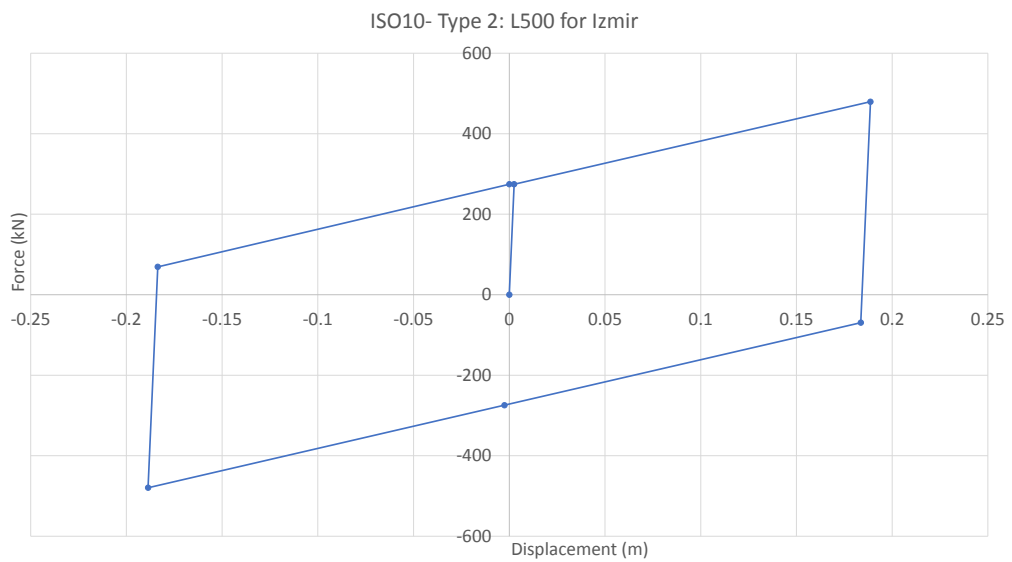


Figure 2.44: ISO10-Nonlinear UB Isolation Characteristics of Type 2: L500, Izmir

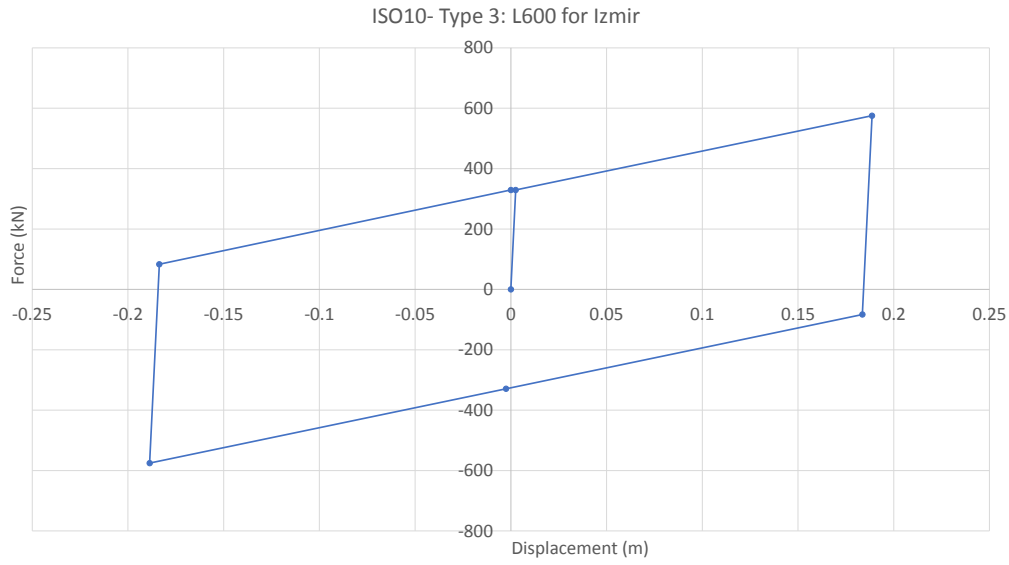


Figure 2.45: ISO10-Nonlinear UB Isolation Characteristics of Type 3: L600, Izmir

Table2.17: Linear Isolator Parameters for ISO10, Izmir & Isparta

Isolator Type	Maximum Vertical Load (kN)	Effective Stiffness (K_{eff}) (kN/m)	Effective Damping (ζ_D) (%)	Damping Coefficient B_D [5]
1	4000	1789	40.43	1.7
2	5000	2236	40.43	1.7
3	6000	2683	40.43	1.7

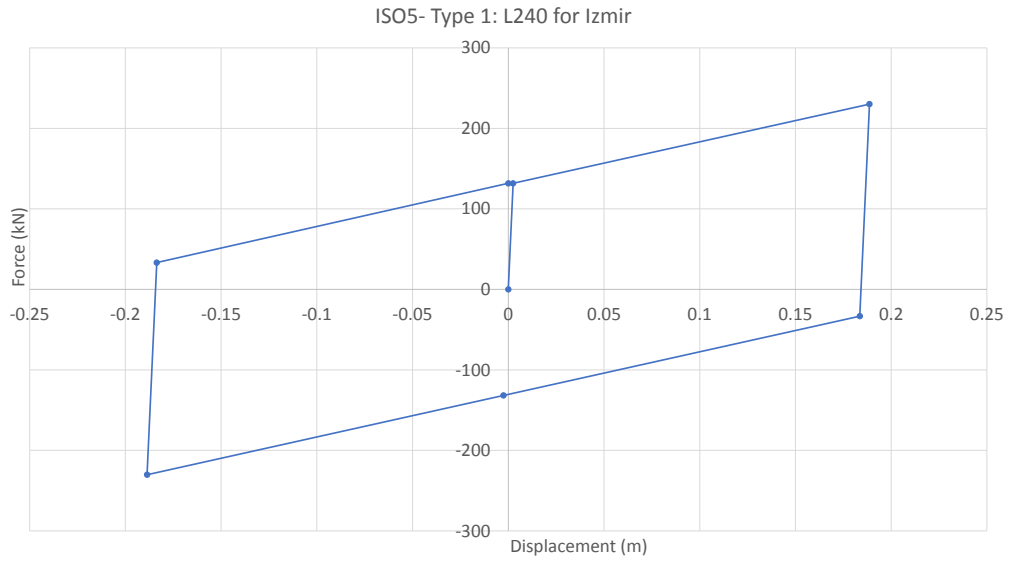


Figure 2.46: ISO5-Nonlinear UB Isolation Characteristics of Type 1: L240, Izmir

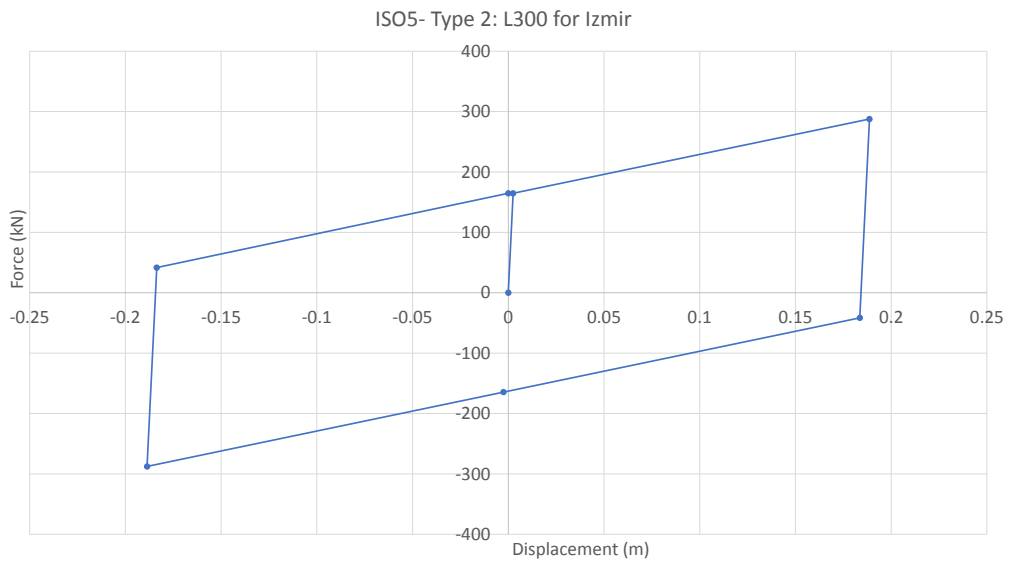


Figure 2.47: ISO5-Nonlinear UB Isolation Characteristics of Type 2: L300, Izmir

Table2.18: Linear Isolator Parameters for ISO5, Izmir & Isparta

Isolator Type	Maximum Vertical Load (kN)	Effective Stiffness (K_{eff}) (kN/m)	Effective Damping (ζ_D) (%)	Damping Coefficient B_D [5]
1	2400	1073	40.43	1.7
2	3000	1342	40.43	1.7

CHAPTER 3

ANALYSIS RESULTS

In this chapter, two significant parameters, namely, interstorey drift ratio (IDR%) and peak floor acceleration (PFA(g)) are evaluated to assess the superstructure behavior by performing Response Spectrum Analysis (RSA) and Fast Nonlinear Analysis (FNA) procedures for DBE level earthquake. Through the next parts, the results obtained from the analyses performed for the structural systems specified in Table 2.1 are presented. As a preliminary assessment of the structural behavior, RSA is performed for Izmir. Note that linear response spectrum analysis gives a rough idea about the overall behavior. To calibrate and validate the RSA results of Izmir, RSA is performed one more time for Isparta, which has higher spectral acceleration values than that of Izmir. Results obtained for Isparta are presented in the Appendix. Finally, FNA is also performed for the three seismically isolated systems; namely, ISOSW15, ISOSW10 and ISOSW5 to examine the behavior of the seismically isolated buildings more accurately by including the nonlinear behavior of the isolators and by taking earthquake directions as plus or minus.

As it is mentioned in Section 2.3, the analyses are performed for two different seismic regions, namely, Izmir and Isparta. Through this chapter, analyses results for Izmir will be delivered in the order of RSA and FNA. RSA results of Isparta are provided in the Appendix. In this chapter, firstly, RSA results for Izmir will be explained. Secondly, nonlinear modal history analysis performed to be more precise in the linear elastic analysis results of ISOSW15, ISOSW10 and ISOSW5 for Izmir will be stated.

Interstorey drift ratio is considered as percentage drift between two adjacent floors divided by the storey height. If a response modification factor is applied to the sys-

tem and the seismic forces are reduced, drift values obtained for these systems are multiplied by the response modification factor applied. Both interstorey drift ratio and floor accelerations are obtained from each floor and from the center of rigidity of the corresponding floor for RSA. For FNA procedure, the time instant when the maximum interstorey drift ratio or floor acceleration occurred is taken as the time instant when the corresponding maximum value occurred in the top floor.

Interstorey drift ratio values obtained through analyses are checked for the limitations per ASCE 7-10 (Chapter 17)[5] and 2013 TMMH[21]. For floor acceleration, the only limitation specified in [21] as a maximum value of 0.2g is also considered.

Table3.1: Limitations on the Maximum Interstorey Drifts

Specification	Limitation
2013 TMMH	Interstorey Drift Ratio (%) ≤ 0.5 [21]
2013 TMMH	Maximum Floor Acceleration (g) ≤ 0.2 [21]
ASCE 7-10, Chapter 17	Interstorey Drift Ratio (%) ≤ 1.5 [5]

3.1 RSA Results for Izmir

To preliminarily assess the superstructure behavior under the seismic action for Izmir, linear response spectrum analysis procedure is employed to evaluate the interstorey drift ratio IDR(%) and peak floor accelerations (PFA). The RSA Results for Izmir will be delivered in the order of IDR(%) and (PFA) for 15,10 and 5 storey structural systems specified in Table 2.1, respectively.

3.1.1 IDR(%) and PFA (g) Results of ISOSW15, ISO15, SWFB15, FB15 for Izmir

Distribution of the interstorey drift ratios (%) in two earthquake directions x and y through the floors of the systems with 15 floors are presented in Figures 3.1 and 3.2 for Izmir.

In Figures 3.1 and 3.2 vertical axis of the curve represents the adjacent floor numbers.

For example, the interstorey drift percentage value in x axis corresponding to "1" in y axis refers to the drift ratio between 1st and 2nd floor and the one stated as "14" in y direction stands for the interstorey drift ratio between 14th and 15th floor.

Figures 3.1 and 3.2 represent how interstorey drift ratios are distributed in different structural systems with 15 floors. The seismic analysis performed is a linear elastic response spectrum analysis of which a linearly damped spectrum is used for Izmir. Damping is applied to the spectral acceleration values beginning from the corresponding isolated periods by a damping coefficient equal to 1.7[5], as specified in Table 1.9.

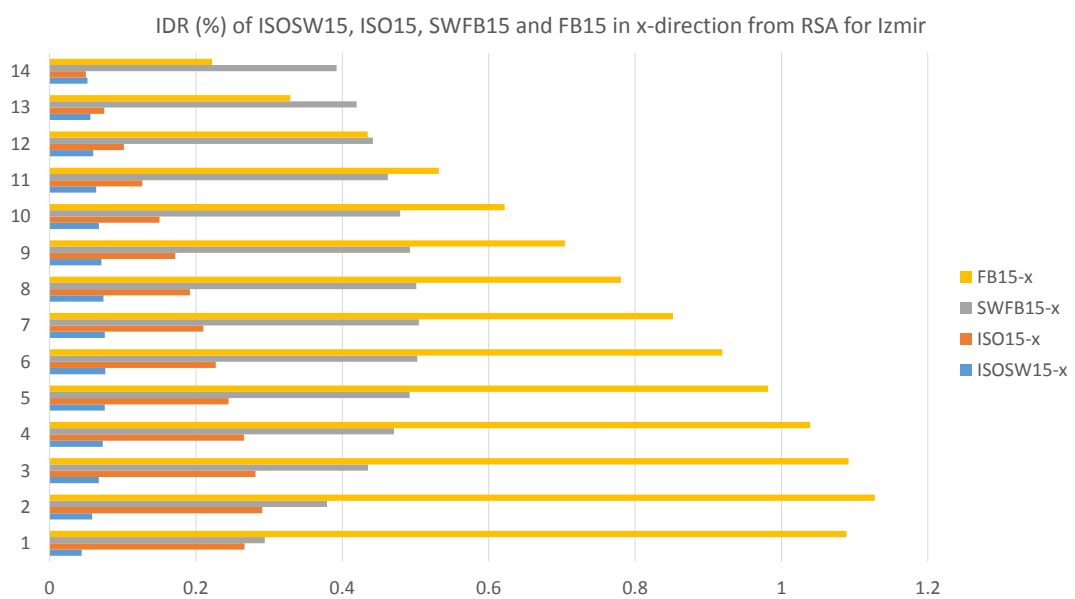


Figure 3.1: IDR(%) (in x direction) through Floors of 15 Storey Systems for Izmir DBE Level from RSA

As it can be seen from Figure 3.1, the system resulting in least drift values is ISOSW15 since the system is configured as both seismically isolated and shear walled frame. The drift values obtained from the system ISOSW15 are far less from the limitations specified in both 2013 TMMH[21] and ASCE 7-10 (Chapter 17)[5]. Similar results are also obtained in y direction for ISOSW15, as it is demonstrated in Figure 3.2. Since the shear wall area of the dual system is higher in x direction than y direction, the drift values are obtained as vice versa. Yet the maximum interstorey drift ratio for ISOSW15 in y direction also does not exceed the limiting values specified in Table

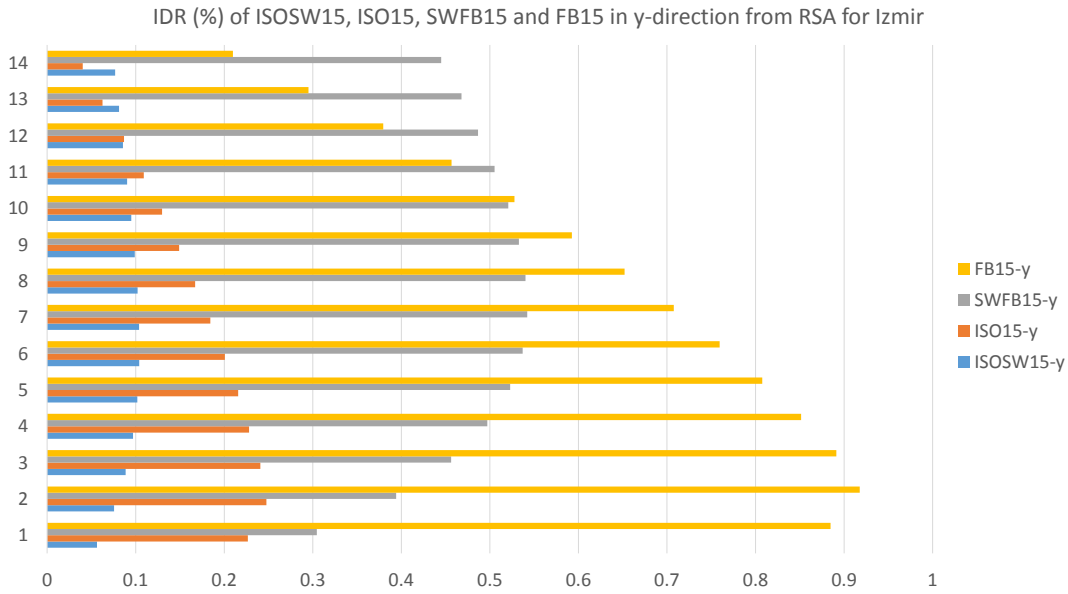


Figure 3.2: IDR(%) (in y direction) through Floors of 15 Storey Systems for Izmir DBE Level from RSA

3.1. Having higher interstorey drift ratio values in y direction can also be figured out from the mass participation ratios given in Table 3.2 such that the majority of the mass is participated in y direction since the weak axis of the system is y direction that have a lower shear wall area compared to x direction. It can also be noticed that the modes of vibration are well separated in both translational directions x and y and one rotational direction. Well separation of modes ensures that seismic isolation design is as it should be. Having well separated modes also is an indication of a superstructure behavior as almost a rigid body motion, which is desired in seismically isolated structures.

Regarding the shape of the interstorey drift ratio distribution through floors, it is obtained as a typical moment frame with shear walls for ISOSW15 in Figure 3.1 and Figure 3.2 where the highest drift values are around mid-heights.

As a second system being alternative to seismically isolated dual system ISOSW15, ISO15 is analyzed, which is a seismically isolated moment frame system (without shear walls). After removing the contribution of shear walls, interstorey drift values are increased without again exceeding the limiting values specified in [21] and in [5]. In the structural model ISO15, the variation in the interstorey drift ratio and floor

Table3.2: Modal Participating Mass Ratios, ISOSW15

Mode (#)	Period (sec)	UX Unitless	UY Unitless	SumUX Unitless	SumUY Unitless	RZ Unitless	SumRZ Unitless
1	3.159	0.002	0.977	0.002	0.977	0.010	0.010
2	3.083	0.966	0.004	0.968	0.981	0.024	0.035
3	2.951	0.026	0.009	0.994	0.989	0.959	0.994
4	0.774	0.000	0.009	0.994	0.998	0.000	0.994
5	0.659	0.005	0.000	0.998	0.998	0.000	0.994
6	0.616	0.000	0.000	0.998	0.998	0.004	0.998
7	0.273	0.000	0.000	0.998	0.998	0.000	0.998
8	0.231	0.000	0.000	0.998	0.998	0.000	0.998
9	0.226	0.000	0.000	0.998	0.998	0.000	0.998
10	0.214	0.000	0.000	0.998	0.998	0.000	0.998
11	0.213	0.000	0.000	0.998	0.998	0.000	0.998
12	0.208	0.000	0.000	0.998	0.998	0.000	0.998

accelerations regarding each earthquake direction x and y are obtained as less than those in ISOSW15. The reason for this is that the lateral stiffness of the system does not differ in the corresponding directions in the absence of shear walls. In contrast to the behavior in ISOSW15, first mode of vibration is encountered in x direction with the higher mass participation ratio specified in Table 3.3. This is simply because of being x direction as the weak axis of the system in the absence of shear walls due to geometric plan dimensions of the structure. Note that the building was 69.3m in x direction and 79.2m in y direction as specified in Table 2.4.

Shape of the interstorey drift ratio distribution through floors is obtained as linearly decreasing throughout upper floors. The reason is that there is no stiffness contribution from shear walls.

As a third system, the system named SWFB15 is analyzed as a conventional fixed base dual system. After removing seismic isolation, interstorey drift values are increased, which is expected. Although the limitations specified in Table 3.1 refer to seismically isolated buildings, change in drifts after excluding seismic isolation that reducing the seismic force demand are evaluated for comparison. In both x and y directions, the maximum drift ratio values are obtained as again lower than the limiting value specified in Table 3.1 and they are close to each other in x and y directions. In

Table3.3: Modal Participating Mass Ratios, ISO15

Mode (#)	Period (sec)	UX Unitless	UY Unitless	SumUX Unitless	SumUY Unitless	RZ Unitless	SumRZ Unitless
1	3.454	0.918	0.007	0.918	0.007	0.042	0.042
2	3.387	0.010	0.953	0.928	0.960	0.007	0.049
3	3.315	0.039	0.011	0.967	0.970	0.921	0.970
4	0.988	0.023	0.000	0.990	0.971	0.002	0.972
5	0.947	0.000	0.021	0.990	0.991	0.000	0.973
6	0.926	0.001	0.000	0.991	0.992	0.020	0.993
7	0.646	0.000	0.000	0.991	0.992	0.000	0.993
8	0.517	0.002	0.000	0.993	0.992	0.000	0.993
9	0.508	0.000	0.000	0.993	0.992	0.000	0.993
10	0.488	0.000	0.001	0.994	0.992	0.001	0.994
11	0.483	0.000	0.001	0.994	0.994	0.001	0.995
12	0.394	0.000	0.000	0.994	0.994	0.000	0.995

SWFB15 system, drift values obtained in y direction as a little higher than those in x direction. Mass participation ratios and period of vibrations for SWFB15 are also given Table 3.4. As it can be seen from Table 3.4, first fundamental mode of vibration is obtained in y direction, as expected. Shape of the drift distribution is also a typical one for a dual system.

Finally, shear walls are removed from the fixed base system and analyzed linearly as a moment frame. As it can be seen from Figure 3.1 and Figure 3.2, the largest interstorey drift values are obtained from the fixed base moment frame system FB15. Maximum interstorey drift values are obtained as 1.127% and 0.918% in x and y directions, respectively. Note that maximum interstorey drift values exceeded the maximum allowable interstorey drift value specified as 0.5% 2013 TMMH[21]. However, note again that 2013 TMMH[21] and ASCE 7-10 (Chapter 17) [5] specifications cover seismically isolated buildings. Nevertheless, interstorey drift ratio values obtained from the fixed base systems are also investigated to make a comparison of efficiency among all the systems considered.

As in the case of ISO15 where there is also no shear walls, in the FB15 system, interstorey drift ratio distribution is linearly decreasing throughout upper floors. In Table 3.5, mass participation and period of vibration of each mode are presented.

Table3.4: Modal Participating Mass Ratios, SWFB15

Mode (#)	Period (sec)	UX Unitless	UY Unitless	SumUX Unitless	SumUY Unitless	RZ Unitless	SumRZ Unitless
1	1.467	0.000	0.701	0.000	0.701	0.006	0.006
2	1.212	0.693	0.000	0.693	0.701	0.010	0.017
3	1.144	0.011	0.006	0.705	0.708	0.693	0.710
4	0.391	0.000	0.158	0.705	0.865	0.002	0.711
5	0.321	0.144	0.001	0.849	0.866	0.016	0.727
6	0.305	0.019	0.002	0.867	0.868	0.143	0.870
7	0.184	0.000	0.057	0.867	0.925	0.001	0.871
8	0.155	0.036	0.001	0.904	0.925	0.019	0.890
9	0.143	0.022	0.000	0.926	0.926	0.038	0.928
10	0.115	0.000	0.028	0.926	0.954	0.001	0.928
11	0.099	0.015	0.000	0.941	0.955	0.013	0.941
12	0.089	0.014	0.000	0.955	0.955	0.015	0.956

As in the previous systems ISOSW15, ISO15 and SWFB15, the modes of vibration seem to be well-separated and there is no coupling behavior between the modes of different directions. Similar to the ISO15 system, mass participation in x direction is the highest one since the weak axis is that one.

3.1.2 PFA (g) Results of ISOSW15, ISO15, SWFB15, FB15 for Izmir

In the subsection 3.1.2, floor acceleration values from linear elastic response spectrum analysis are presented for the structural systems ISOSW15, ISO15, SWFB15 and FB15 to preliminarily assess the behavior of each system compared to one another. The comparison of floor accelerations in terms of both different structural systems and number of floors will be tabulated and presented in the end of this chapter.

In Figures 3.3 and 3.4, distribution of floor accelerations are demonstrated for the systems with 15 stories.

Table3.5: Modal Participating Mass Ratios, FB15

Mode (#)	Period (sec)	UX Unitless	UY Unitless	SumUX Unitless	SumUY Unitless	RZ Unitless	SumRZ Unitless
1	2.179	0.710	0.007	0.710	0.007	0.087	0.087
2	2.061	0.019	0.759	0.728	0.766	0.022	0.109
3	2.030	0.074	0.034	0.802	0.800	0.699	0.808
4	0.712	0.087	0.001	0.889	0.801	0.012	0.820
5	0.672	0.004	0.091	0.893	0.891	0.008	0.828
6	0.666	0.009	0.012	0.902	0.903	0.077	0.905
7	0.410	0.030	0.000	0.932	0.903	0.006	0.911
8	0.387	0.006	0.004	0.938	0.908	0.025	0.936
9	0.384	0.000	0.032	0.938	0.939	0.004	0.940
10	0.283	0.015	0.000	0.953	0.939	0.004	0.944
11	0.268	0.004	0.001	0.957	0.941	0.014	0.958
12	0.265	0.000	0.018	0.957	0.958	0.001	0.959

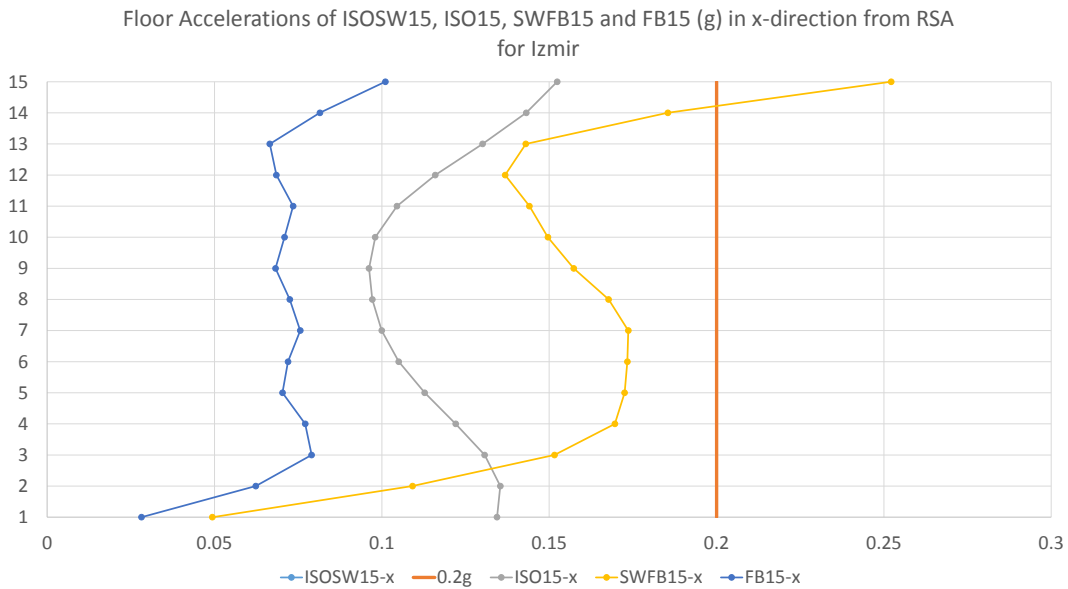


Figure 3.3: PFA(g) (in x direction) through Floors of 15 Storey Systems for Izmir DBE Level from RSA

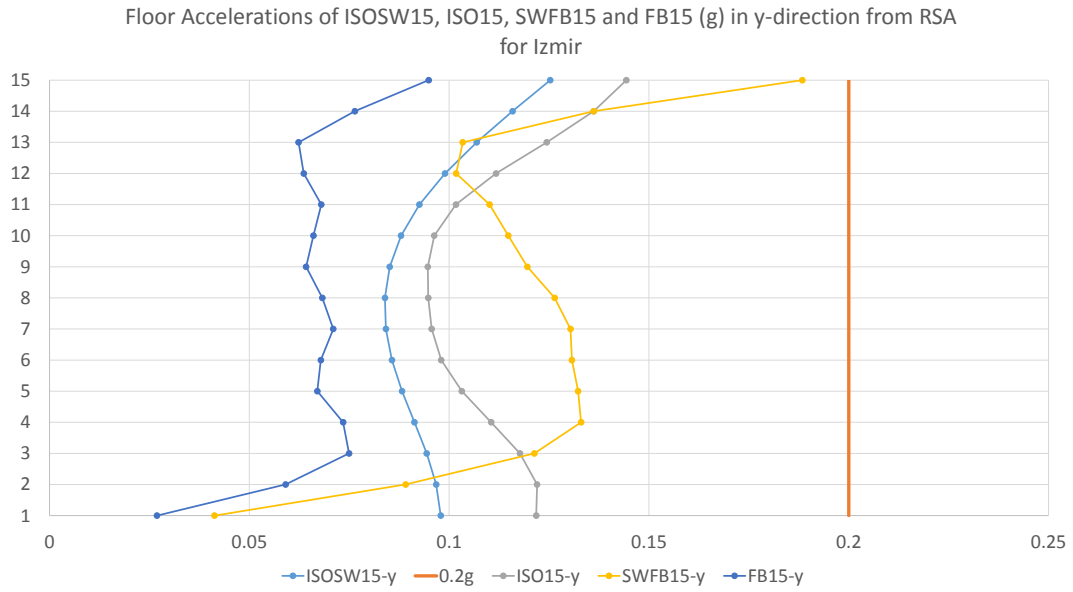


Figure 3.4: PFA(g) (in y direction) through Floors of 15 Storey Systems for Izmir DBE Level from RSA

Based on Figure 3.3 and Figure 3.4, there is no seismically isolated system where acceleration values exceeding $0.2g$ as mentioned in Table 3.1. The only system where maximum acceleration value exceeds $0.2g$ is SWFB15. In x-direction, since the rigidity of the system is higher in x- direction, floor acceleration values in x-direction are found to be higher than those in y-direction and also exceeding $0.2g$. However, maximum floor acceleration limitation is not valid for conventionally designed fixed base systems based on [21]. Note also that linear elastic response spectrum analysis underestimates the acceleration values [19]. In addition, the direction of accelerations under seismic action cannot be traced when RSA performed. For this reason, the acceleration values obtained from linear elastic response spectrum analysis should not be directly used for a non-structural damage assessment. However, they will be used to compare the behavior of different structural systems as well as efficiency in reduction of forces via seismic isolation.

In the next subsection 3.1.3, the four structural systems analyzed as having 10 floors and the corresponding results are presented.

3.1.3 IDR(%) Results of ISOSW10, ISO10, SWFB10, FB10 for Izmir

In the systems with 10 floors, general structural behavior regarding interstorey drift ratio is obtained as similar to those in Figure 3.1 and 3.2. In addition, interstorey drift ratio values are found to be lower than those in the systems with 15 floors, as expected.

In Figures 3.5 and 3.6, interstorey drift ratio distributions of each structural system having 10 floors are demonstrated.

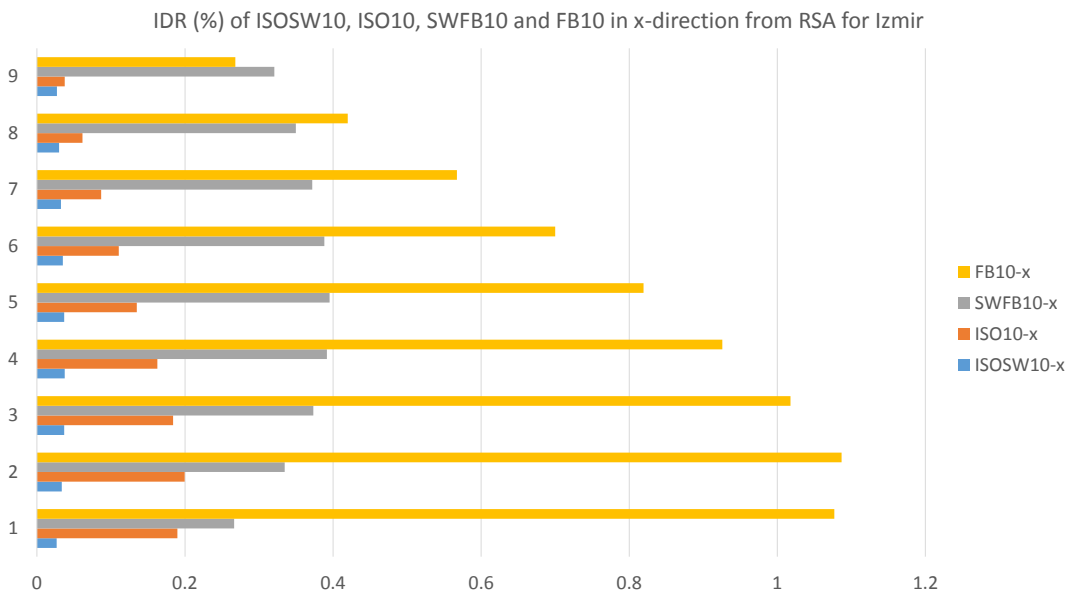


Figure 3.5: IDR(%) (in x direction) through Floors of 10 Storey Systems for Izmir DBE Level from RSA

Mass participating ratios and fundamental periods of vibration values can also be seen in Tables 3.6, 3.7, 3.8 and 3.9.

Based on Table 3.6 and Table 3.7, the modes of vibration are well-separated, ensuring the appropriate seismic isolation design. In addition, well mode separation is also achieved in the systems SWFB10 and FB10 which is structurally desired regarding behavior.

Another significant point is that although the targeted seismic isolation period is the same as being 3 sec in all systems having different floors, the periods of fundamental

Table3.6: Modal Participating Mass Ratios, ISOSW10

Mode (#)	Period (sec)	UX Unitless	UY Unitless	SumUX Unitless	SumUY Unitless	RZ Unitless	SumRZ Unitless
1	2.912	0.000	0.993	0.000	0.993	0.003	0.003
2	2.886	0.995	0.000	0.995	0.993	0.002	0.005
3	2.784	0.002	0.003	0.997	0.996	0.991	0.997
4	0.463	0.000	0.001	0.997	0.998	0.000	0.997
5	0.385	0.001	0.000	0.998	0.998	0.000	0.997
6	0.363	0.000	0.000	0.998	0.998	0.001	0.997
7	0.162	0.000	0.000	0.998	0.998	0.000	0.997
8	0.153	0.000	0.000	0.998	0.998	0.000	0.997
9	0.152	0.000	0.000	0.998	0.998	0.000	0.997
10	0.151	0.000	0.000	0.998	0.998	0.000	0.997
11	0.149	0.000	0.000	0.998	0.998	0.000	0.997
12	0.146	0.000	0.000	0.998	0.998	0.000	0.997

Table3.7: Modal Participating Mass Ratios, ISO10

Mode (#)	Period (sec)	UX Unitless	UY Unitless	SumUX Unitless	SumUY Unitless	RZ Unitless	SumRZ Unitless
1	3.106	0.918	0.000	0.918	0.000	0.068	0.068
2	3.070	0.000	0.983	0.918	0.983	0.003	0.070
3	2.977	0.066	0.003	0.984	0.986	0.916	0.987
4	0.689	0.006	0.000	0.990	0.986	0.001	0.987
5	0.652	0.000	0.005	0.990	0.990	0.001	0.988
6	0.645	0.000	0.001	0.991	0.991	0.005	0.993
7	0.503	0.000	0.000	0.991	0.991	0.000	0.993
8	0.433	0.000	0.000	0.991	0.991	0.000	0.993
9	0.347	0.000	0.000	0.991	0.991	0.000	0.993
10	0.340	0.000	0.000	0.991	0.991	0.000	0.993
11	0.322	0.000	0.000	0.991	0.991	0.000	0.993
12	0.320	0.000	0.000	0.991	0.991	0.000	0.993

Table3.8: Modal Participating Mass Ratios, SWFB10

Mode (#)	Period (sec)	UX Unitless	UY Unitless	SumUX Unitless	SumUY Unitless	RZ Unitless	SumRZ Unitless
1	0.854	0.000	0.706	0.000	0.706	0.008	0.008
2	0.698	0.711	0.000	0.711	0.706	0.002	0.010
3	0.664	0.002	0.008	0.713	0.714	0.709	0.719
4	0.223	0.000	0.171	0.713	0.885	0.002	0.721
5	0.186	0.121	0.001	0.835	0.886	0.045	0.766
6	0.174	0.053	0.001	0.888	0.888	0.125	0.890
7	0.107	0.000	0.056	0.888	0.943	0.001	0.892
8	0.093	0.029	0.001	0.917	0.944	0.025	0.917
9	0.083	0.028	0.000	0.945	0.945	0.029	0.946
10	0.069	0.000	0.025	0.945	0.970	0.001	0.947
11	0.061	0.012	0.001	0.957	0.971	0.013	0.960
12	0.054	0.014	0.000	0.971	0.971	0.011	0.971

Table3.9: Modal Participating Mass Ratios, FB10

Mode (#)	Period (sec)	UX Unitless	UY Unitless	SumUX Unitless	SumUY Unitless	RZ Unitless	SumRZ Unitless
1	1.430	0.692	0.006	0.692	0.006	0.110	0.110
2	1.348	0.053	0.599	0.745	0.605	0.157	0.267
3	1.339	0.063	0.202	0.808	0.807	0.546	0.813
4	0.463	0.084	0.001	0.891	0.808	0.016	0.828
5	0.437	0.012	0.042	0.904	0.850	0.046	0.874
6	0.434	0.004	0.060	0.908	0.910	0.037	0.911
7	0.263	0.029	0.000	0.937	0.910	0.008	0.919
8	0.249	0.008	0.002	0.946	0.912	0.027	0.945
9	0.246	0.000	0.035	0.946	0.947	0.002	0.948
10	0.177	0.015	0.000	0.960	0.947	0.006	0.953
11	0.168	0.006	0.001	0.966	0.948	0.014	0.967
12	0.166	0.000	0.019	0.966	0.968	0.001	0.968

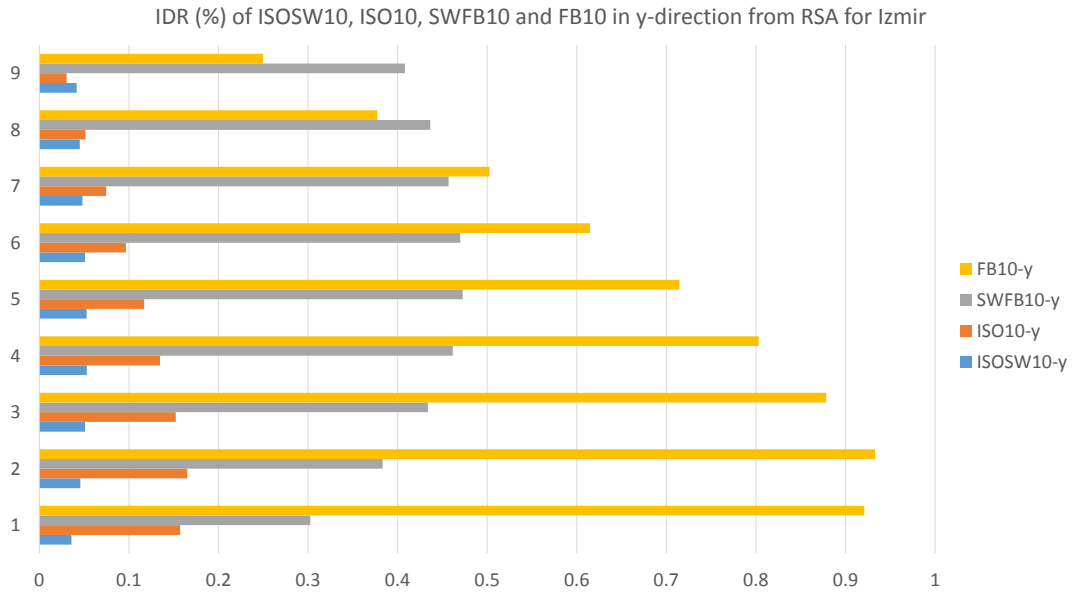


Figure 3.6: IDR(%) (in y direction) through Floors of 10 Storey Systems for Izmir DBE Level from RSA

modes are different from each other, meaning that the rigidity of the superstructure is also crucial besides isolated seismic mass.

Moreover, the percentage of the mass participation values obtained from modal analyses are achieved as above 90% in the first mode of vibration in all of the seismically isolated systems up to now. This means that, seismically isolated systems are oscillating as almost a rigid body. Efficiency in the reduction of floor accelerations for each structural system having different number of floors will be presented in Table 3.26 and 3.27 for Izmir.

3.1.4 PFA(g) Results of ISOSW10, ISO10, SWFB10, FB10 for Izmir

In Figures 3.7 and 3.8, floor acceleration values for the systems with 10 floors are delivered.

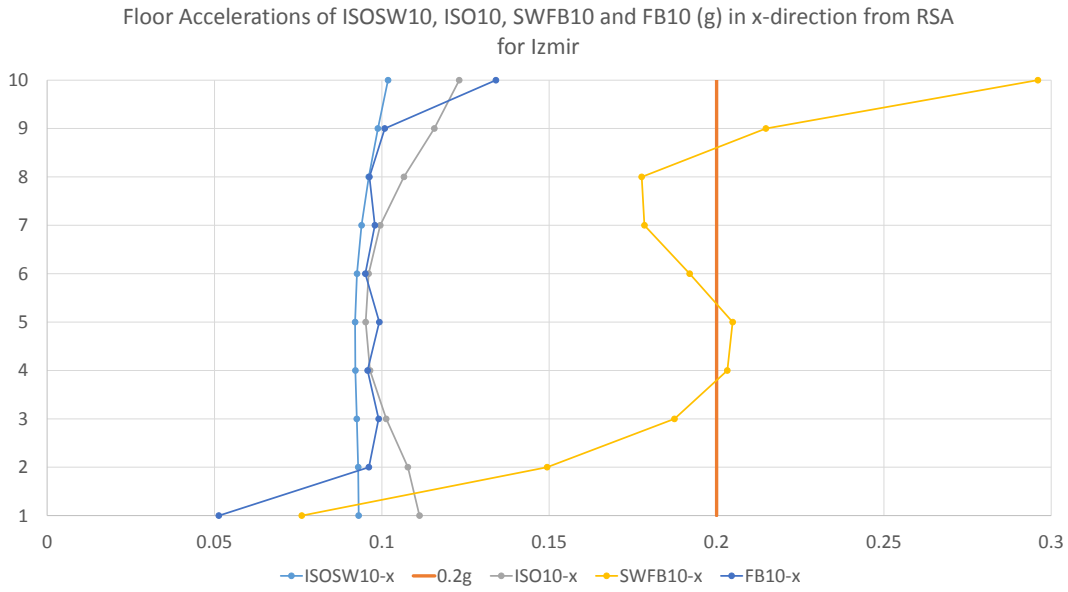


Figure 3.7: PFA(g) (in x direction) through Floors of 10 Storey Systems for Izmir DBE Level from RSA

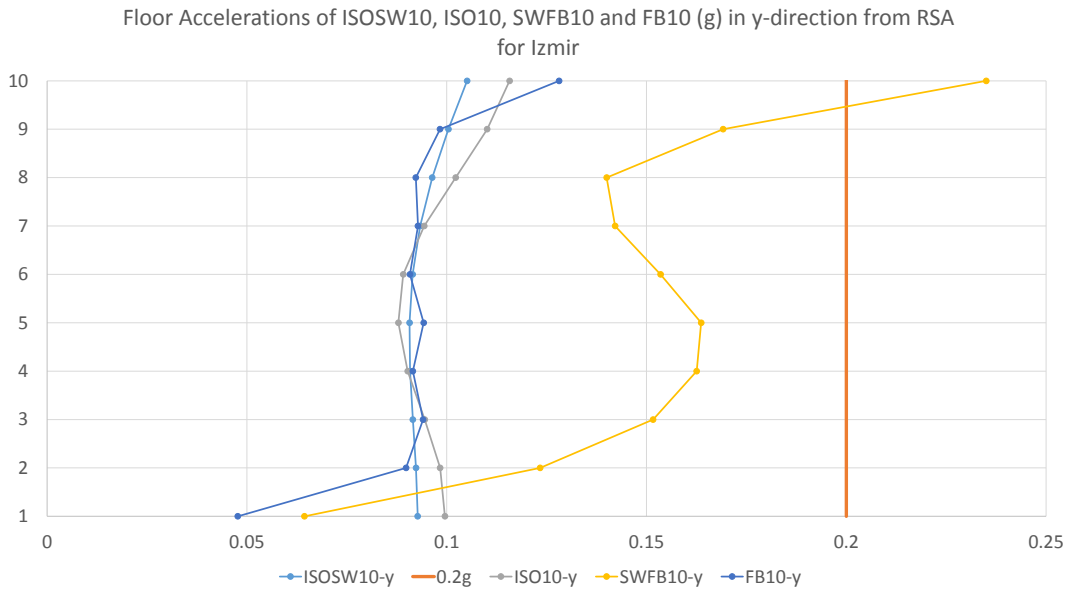


Figure 3.8: PFA(g) (in y direction) through Floors of 10 Storey Systems for Izmir DBE Level from RSA

For the seismically isolated systems ISOSW10 and ISO10, there is a subtle decrease in maximum floor acceleration value compared to ISOSW15 and ISO15, respectively.

On the other hand, for the seismically non-isolated systems, which are SWFB10 and FB10, acceleration values are found to be increased in the case of reduction in number of floors from 15 to 10. For the fixed based dual system SWFB10, in both x and y directions, maximum floor acceleration limit of $0.2g$ is exceeded.

Final linear elastic response spectrum analysis conducted for Izmir is presented in subsection 3.1.5 and 3.1.6 with the systems having 5 floors.

3.1.5 IDR(%) Results of ISOSW5, ISO5, SWFB5, FB5 for Izmir

For the structural systems ISOSW5, ISO5, SWFB5 and FB5, interstorey drift ratio distribution is given in Figure 3.9 and 3.10.

As it is expected, interstorey drift ratio values are obtained as lower than those of the systems with 10 floors and, obviously, 15 floors.

General behavior in the distribution of drift values are obtained as similar to the systems with 10 and 15 floors.

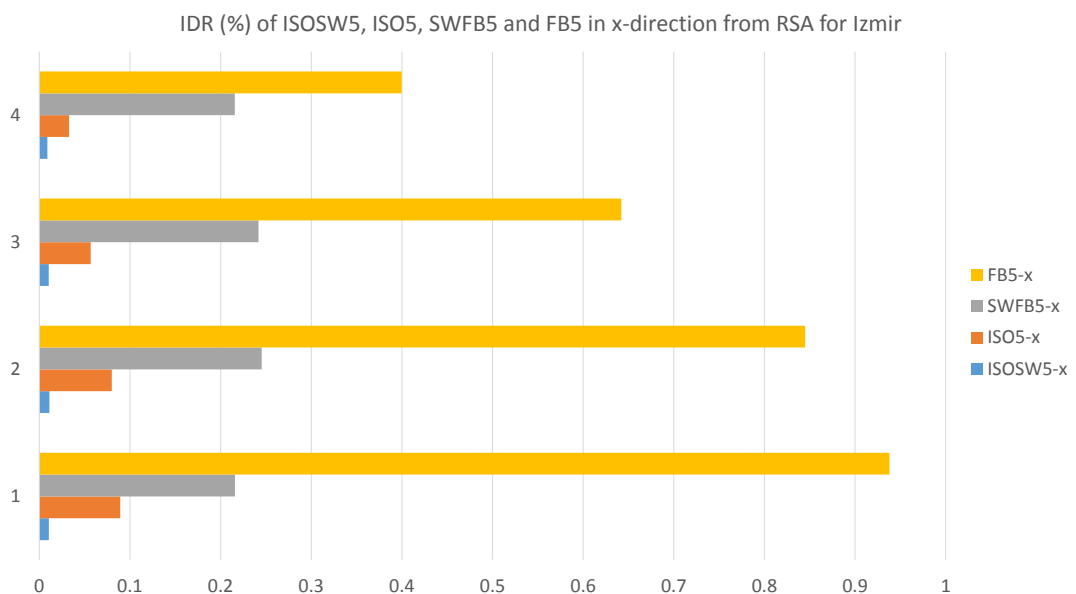


Figure 3.9: IDR(%) (in x direction) through Floors of 5 Storey Systems for Izmir DBE Level from RSA

Table3.10: Modal Participating Mass Ratios, ISOSW5

Mode (#)	Period (sec)	UX Unitless	UY Unitless	SumUX Unitless	SumUY Unitless	RZ Unitless	SumRZ Unitless
1	2.753	0.000	0.990	0.990	0.000	0.005	0.005
2	2.749	0.995	0.000	0.990	0.000	0.000	0.005
3	2.647	0.000	0.005	0.995	0.000	0.989	0.994
4	0.173	0.000	0.000	0.995	0.000	0.000	0.994
5	0.145	0.000	0.000	0.995	0.000	0.000	0.994
6	0.136	0.000	0.000	0.995	0.000	0.000	0.994
7	0.087	0.000	0.000	0.995	0.336	0.000	0.994
8	0.084	0.000	0.000	0.995	0.369	0.000	0.994
9	0.083	0.000	0.000	0.995	0.376	0.000	0.994
10	0.082	0.000	0.000	0.995	0.388	0.000	0.994
11	0.082	0.000	0.000	0.995	0.389	0.000	0.994
12	0.081	0.000	0.000	0.995	0.389	0.000	0.994

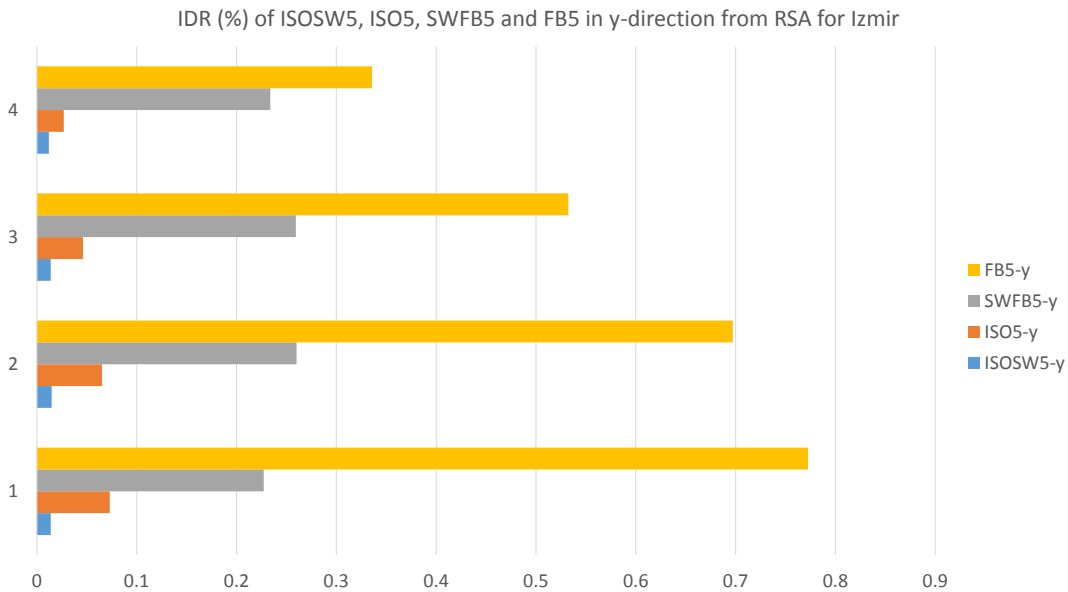


Figure 3.10: IDR(%) (in y direction) through Floors of 5 Storey Systems for Izmir DBE Level from RSA

In Tables 3.10, 3.11, 3.12 and 3.13, modal parameters of period and mass participation ratio values for fundamental modes of vibration are presented. Similar results are obtained regarding well-separation of modes.

Table3.11: Modal Participating Mass Ratios, ISO5

Mode (#)	Period (sec)	UX Unitless	UY Unitless	SumUX Unitless	SumUY Unitless	RZ Unitless	SumRZ Unitless
1	2.852	0.849	0.016	0.849	0.016	0.122	0.122
2	2.831	0.021	0.961	0.870	0.977	0.001	0.122
3	2.727	0.113	0.006	0.982	0.982	0.864	0.986
4	0.342	0.000	0.000	0.983	0.982	0.000	0.986
5	0.325	0.000	0.000	0.983	0.982	0.000	0.986
6	0.321	0.000	0.000	0.983	0.983	0.000	0.986
7	0.152	0.000	0.000	0.983	0.983	0.000	0.986
8	0.145	0.000	0.000	0.983	0.983	0.000	0.986
9	0.143	0.000	0.000	0.983	0.983	0.000	0.986
10	0.088	0.000	0.000	0.983	0.983	0.000	0.986
11	0.087	0.000	0.000	0.983	0.983	0.000	0.986
12	0.085	0.000	0.000	0.983	0.983	0.000	0.986

Note that as the number of floor decreases, the rigidity of the systems increases. For the seismically isolated systems ISOSW5 and ISO5, dominant isolated period values are found as 2.753 sec and 2.852 sec, respectively. In the previous cases, isolated period of the systems ISOSW10 and ISO10 were determined as 2.912 sec and 3.106 sec. For ISOSW15 and ISO15, corresponding isolated period values were 3.159 sec and 3.454 sec. Note that, the targeted isolation period for all of the systems regardless of their number of floors were 3 sec. This means that the overall isolated period is affected by the rigidity of the superstructure as well. That is, while determining targeted value of the isolated period, one of the main parameter is the seismically isolated mass. Analysis results indicated that, the targeted isolation period is not perfectly achieved since the rigidity of the system affected the isolated period.

For the non-isolated systems, it is obvious that as the number of floors decreases, the period of the structure decreases. It is also explicit that the vibration frequency of shear walled frames is higher than that of moment frame systems as the rigidity of the system increases, period of vibration decreases and natural frequency increases since it is inversely proportional to the natural period of vibration.

Table3.12: Modal Participating Mass Ratios, SWFB5

Mode (#)	Period (sec)	UX Unitless	UY Unitless	SumUX Unitless	SumUY Unitless	RZ Unitless	SumRZ Unitless
1	0.334	0.000	0.748	0.000	0.748	0.011	0.011
2	0.275	0.617	0.004	0.617	0.752	0.141	0.152
3	0.261	0.142	0.008	0.759	0.760	0.613	0.765
4	0.092	0.000	0.173	0.760	0.933	0.004	0.769
5	0.080	0.085	0.003	0.845	0.936	0.082	0.851
6	0.072	0.092	0.001	0.937	0.937	0.086	0.938
7	0.047	0.000	0.042	0.937	0.979	0.002	0.940
8	0.047	0.000	0.000	0.937	0.979	0.000	0.940
9	0.046	0.000	0.000	0.938	0.979	0.000	0.940
10	0.044	0.007	0.000	0.944	0.979	0.000	0.941
11	0.043	0.013	0.002	0.958	0.982	0.026	0.966
12	0.040	0.000	0.000	0.958	0.982	0.000	0.966

Table3.13: Modal Participating Mass Ratios, FB5

Mode (#)	Period (sec)	UX Unitless	UY Unitless	SumUX Unitless	SumUY Unitless	RZ Unitless	SumRZ Unitless
1	0.701	0.665	0.005	0.665	0.005	0.155	0.155
2	0.662	0.151	0.105	0.816	0.110	0.569	0.724
3	0.657	0.007	0.715	0.822	0.825	0.104	0.828
4	0.218	0.081	0.001	0.904	0.825	0.026	0.854
5	0.207	0.027	0.010	0.930	0.835	0.071	0.925
6	0.205	0.001	0.098	0.931	0.934	0.009	0.934
7	0.118	0.027	0.000	0.958	0.934	0.015	0.949
8	0.112	0.016	0.004	0.973	0.937	0.023	0.973
9	0.111	0.001	0.038	0.974	0.975	0.003	0.975
10	0.077	0.010	0.000	0.984	0.975	0.009	0.984
11	0.073	0.002	0.015	0.987	0.991	0.002	0.986
12	0.073	0.008	0.004	0.994	0.994	0.008	0.994

3.1.6 PFA(g) Results of ISOSW5, ISO5, SWFB5, FB5 for Izmir

In this subsection , floor acceleration distributions through floors of 5 storey systems in each earthquake direction is presented, as previously demonstrated for 10 storey and 15 storey systems.

In Figure 3.11 and Figure 3.12, floor acceleration values resulted from linear elastic response spectrum analysis are provided consecutively.

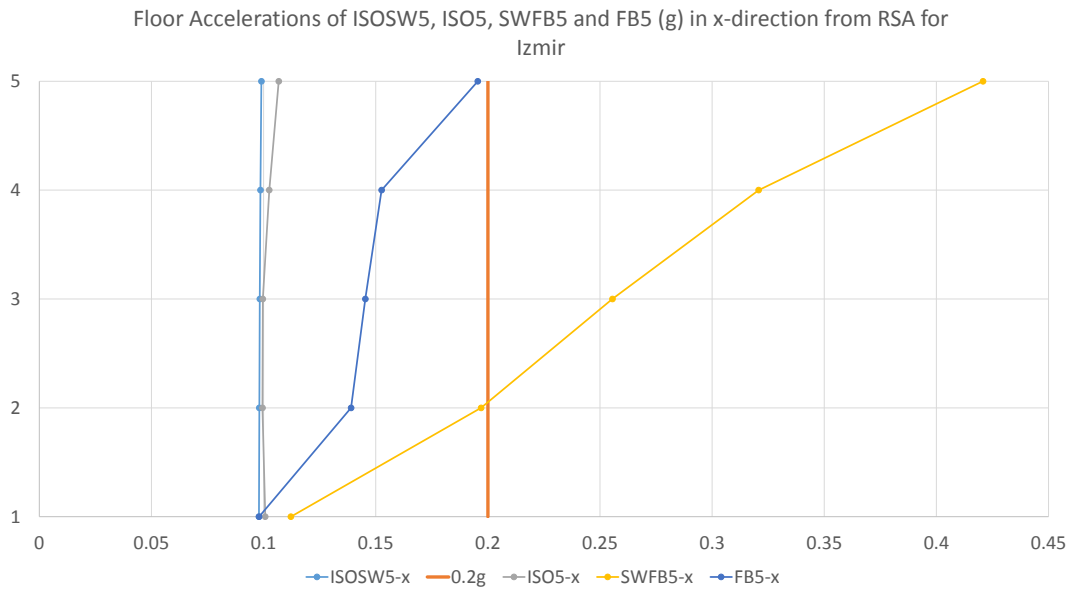


Figure 3.11: PFA(g) (in x direction) through Floors of 5 Storey Systems for Izmir DBE Level from RSA

It can be deduced from Figures 3.11 and 3.12, as the rigidity of the 5 storey fixed base systems is higher than those of the previous systems with 10 and 15 floors, the floor acceleration values are resulted in higher values compared to the ones in Figures 3.3, 3.4, 3.7 and 3.8. In contrast, floor accelerations resulted from seismically isolated system is in a slightly decreasing trend as the number of floors decreases. Since the analysis performed is a linear elastic response spectrum analysis in modal space, higher modes effect may be dominant in the systems having higher number of floors.

Moreover, as the number of floors decreases, the contribution of shear walls to the overall behavior also decreases in both seismically isolated and non-isolated systems.

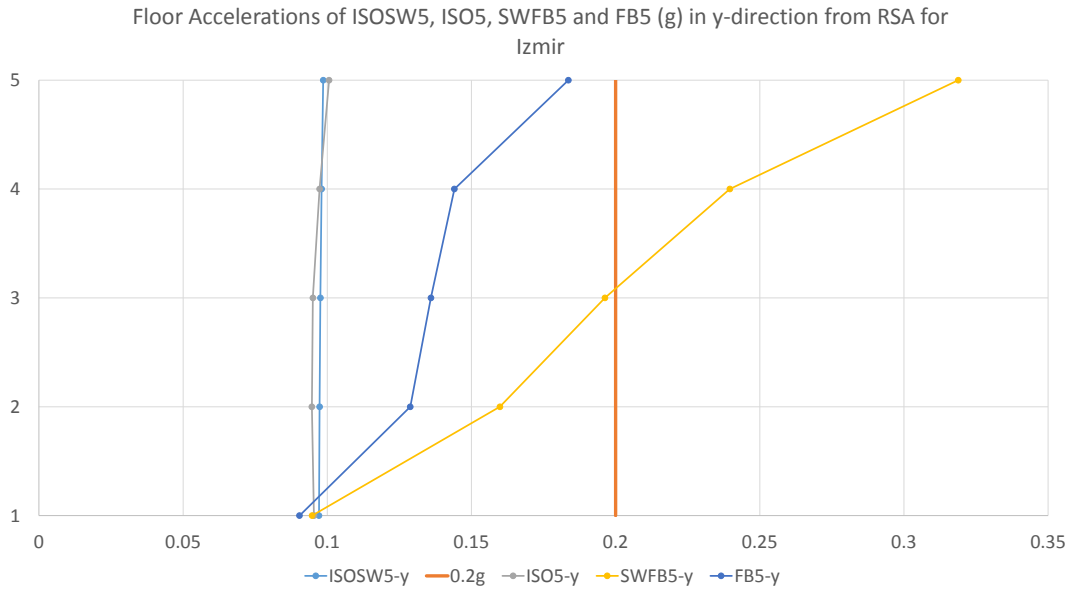


Figure 3.12: PFA(g) (in y direction) through Floors of 5 Storey Systems for Izmir DBE Level from RSA

This means that, as the number of floors decreases, the structural behavior of a shear walled system gets very close to the one without shear walls.

Note that no seismically isolated system exceeded the maximum allowed floor acceleration of 0.2g, which is specified in Table 3.1. Being aware of that linear elastic analysis method underestimates the acceleration values[19], acceleration values derived from RSA will not be taken as the ones to be check against the maximum allowable acceleration value of 0.2g from the Table 3.1. Instead, nonlinear analysis procedures will be followed to investigate the floor accelerations. Nevertheless, to validate the trend of floor acceleration distribution observed in the linear analysis procedures performed for Izmir, the same analysis will be repeated for Isparta that has higher spectral acceleration values to investigate the seismic isolation efficiency between different systems.

Note also that there are not any seismically isolated systems where maximum allowable drift values exceeded based on neither ASCE 7-10 [5] nor 2013 TMMH [21] criterion. To validate the structural behavior regarding interstorey drift ratios, the same linear elastic analysis procedure had been followed for Isparta, where seismicity is higher than Izmir.

In the Appendix, linear elastic response spectrum analysis results for Isparta are provided. The results found to be very similar to those obtained for Izmir. Since the method of analysis is linear elastic, the results obtained for Isparta are linearly scaled versions of the ones for Izmir with higher response values.

3.2 FNA Results of ISOSW15, ISOSW10 and ISOSW5 for Izmir

Non-linear analysis procedures are needed to be followed especially to assess floor accelerations more diligently. In this Section 3.2, results from FNA performed for the seismically isolated dual systems with different number of floors; ISOSW15, ISOSW10 and ISOSW5 to exemplify the difference in results obtained from linear elastic and nonlinear analysis methods.

Interstorey drift and floor acceleration values are obtained from the mean resultant of 7 ground motions selected and scaled based on the site specific response spectrum curve for Izmir, as specified in Section 2.3.

In the subsections 3.2.1, 3.2.2 and 3.2.3, acceleration values read from the center of rigidity of each floor are presented. Interstorey drift ratio distribution for each system will be delivered in the subsections 3.2.4, 3.2.5 and 3.2.6.

In Figure 3.13, one of the floor acceleration responses of the 15 storey seismically isolated dual system (ISOSW15) is presented. The maximum floor acceleration of the 15th floor occurs at 9.96 sec as $0.468g$, as it is tabulated in Table 3.14.

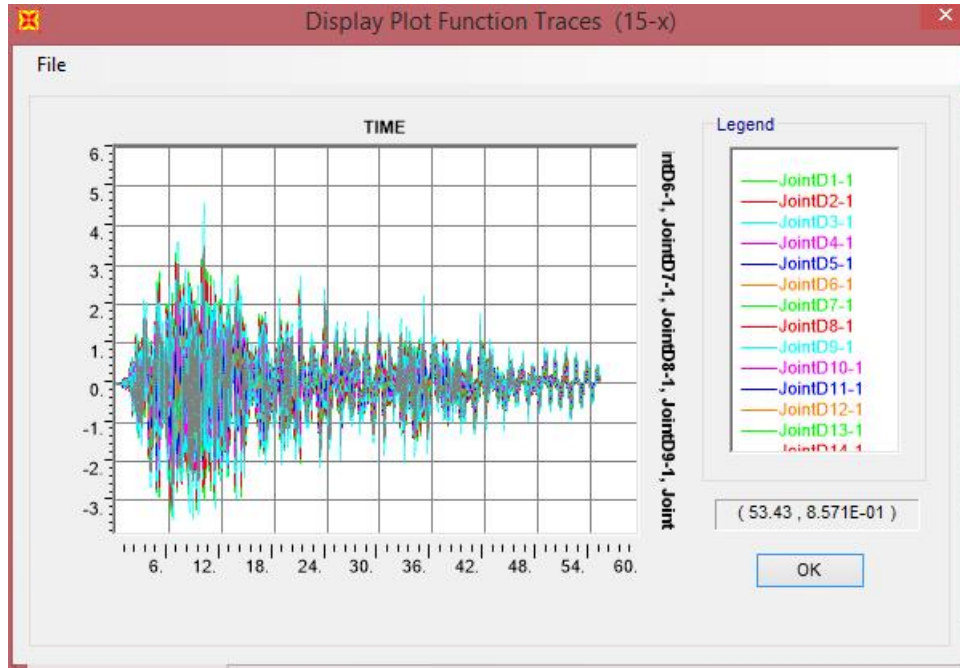


Figure 3.13: Acceleration of CoR of each Floor under GM:0015 Excitation in x-direction

Table3.14: PFA (g) of the Top Floor under GM:0015 Excitation in x-direction

Time of PFA Occurrence (sec)	PFA (g)
9.96	0.468

In Figure 3.13, each different colored line corresponds to a storey from 1 to 15. As it can be seen from Figure 3.13, all of the lines coincide with each other at the same time instants. This is simply due to the (almost) rigid body motion achieved by seismic isolation.

3.2.1 PFA(g) Results of ISOSW15 for Izmir from FNA

In this section, the original hospital block, which is a seismically isolated dual system, ISOSW15 is analyzed via fast nonlinear analysis procedure. To compare the seismic performance based on building height; ISOSW10 and ISOSW5, which have 10 floors and 5 floors, respectively, are analyzed in the same way. The main pur-

pose of performing fast nonlinear analysis is to include nonlinear characteristics of the seismically isolated system and to determine the difference of responses obtained from linear and nonlinear procedures.

In Figure 3.14, floor acceleration distribution of ISOSW15 through each floor obtained from 7 ground motion is presented.

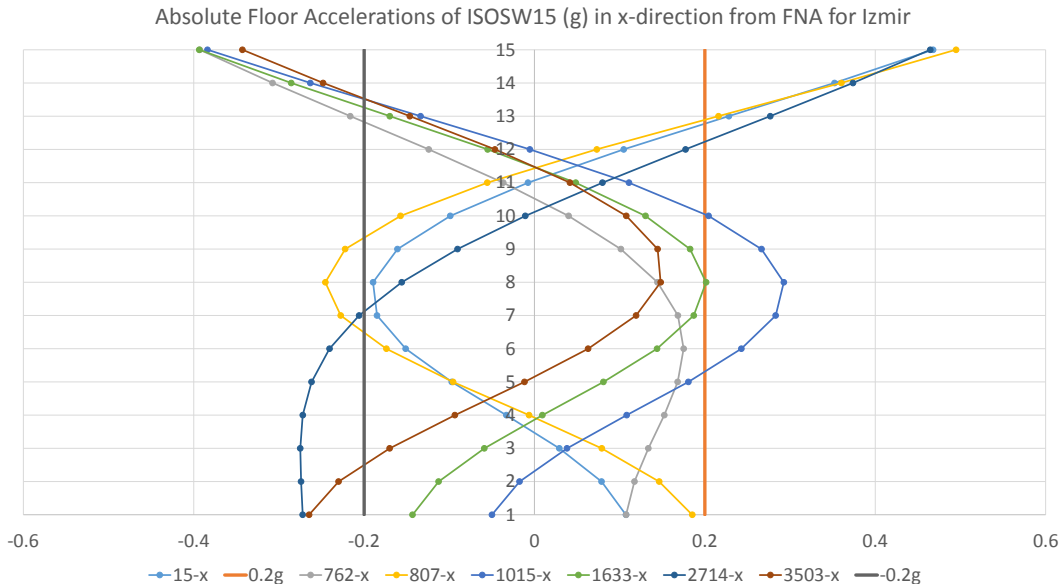


Figure 3.14: PFA(g) (in x direction) through Floors of ISOSW15 for Izmir DBE Level from FNA

Table3.15: Mean PFA (g) of ISOSW15 from the 7 GM Records in x-direction

	15-x	762-x	807-x	1015-x	1633-x	2714-x	3503-x
Maximum top floor acceleration (g)	0.468	-0.393	0.495	-0.384	-0.393	0.465	-0.343
Mean (g)	0.420						

In Figures 3.14 and 3.15, peak floor accelerations obtained from the earthquake excitation in x-direction and y-direction, respectively, are presented. Peak floor acceleration values are determined at the time instant where maximum value observed at the top floor, namely, at the 15th floor. The reason for is that due to dynamic amplification phenomena, the maximum acceleration value is expected to occur at the uppermost floor.

As it can be seen from Figure 3.14 and Figure 3.15, each ground motion is resulted in different peak acceleration value regarding order of magnitude. As it is specified in [5], the average of peak floor accelerations obtained from the 7 ground motion records. The average of peak floor accelerations resulted from 7 ground motions is tabulated in Table 3.15.

Earthquake excitation in y-direction is treated in the same way to obtain the distribution of floor acceleration values through 15 floor. In Figure 3.15, distribution of floor accelerations is demonstrated.

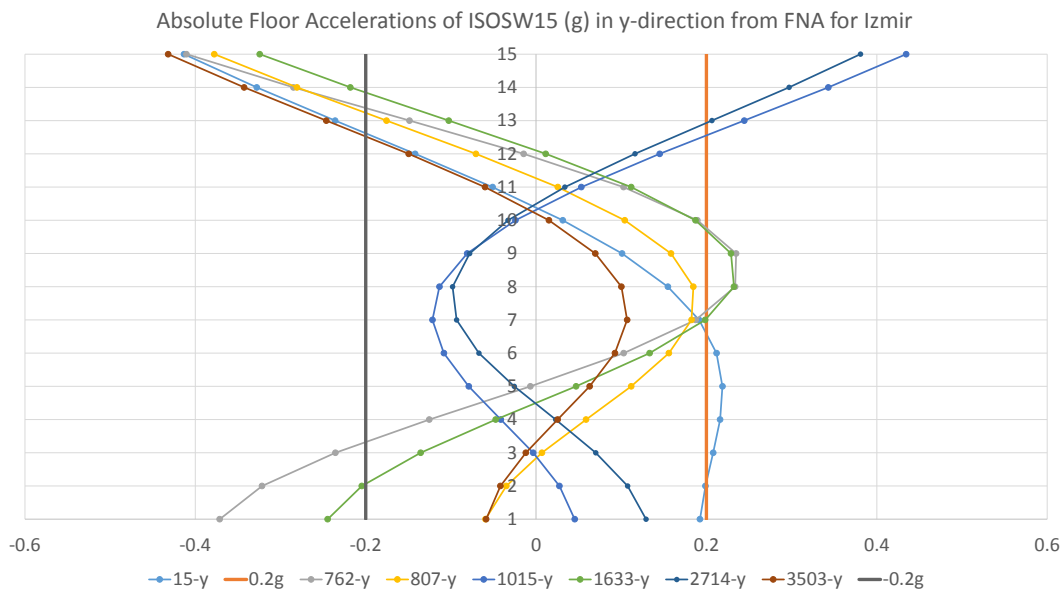


Figure 3.15: PFA(g) (in y direction) through Floors of ISOSW15 for Izmir DBE Level from FNA

The average of peak floor accelerations is presented in a tabular way in 3.16 by specifying peak floor acceleration response of each time history.

Table3.16: Mean PFA (g) of ISOSW15 from the 7 GM Records in y-direction

	15-y	762-y	807-y	1015-y	1633-y	2714-y	3503-y
Maximum top floor acceleration (g)	-0.413	-0.410	-0.378	0.434	-0.324	0.381	-0.432
Mean (g)	0.396						

Note that, performing nonlinear modal history analysis provided the detection of sign of acceleration response direction.

FNA resulted in an average acceleration value of $0.420g$ in x direction and RSA in a maximum acceleration value of $0.117g$; meaning that FNA resulted in an acceleration value of 3.59 times higher than the value obtained from RSA. In y direction, it is 3.17 times higher than the acceleration value obtained from RSA.

3.2.2 PFA(g) Results of ISOSW10 for Izmir from FNA

In this subsection, seismically isolated dual system with 10 floors is analyzed in modal space non-linearly to compare the results with the ones obtained from ISOSW15.

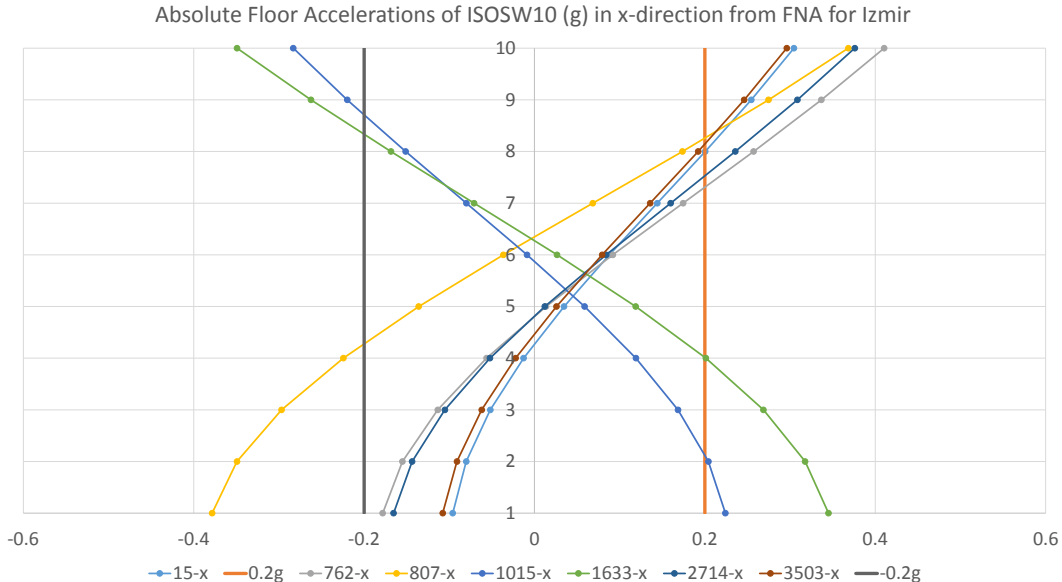


Figure 3.16: PFA(g) (in x direction) through Floors of ISOSW10 for Izmir DBE Level from FNA

Table3.17: Mean PFA (g) of ISOSW10 from the 7 GM Records in x-direction

	15-x	762-x	807-x	1015-x	1633-x	2714-x	3503-x
Maximum top floor acceleration (g)	0.305	0.410	-0.378	-0.283	-0.349	0.376	0.296
Mean (g)	0.343						

Based on Figure 3.16 and Table 3.17, maximum top floor acceleration values are obtained as higher than those from RSA, (3.39 times higher in x direction and 3.81 in y direction) as in the case for 15 floors. The floor acceleration distribution for y direction is provided in Figure 3.17 and the mean value of maximum top floor accelerations is in Table 3.18.

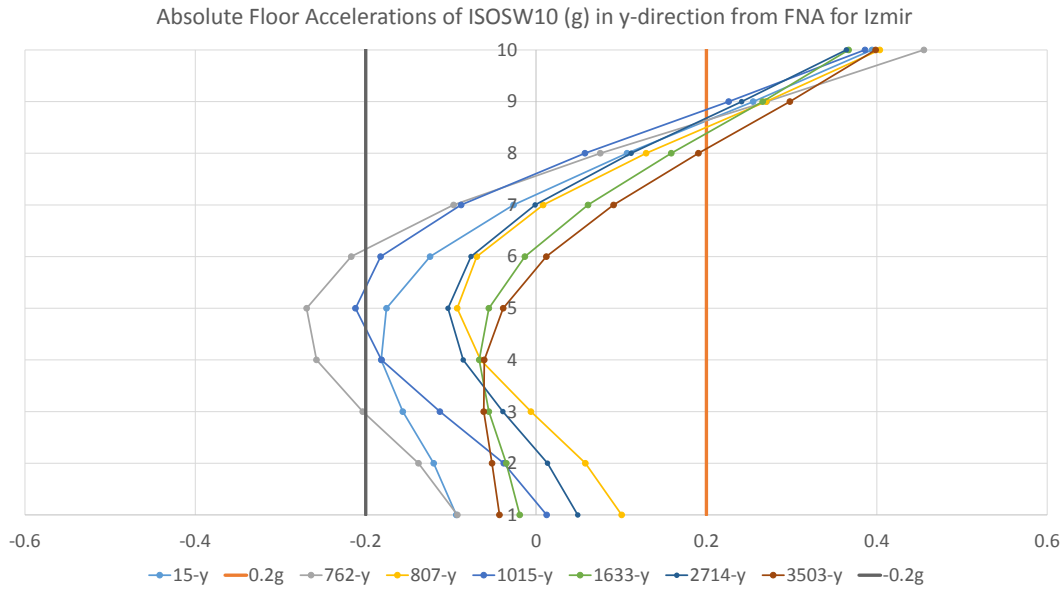


Figure 3.17: PFA(g) (in y direction) through Floors of ISOSW10 for Izmir DBE Level from FNA

Table3.18: Mean PFA (g) of ISOSW10 from the 7 GM Records in y-direction

	15-y	762-y	807-y	1015-y	1633-y	2714-y	3503-y
Maximum top floor acceleration (g)	0.394	0.455	0.403	0.386	0.367	0.364	0.399
Mean (g)	0.396						

3.2.3 PFA(g) Results of ISOSW5 for Izmir from FNA

Finally, seismically isolated dual system with 5 floors is analyzed via FNA. Figures 3.18 and 3.19 demonstrates the floor acceleration distribution of the 5 floor system.

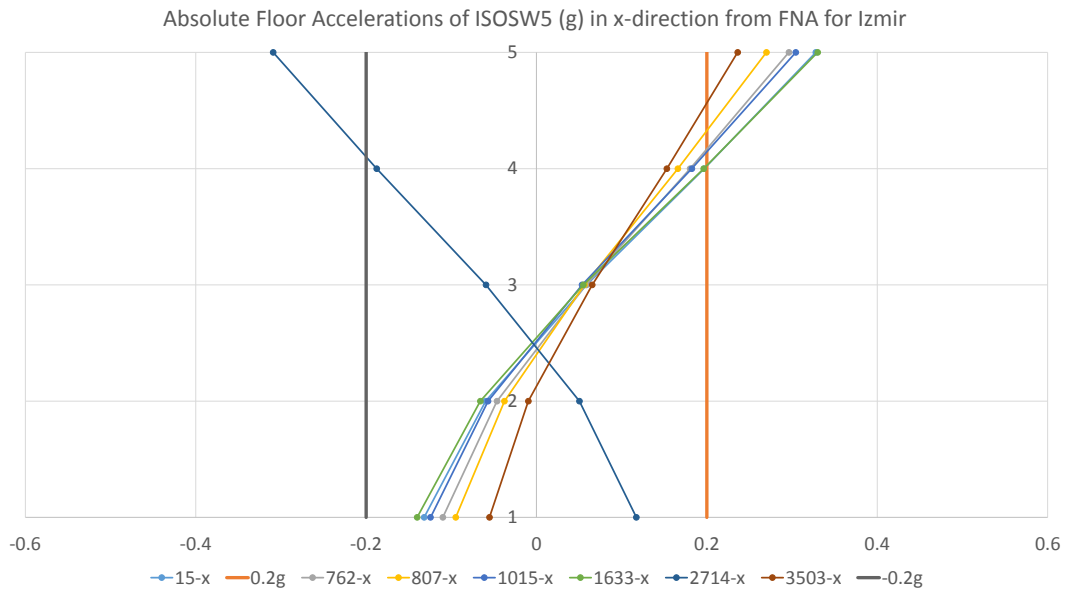


Figure 3.18: PFA(g) (in x direction) through Floors of ISOSW5 for Izmir DBE Level from FNA

Table3.19: Mean PFA (g) of ISOSW5 from the 7 GM Records in x-direction

	15-x	762-x	807-x	1015-x	1633-x	2714-x	3503-x
Maximum top floor acceleration (g)	0.328	0.296	0.270	0.304	0.330	-0.309	0.236
Mean (g)	0.296						

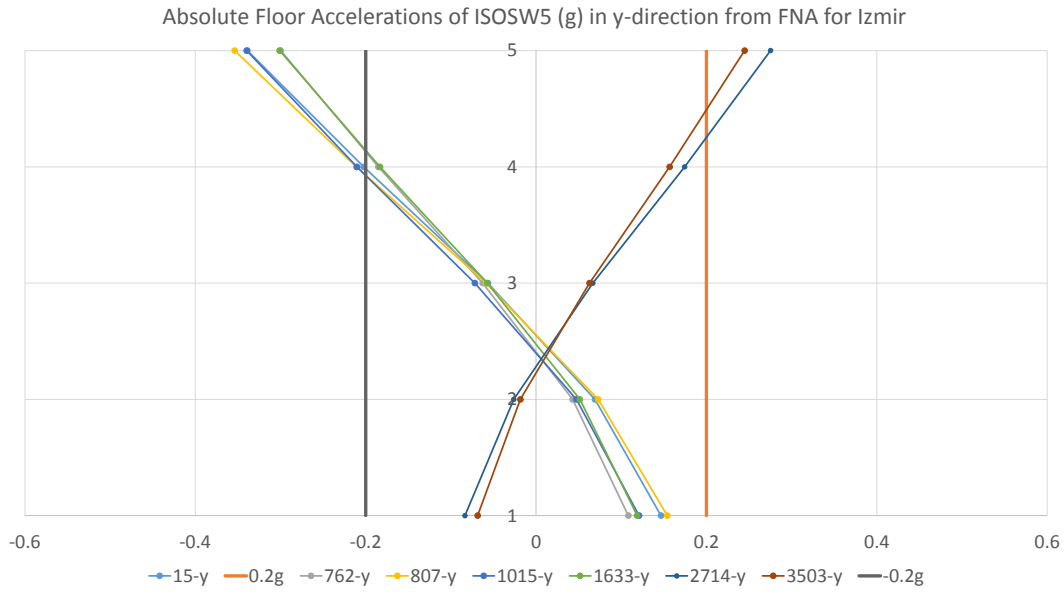


Figure 3.19: PFA(g) (in y direction) through Floors of ISOSW5 for Izmir DBE Level from FNA

Table3.20: Mean PFA (g) of ISOSW5 from the 7 GM Records in y-direction

	15-y	762-y	807-y	1015-y	1633-y	2714-y	3503-y
Maximum top floor acceleration (g)	-0.339	-0.300	-0.354	-0.340	-0.301	0.275	0.245
Mean (g)	0.308						

Based on Tables 3.19 and 3.20, mean value of the maximum top floor accelerations are decreased through 15, 10 and 5 floors as $0.420g$, $0.342g$ and $0.307g$, respectively. None of these values satisfies the maximum floor acceleration value of $0.2g$. However, linear elastic response spectrum analysis results had given desirable results regarding floor accelerations. This issue will be discussed in Chapter 4.

3.2.4 IDR(%) Results of ISOSW15 for Izmir from FNA

In this subsection, interstorey drift ratio distribution for ISOSW15 is represented by the results obtained from FNA.

In Figure 3.20 and 3.21, one can found the interstorey drift distribution through floors

of ISOSW15, which is the seismically isolated dual system.

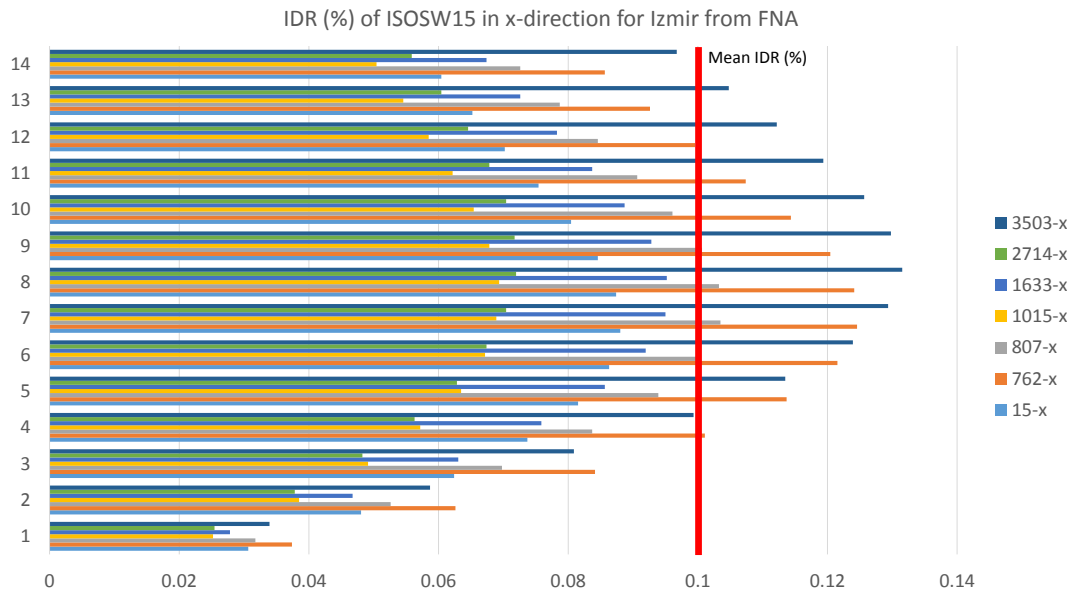


Figure 3.20: IDR(%) (in x direction) through Floors of ISOSW15 for Izmir DBE Level from FNA

Table3.21: Mean IDR(%) of 7 GM Records in x-direction for ISOSW15

	15-x	762-x	807-x	1015-x	1633-x	2714-x	3503-x
Maximum IDR (%)	0.088	0.125	0.103	0.069	0.095	0.072	0.131
Mean (%)	0.098						

As it can be seen from Figure 3.20 and 3.21, distribution trend of the interstorey drift values are different than those obtained from RSA, as presented in Figure 3.1 and 3.2, where the distribution was linearly decreasing through the upper floors.

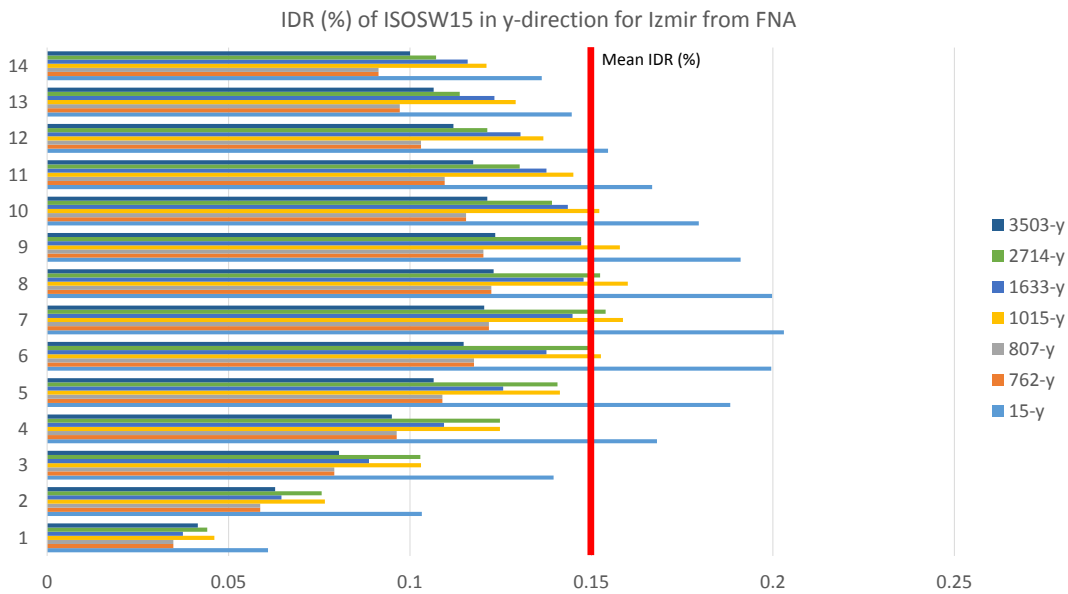


Figure 3.21: IDR(%) (in y direction) through Floors of ISOSW15 for Izmir DBE Level from FNA

Table3.22: Mean IDR(%) of 7 GM Records in y-direction for ISOSW15

	15-y	762-y	807-y	1015-y	1633-y	2714-y	3503-y
Maximum IDR (%)	0.203	0.122	0.122	0.160	0.147	0.154	0.123
Mean (%)	0.148						

It can also be deduced from Table 3.23 and 3.24 that RSA may underestimate also interstorey drift besides floor accelerations. Interstorey drift values that had been obtained from RSA were 0.077(%) for x direction and 0.104(%) for y direction. For x direction, interstorey drift ratio is observed to be underestimated by 1.28 times lower in case of RSA. In y direction, this value is equal to 1.42.

3.2.5 IDR(%) Results of ISOSW10 for Izmir from FNA

In this section, interstorey drift ratio values obtained from FNA for the 10 storey seismically isolated dual system are demonstrated. In Figure 3.22, interstorey drift values in x direction are obtained. It can be seen that the interstorey drift values are decreased as compared to the ones for ISOSW15.

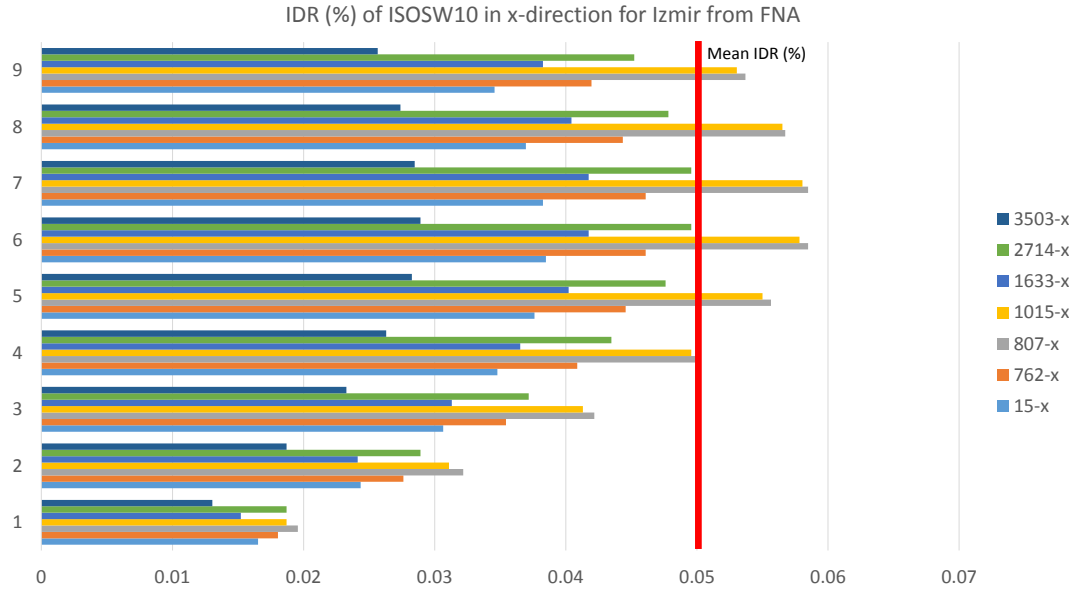


Figure 3.22: IDR(%) (in x direction) through Floors of ISOSW10 for Izmir DBE Level from FNA

Table3.23: Mean IDR(%) of 7 GM Records in x-direction for ISOSW10

	15-x	762-x	807-x	1015-x	1633-x	2714-x	3503-x
Maximum IDR (%)	0.038	0.046	0.058	0.058	0.042	0.050	0.029
Mean (%)	0.046						

From RSA for ISOSW10, maximum interstorey drift ratio was obtained as 0.038(%). This value is obtained as 0.046(%); which is 1.21 times higher than the interstorey drift value obtained from RSA.

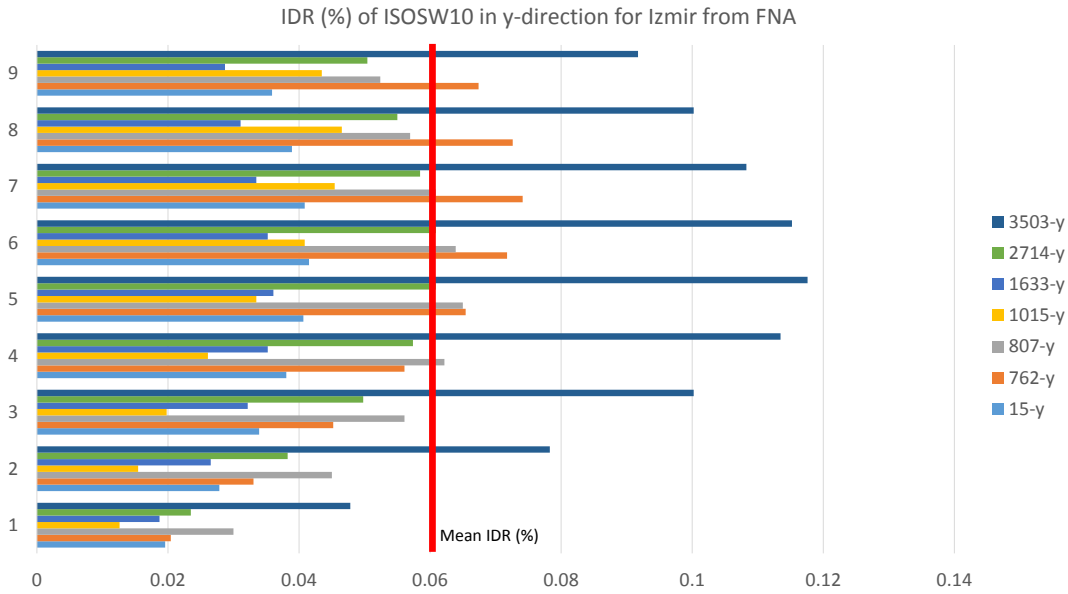


Figure 3.23: IDR(%) (in y direction) through Floors of ISOSW10 for Izmir DBE Level from FNA

In Figure 3.23, interstorey drift distribution in y direction is presented. Similar to the case in x direction, interstorey drift values are lower than those obtained from ISOSW15.

Table3.24: Mean IDR(%) of 7 GM Records in y-direction for ISOSW10

	15-y	762-y	807-y	1015-y	1633-y	2714-y	3503-y
Maximum IDR (%)	0.041	0.074	0.065	0.046	0.036	0.061	0.118
Mean (%)	0.063						

As it can be seen from Table 3.24, mean value of the maximum interstorey drift values obtained from 7 ground motion records from the modal response history is 0.063(%). This value had previously been obtained as 0.053(%) from RSA, which is 1.19 times lower.

3.2.6 IDR(%) Results of ISOSW5 for Izmir from FNA

In this subsection 3.2.6, interstorey drift ratios obtained from FNA procedures for ISOSW5 are presented.

In Figures 3.24 and 3.25, interstorey drift distribution from each 7 ground motion input are demonstrated for the two corresponding earthquake direction, x and y, respectively.

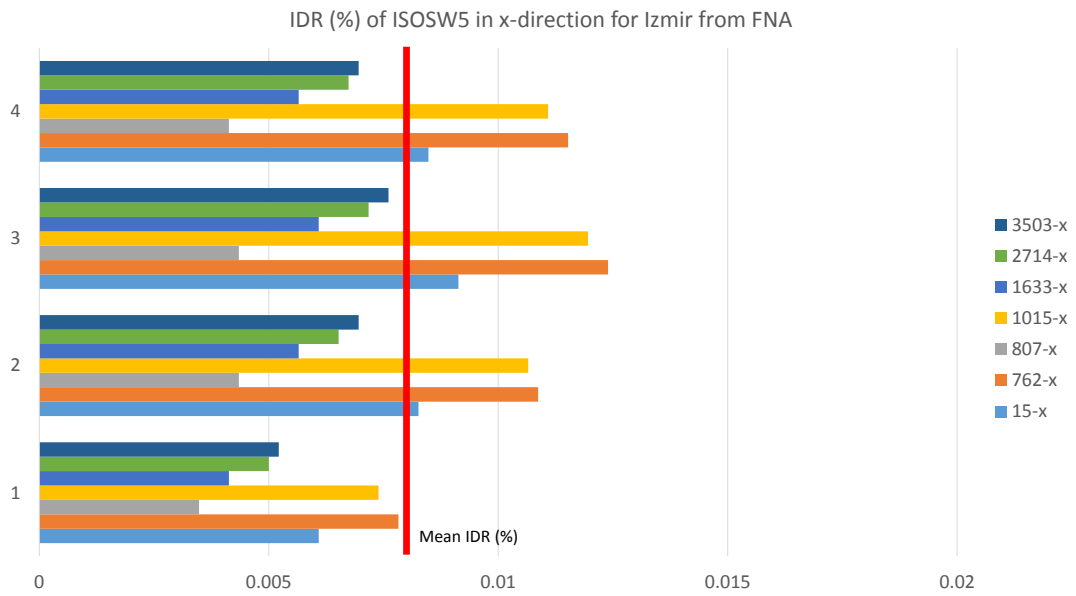


Figure 3.24: IDR(%) (in x direction) through Floors of ISOSW5 for Izmir DBE Level from FNA

Table3.25: Mean IDR(%) of 7 GM Records in x-direction for ISOSW5

	15-x	762-x	807-x	1015-x	1633-x	2714-x	3503-x
Maximum IDR (%)	0.009	0.012	0.004	0.012	0.006	0.007	0.008
Mean (%)	0.008						

Maximum interstorey drift values obtained as a mean of 7 ground motion response is stated in Tables 3.25 and 3.26 as 0.008(%) and 0.016(%) for x and y directions, respectively.

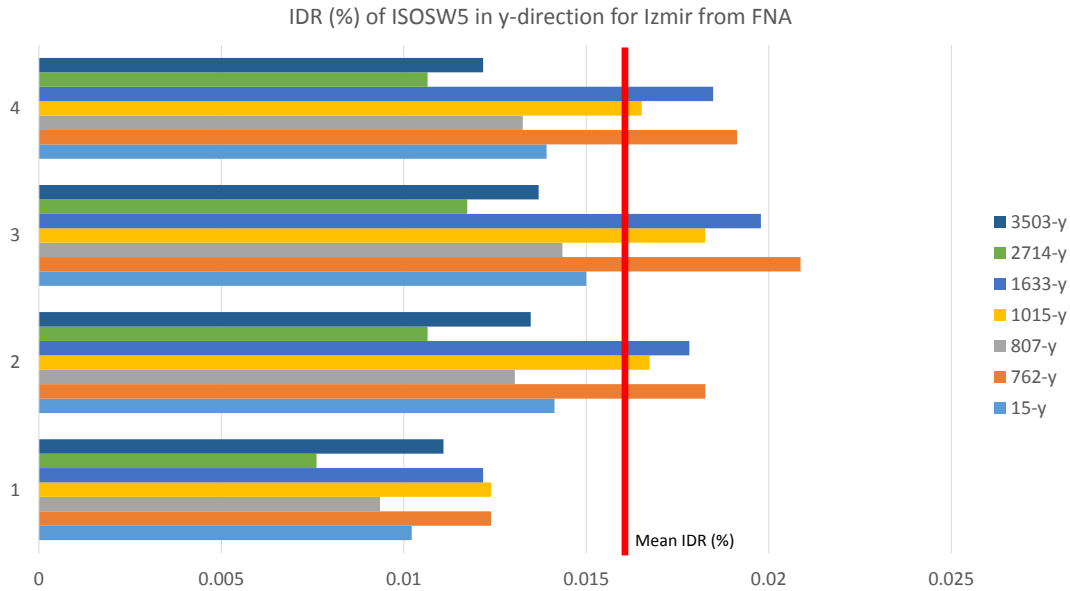


Figure 3.25: IDR(%) (in y direction) through Floors of ISOSW5 for Izmir DBE Level from FNA

Table3.26: Mean IDR(%) of 7 GM Records in y-direction for ISOSW5

	15-y	762-y	807-y	1015-y	1633-y	2714-y	3503-y
Maximum IDR (%)	0.015	0.021	0.014	0.018	0.02	0.012	0.014
Mean (%)	0.016						

From RSA, maximum interstorey drift values for ISOSW5 for x and y directions had been obtained as 0.012(%) and 0.014(%), respectively. In x direction, FNA is resulted in 1.5 times lower than the one obtained from RSA this time. In y direction, however, it is obtained from FNA as 1.14 times higher than the maximum interstorey drift ratio resulted from RSA.

It can be stated that the difference in the amount of response regarding interstorey drift ratio values resulted from FNA and RSA methods decreases as the number of

floors decreases from 15 through 10 and 5.

3.3 Summary and Discussion of Analysis Results

From linear elastic response spectrum analysis, maximum values obtained for interstorey drift ratio and floor accelerations from the corresponding structural systems are tabulated in Figures 3.26 to 3.29. In the same figures, the efficiency ratios (%) are also provided regarding the reduction in response of each structural system in the case of being seismically isolated or non-isolated 15, 10 and 5 storey systems from RSA of Izmir and Isparta separately. Based on Figure 3.26, seismic isolation application

Interstorey Drift Ratio (%)						
izmir, Tiso=3 sec			shear walled systems	Isparta, Tiso=3 sec		
	max IDR (%)				max IDR (%)	
	x	y		x	y	
ISOSW15	0.077	0.104		ISOSW15	0.124	0.169
SWFB15	0.504	0.542		SWFB15	0.779	0.953
ISOSW15/SWFB15	658	521 (%)		ISOSW15/SWFB15	631	564 (%)
	max IDR (%)			max IDR (%)		
	x	y		x	y	
ISOSW10	0.038	0.053		ISOSW10	0.061	0.087
SWFB10	0.395	0.473		SWFB10	0.627	0.719
ISOSW10/SWFB10	1048	888 (%)		ISOSW10/SWFB10	1026	825 (%)
	max IDR (%)			max IDR (%)		
	x	y		x	y	
ISOSW5	0.012	0.014		ISOSW5	0.018	0.025
SWFB5	0.246	0.260		SWFB5	0.317	0.355
ISOSW5/SWFB5	2100	1818 (%)		ISOSW5/SWFB5	1743	1437 (%)

Figure 3.26: (%) Reduction in Interstorey Drift Ratio (%) for Dual Systems Izmir & Isparta

to the fixed base dual system with 5 floors is found to be the most efficient, such that, for Izmir, interstorey drift values found to be 18-21 times lower (1818% in y direction and 2100% in x direction) in the seismically isolated system compared to the same system as it is conventionally designed. The reduction ratio in interstorey drift values

through decreasing number of floors from 15 to 10 and 5 are getting lower. In 10 storey systems, the ratio is 8.88 for x direction and 10.48 for y direction. In 5 storey systems, these values are 6.58 for x direction and 5.21 for y direction. Since the rigidity of fixed base dual systems were higher in x direction, the reduction in interstorey drift values is observed to be higher in x direction.

In Figure 3.26, it can also be noticed that the order of magnitude of the reduction ratios for Isparta are almost the same as those in Izmir. This is a natural consequence of the method of analysis being linear.

Interstorey Drift Ratio (%)						
Izmir, Tiso=3 sec			moment frame systems	Isparta, Tiso=3 sec		
max IDR (%)				max IDR (%)		
	x	y			x	y
ISO15	0.290	0.247		ISO15	0.478	0.407
FB15	1.127	0.918		FB15	1.876	1.528
ISO15/FB15	389	372 (%)		ISO15/FB15	392	375 (%)
max IDR (%)			max IDR (%)			
	x	y		x	y	
ISO10	0.199	0.165	ISO10	0.326	0.269	
FB10	1.087	0.933	FB10	1.868	1.528	
ISO10/FB10	546	565 (%)	ISO10/FB10	573	568 (%)	
max IDR (%)			max IDR (%)			
	x	y		x	y	
ISO5	0.090	0.073	ISO5	0.146	0.120	
FB5	0.939	0.772	FB5	1.469	1.217	
ISO5/FB5	1046	1061 (%)	ISO5/FB5	1009	1017 (%)	

Figure 3.27: (%) Reduction in Interstorey Drift Ratio (%) for Moment Frame Systems Izmir & Isparta

In Figure 3.27, interstorey drift reduction ratios of the systems considered are presented for the moment frame systems. Based on Figure 3.27, most efficient seismically isolated system is observed to be the one with 5 floor as compared to the ones with 10 and 15 floors. However, the highest reduction ratio is 10.46 for x direction and 10.61 for y direction, which are about the half of the 5 storey dual system. This is simply because of the difference in rigidity of dual systems and moment frame sys-

tems, such that dual systems obviously undergo higher base shear. Compatibility of results for Izmir and Isparta is also valid for the moment frame systems.

Top Floor Acceleration (g)								
Izmir, Tiso=3 sec				shear walled systems	Isparta, Tiso=3 sec			
max TFA (g)					max TFA (g)			
	x	y			x	y		
ISOSW15	0.117	0.125			ISOSW15	0.189	0.197	
SWFB15	0.252	0.188			SWFB15	0.338	0.271	
ISOSW15/SWFB15	216	151	(%)		ISOSW15/SWFB15	179	138	(%)
max TFA (g)					max TFA (g)			
	x	y			x	y		
ISOSW10	0.101	0.104			ISOSW10	0.164	0.170	
SWFB10	0.296	0.235			SWFB10	0.404	0.316	
ISOSW10/SWFB10	292	226	(%)	ISOSW10/SWFB10	247	185	(%)	
max TFA (g)				max TFA (g)				
	x	y		x	y			
ISOSW5	0.099	0.099		ISOSW5	0.162	0.161		
SWFB5	0.421	0.319		SWFB5	0.534	0.423		
ISOSW5/SWFB5	426	323	(%)	ISOSW5/SWFB5	330	263	(%)	

Figure 3.28: (%) Reduction in Top Floor Accelerations (g) for Dual Systems Izmir & Isparta

In Figure 3.28, reduction ratios for the maximum top floor acceleration values of dual systems are presented. Similar to interstorey drift reduction ratios, efficacy of the systems increases as the number of floor decreases.

Finally, in Figure 3.29, reduction ratios for the maximum top floor acceleration values of moment frame systems are tabulated. Having lower reduction factors compared to dual systems, the trend of change is similar to dual systems. Note that, in the moment frame system with 15 floors, the reduction in top floor acceleration in case of seismic isolation found to be lower than conventionally designed case as having a reduction factor 0.66 in x direction and 0.66 in y direction. Similar results obtained from RSA of Isparta with a reduction factor in x direction as 0.79 and 0.74 in y direction. Although linear elastic response spectrum analysis is unfavorable to estimate the floor accelerations accurately, these reduction factors are the indication of inefficiency of seismic isolation application to 15 floor moment frame system regarding the reduction

Top Floor Acceleration (g)							
İzmir, Tiso=3 sec				moment frame systems	Isparta, Tiso=3 sec		
max TFA (g)					max TFA (g)		
	x	y			x	y	
ISO15	0.152	0.144			ISO15	0.195	0.196
FB15	0.101	0.095			FB15	0.155	0.145
ISO15/FB15	66	66	(%)		ISO15/FB15	79	74 (%)
max TFA (g)					max TFA (g)		
	x	y			x	y	
ISO10	0.124	0.116			ISO10	0.198	0.186
FB10	0.134	0.127			FB10	0.205	0.191
ISO10/FB10	108	110	(%)	ISO10/FB10	104	103 (%)	
max TFA (g)				max TFA (g)			
	x	y		x	y		
ISO5	0.107	0.100		ISO5	0.172	0.163	
FB5	0.196	0.184		FB5	0.283	0.268	
ISO5/FB5	183	183	(%)	ISO5/FB5	165	165 (%)	

Figure 3.29: (%) Reduction in Top Floor Accelerations (g) for Moment Frame Systems Izmir & Isparta

in floor accelerations.

Through FNA performed for the seismically isolated dual systems with 15, 10 and 5 floors (ISOSW15, ISOSW10, ISOSW5), it is observed that linear elastic analysis procedure underestimates especially top floor acceleration such that; in RSA, maximum top floor acceleration observed for ISOSW15 in the case of Izmir seismicity was found as $0.117g$ and $0.125g$ in x and y directions, respectively. However, FNA resulted in a maximum of $0.420g$ in x direction and $0.396g$ in y direction. For ISOSW10, these values obtained as $0.101g$ in x direction and $0.104g$ in y direction, whereas FNA resulted in $0.343g$ in x direction and $0.396g$ in y direction. Similarly, seismically isolated dual system with 5 floors (ISOSW5) had top floor accelerations of $0.099g$ for both x and y directions from RSA; on the other hand, FNA resulted in top floor acceleration values of $0.296g$ in x direction and $0.308g$ in y direction.

CHAPTER 4

SUMMARY AND CONCLUSIONS

4.1 Summary

In this study, different structural systems which are:

- Seismically Isolated Dual System,
- Seismically Isolated Moment Frame System,
- Fixed Base Dual System and
- Fixed Base Moment Frame System

are seismically analyzed and compared to each other in the cases of these systems having different number of floors as 15, 10 and 5. The seismic analysis is performed for two site-specific seismicity levels, namely, Izmir and Isparta, each of which first degree seismic zones from Turkey. To compare the seismic isolation efficiency level of each system regarding its fixed base and seismically isolated cases, linear elastic response spectrum analysis is performed for DBE level earthquake for both Izmir and Isparta. The main parameters to assess the seismic isolation efficiency are selected as i) interstorey drift ratio and ii) floor acceleration.

4.2 Conclusion

Based on this study, following aspects can be deduced:

- For both dual systems and moment frame systems, seismic isolation efficiency observed to be decreased as the number of floor increases. In other words, seismic isolation is more efficient for short period structures.
- The amount of seismic isolation efficiency is structural system dependent. This can be concluded from the fact that the efficiency obtained from seismically isolated moment frame systems is about half of the efficiency that from dual systems.
- Linear elastic response spectrum analysis is found to be consistent as the order of magnitude of the responses obtained from different seismicity levels, Izmir and Isparta is almost the same for the same targeted seismic isolation performance.
- For the reason specified in the previous item, linear elastic response spectrum analysis may be used as a tool to compare the reduction or amplification of responses between different systems. However, since it may underestimate the exact response, especially floor accelerations, making use of the acceleration responses obtained from linear elastic procedures for nonstructural damage sensitivity assessment may be unfavorable.
- Maximum floor acceleration criteria specified in [21] may be open to discussion due to the fact that it is highly dependent on the method of analysis and selected ground motions used in nonlinear analysis procedures.
- Appropriate seismic isolation design ends up with satisfying modal mass participation from the fundamental mode of vibration, which ensures almost a rigid body motion in the system where interstorey drift values are significantly minimized.

4.3 Recommendation for Future Work

To assess non-structural damage, estimation of peak floor acceleration distribution needs to be studied in detail, as in the work of [10], [13], [18] and [26] several methods may be generated to estimate peak floor accelerations. It seems that non-structural damage assessment requires deep and extensive research.

REFERENCES

- [1] AASHTO, American Association of State Highway and Transportation Officials. Guide Specifications for Seismic Isolation Design, 4th Edition, 2014.
- [2] A.B.M. Saiful Islam, M. Jameel, M.A. Uddin and Syed Ishtiaq Ahmed. Simplified design guidelines for seismic base isolation in multi-storey buildings for Bangladesh National Building Code (BNBC). *International Journal of the Physical Sciences*, 2011.
- [3] ASCE. Prestandard and Commentary for the Seismic Rehabilitation of Buildings. Prepared for "Federal Emergency Management Agency" (FEMA), 2000.
- [4] ASCE. Seismic Rehabilitation of Existing Buildings (ASCE/SEI 41-06), 2006.
- [5] ASCE. Minimum Design Loads for Buildings and Other Structures (ASCE 7-10), 2010.
- [6] ASCE. Minimum Design Loads for Buildings and Other Structures (ASCE 7-16), 2016.
- [7] B. O. Ay and S. Akkar. A procedure on ground motion selection and scaling for nonlinear response of simple structural systems. Published online in Wiley Online Library, 2012.
- [8] A. Baratta and I. Corbi. Optimal design of base-isolators in multi-storey buildings. *Computers & Structures*, 82(23–26):2199 – 2209, 2004. Computational Structures Technology.
- [9] Computers & Structures, Inc. (CSI). Integrated Software for Structural Analysis and Design, 2016.
- [10] D. Lopez Garcia, P. Price, P. Wichmann. Peak floor accelerations in multistory buildings subjected to earthquakes. The 14th World Conference on Earthquake Engineering, 2008.
- [11] J. E. Dairesi. İzmir Yakın Çevresinin Diri Fayları ve Deprem Potansiyelleri. MTA Rapor No: 10754, 2005.
- [12] Dimos C. Charmpis, Petros Komodromos and Marios C. Phocas. Optimized earthquake response of multi-storey buildings with seismic isolation at various elevations. Published online 27 March 2012 in Wiley Online Library, 2012.

- [13] H. Akhlaghi and A.S. Moghadam. Height-wise distribution of peak horizontal floor acceleration (PHFA). The 14th World Conference on Earthquake Engineering, 2008.
- [14] Haider S. AL-Jubair and Fareed H. Majeed. The effect of shear walls on seismically isolated buildings of variable geometric configurations. International Journal of Engineering Research & Technology, 2014.
- [15] A. B. M. S. Islam, M. Jameel, M. Z. Jumaat, and M. M. Rahman. Optimization in structural altitude for seismic base isolation at medium risk earthquake disaster region. *Disaster advances*, 6(1):23–34, 2013.
- [16] Kamrava A. Seismic isolators and their types. Special Issue of Current World Environment 2015, 2015.
- [17] M. C. Phocas and G. Pamboris. Multi-storey structures with compound seismic isolation. WIT Transactions on The Built Environment, 2009.
- [18] M. Saatcioglu, M. Shooshtari, N. Naumoski and S. Foo. Development of floor design spectra for operational and functional components of concrete buildings in Canada. 14th World Conference on Earthquake Engineering, 2008.
- [19] E. Mavronicola and P. Komodromos. Assessing the suitability of equivalent linear elastic analysis of seismically isolated multi-storey buildings. *Comput. Struct.*, 89(21-22):1920–1931, Nov. 2011.
- [20] Mehmet Halis Gunel and Huseyin Emre Ilgin . Tall Buildings Structural Systems and Aerodynamic Form, 2014.
- [21] Ministry of Health, Republic of Turkey. Deprem Yalıtımlı olarak İnşa Edilecek Yapılara Ait Proje ve Yapım İşlerinde Uyulması Gereken Asgari Standartlar, 2013.
- [22] Ministry of Public Works and Settlement Government of Republic of Turkey. Specification for Buildings to be Built in Seismic Zones (TEC 2007), 2007.
- [23] N. T. Ozcan. Site Specific Probabilistic Seismic Hazard Analysis for Isparta, 2015.
- [24] N. T. Ozcan. Site Specific Probabilistic Seismic Hazard Analysis for Izmir, 2015.
- [25] Prota Software. Probina Orion 2013 v.13, 2015.
- [26] Samit Ray Chaudhuri and Tara C. Hutchinson. Distribution of peak horizontal floor acceleration for estimating nonstructural element vulnerability. 13th World Conference on Earthquake Engineering, 2004.
- [27] Seismo Soft. SeismoSignal, a software processing strong ground motion, 2015.

- [28] Shanmuga Priya D., Cinitha A., Umesha P. K. and Nagesh R. Iyer. Enhancing the seismic response of buildings with energy dissipation methods –An overview. *Journal of Civil Engineering Research*, 2014.
- [29] H. R. E. Siller. *Non-linear Modal Analysis Methods for Engineering Structures*. A thesis submitted for the degree of Doctor of Philosophy in Mechanical Engineering, University of London, 2004.
- [30] S. Trevor E Kelly. *Base Isolation Design Guidelines*, 2001.
- [31] Turkish Standards Institute (TSE). *Design Loads for Buildings (TS 498)*, 1997.
- [32] Turkish Standards Institute (TSE). *Requirements for Design and Construction of Reinforced Concrete Structures (TS 500)*, 2000.
- [33] William J. McVitty and Michael C. Constantinou. *Property Modification Factors for Seismic Isolators: Design Guidance for Buildings*, 2015.
- [34] E. L. Wilson. *Three Dimensional Static and Dynamic Analysis of Structures*, 2000.

APPENDIX A

SEISMIC PARAMETERS OF PSHA FOR IZMIR

This appendix chapter is based on [24].

TableA.1: Seismic sources defined for Izmir site

No	Seismic Source Zone
3	North Anatolian Fault System - Segment C
17	Alaşehir - İzmir (Gediz) Graben
18	Büyük Menderes Graben
19	Gökova Fault Zone
24	Simav - Akşehir Fault Zone
35	Background Seismic Activity - West A
36	Background Seismic Activity - West B
41	Background Seismic Activity - Inner 1

TableA.2: Standard Least Square Regression, All Earthquakes

Region No	3	17	18	19	24	35	36	41
Minimum Magnitude	4.5	4.5	4.5	4.5	4.5	4.5	4.5	4.5
Maximum Magnitude	7.4	7.2	7.1	7.8	7.2	5.3	5.9	5.4
Activity Rate (#/year)	2.400	2.188	0.430	5.001	2.762	0.228	5.155	1.204
β	1.699	2.326	1.516	2.236	2.083	3.129	2.828	2.025
A (Rupture Length p.)	-2.57	-2.57	-2.57	-2.57	-2.57	-2.57	-2.57	-2.57
B (Rupture Length p.)	0.62	0.62	0.62	0.62	0.62	0.62	0.62	0.62



Figure A.1: Dominant seismic sources for Izmir site

TableA.3: Maximum Likelihood Method, All Earthquakes

Region No	3	17	18	19	24	35	36	41
Minimum Magnitude	4.5	4.5	4.5	4.5	4.5	4.5	4.5	4.5
Maximum Magnitude	7.4	7.2	7.1	7.8	7.2	5.3	5.9	5.4
Activity Rate (#/year)	2.400	2.188	0.430	5.001	2.762	0.228	5.155	1.204
β	3.062	2.395	3.454	3.247	2.809	3.129	2.828	2.025
A (Rupture Length p.)	-2.57	-2.57	-2.57	-2.57	-2.57	-2.57	-2.57	-2.57
B (Rupture Length p.)	0.62	0.62	0.62	0.62	0.62	0.62	0.62	0.62

TableA.4: Standard Least Square Regression, Main Shocks Only

Region No	3	17	18	19	24	35	36	41
Minimum Magnitude	4.5	4.5	4.5	4.5	4.5	4.5	4.5	4.5
Maximum Magnitude	7.4	7.2	7.1	7.8	7.2	5.3	5.9	5.4
Activity Rate (#/year)	1.138	1.330	0.336	2.659	0.940	0.169	4.248	0.978
β	1.380	2.050	1.350	2.013	1.504	2.408	2.842	2.290
A (Rupture Length p.)	-2.57	-2.57	-2.57	-2.57	-2.57	-2.57	-2.57	-2.57
B (Rupture Length p.)	0.62	0.62	0.62	0.62	0.62	0.62	0.62	0.62

TableA.5: Maximum Likelihood Method, Main Shocks Only

Region No	3	17	18	19	24	35	36	41
Minimum Magnitude	4.5	4.5	4.5	4.5	4.5	4.5	4.5	4.5
Maximum Magnitude	7.4	7.2	7.1	7.8	7.2	5.3	5.9	5.4
Activity Rate (#/year)	1.138	1.330	0.336	2.659	0.940	0.169	4.248	0.978
β	2.162	2.075	1.294	2.579	1.695	2.947	2.842	2.290
A (Rupture Length p.)	-2.57	-2.57	-2.57	-2.57	-2.57	-2.57	-2.57	-2.57
B (Rupture Length p.)	0.62	0.62	0.62	0.62	0.62	0.62	0.62	0.62

TableA.6: Subjective Probabilities of Alternative Assumptions (Logic Tree Method)

	Alternative Assumptions	Subjective Probability
Catalogues	All Earthquakes	0.50
	Main Shocks Only	0.50
Recurrence Relations	Standard Least Squares Regression	0.40
	Maximum Likelihood Method	0.60
Ground Motion Prediction Equations	Boore & Joyner & Fumal 1997	0.33
	Kalkan & Gülkan 2004	0.33
	Abrahamson & Silva 2008 NGA	0.33

TableA.7:

Ground Motion Prediction Equations
Boore Joyner Fumal (1997)
Kalkan and Gülkan (2004)
Abrahamson Silva (2008) NGA

TableA.8:

V_{s30} (m/s)
750

APPENDIX B

SEISMIC PARAMETERS OF PSHA FOR ISPARTA

This appendix chapter is based on [23].

TableB.1: Seismic Source Zones for Isparta

No	Seismic Source Zone
17	Alaşehir-İzmir (Gediz) Graben
18	Büyük Menderes Graben
19	Gökova Fault Zone
20	Finike Fault Zone
22	İnönü Eskişehir Fault Zone
23	Kütahya Fault Zone
24	Simav-Alaşehir Fault Zone
25	Çameli-Burdur Fault Zone
26	Kovada Fault Zone
45	Background Seismic Activity Region 5

TableB.2: Parameters for seismic source zones

Region No	17	18	19	20	22	23	24	25	26	45
Minimum Magnitude	5.0	5.0	5.0	5.0	5.0	5.0	5.0	5.0	5.0	5.0
Maximum Magnitude	7.2	7.1	7.6	7.2	7.1	6.9	7.2	7.1	6.1	5.6
Activity Rate (#/year)	1.330	0.336	1.657	0.804	0.207	0.192	0.940	0.289	0.229	1.996
β	2.075	1.294	1.407	2.924	1.445	2.855	1.695	1.439	2.924	2.395
A (Rupture Length p.)	-2.57	-2.57	-2.57	-2.57	-2.57	-2.57	-2.57	-2.57	-2.57	-2.57
B (Rupture Length p.)	0.62	0.62	0.62	0.62	0.62	0.62	0.62	0.62	0.62	0.62

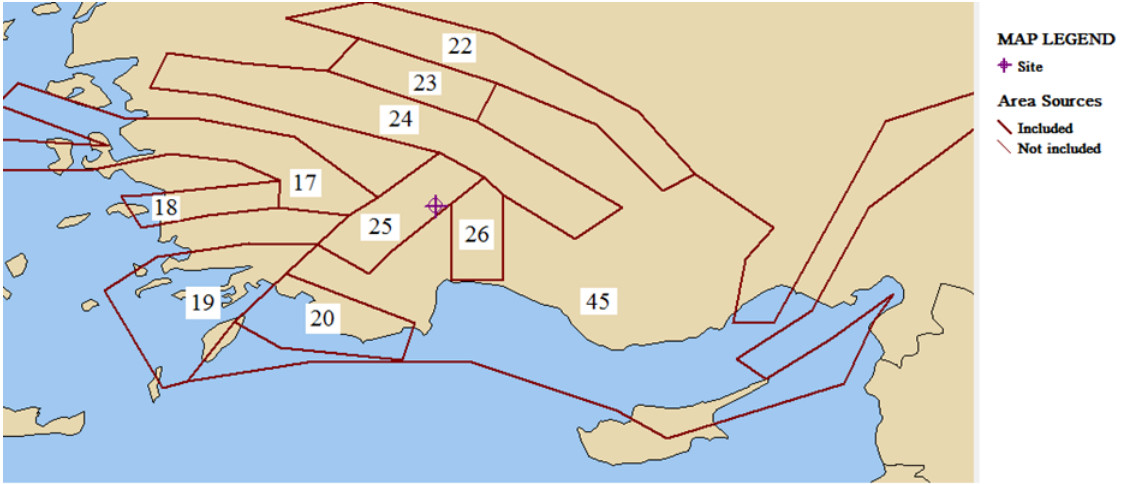


Figure B.1: Seismic Source Zones Defined for Europe and Eastern Mediterian Regions

TableB.3:

Ground Motion Prediction Equation
Boore Joyner Fumal (1997)

TableB.4:

V_{s30} (m/s)
350

APPENDIX C

RSA RESULTS FOR ISPARTA

RSA had been performed for Isparta as well to investigate the effect of higher seismic demands to the efficiency of seismic isolated applied to different structural systems with dissimilar number of floors.

The RSA Results for Isparta had been delivered as well in the order of IDR(%) and PFA(g) for 15,10 and 5 storey structural systems specified in Table 2.1, respectively.

For the seismically isolated systems, targetted seismic isolation period will be the same as the ones for Izmir, as it is stated in Tables 2.11 and 2.12 in Chapter 2.

In subsection C.1, interstorey distribution of 15 storey systems are presented for linear elastic RSA.

C.1 IDR(%) Results of ISOSW15, ISO15, SWFB15, FB15 for Isparta

In Figures C.1 and C.2; similar results are obtained as in Figures 3.1 and 3.2, respectively.

Under the seismicity of Isparta, as well, there is no seismically isolated system exceeding maximum interstorey drift limit specified in Table 3.1 for the structural systems with 15 floors. Naturally, interstorey drift ratio values obtained for Isparta are greater than those from Izmir.

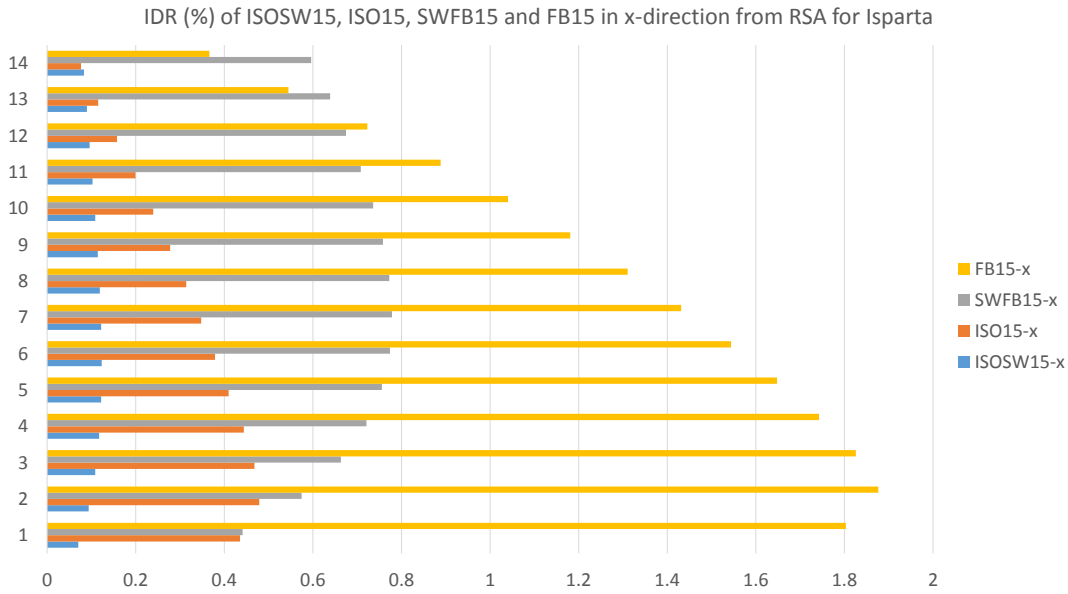


Figure C.1: IDR(%) (in x direction) through Floors of 15 Storey Systems for Isparta DBE Level from RSA

C.2 PFA(g) Results of ISOSW15, ISO15, SWFB15, FB15 for Isparta

In this subsection C.2, floor acceleration values obtained from the seismic action for Isparta are figured out.

In Figures C.3 and C.4, general trend of behavior is similar to the ones obtained for Izmir for 15 storey systems. However, magnitude of floor accelerations are higher because of higher spectral acceleration input from Isparta is present.

C.3 IDR(%) Results of ISOSW10, ISO10, SWFB10, FB10 for Isparta

In Figures C.5 and C.6; similar results are obtained again as in the 10 storey systems analyzed for Izmir.

As it is expected, interstorey drift values obtained from the systems with 10 floors are lower than those from 15 floors, as in the case of Izmir.

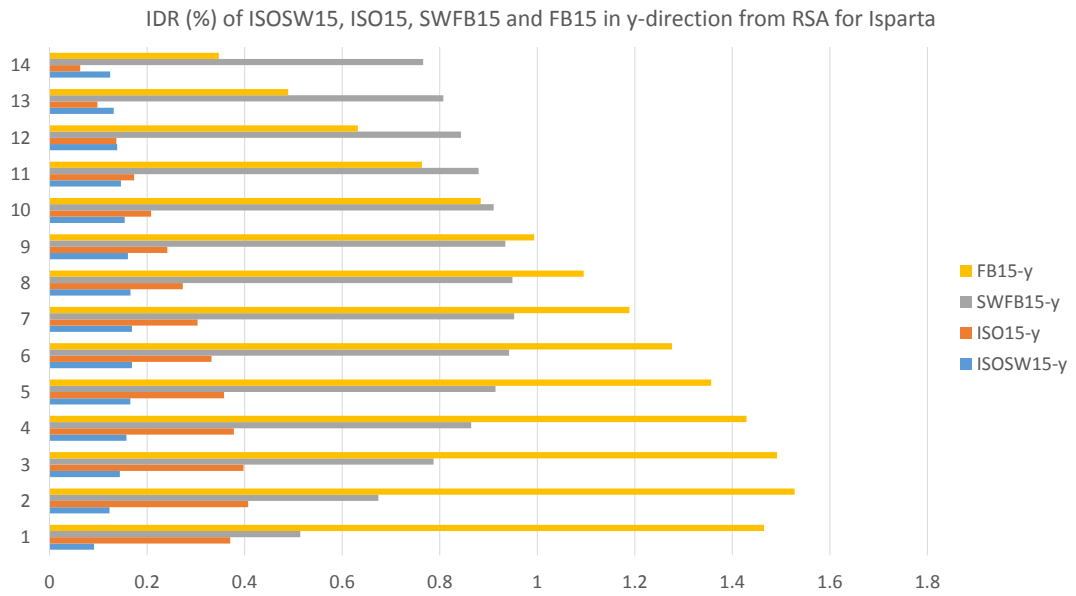


Figure C.2: IDR(%) (in y direction) through Floors of 15 Storey Systems for Isparta DBE Level from RSA

C.4 PFA(g) Results of ISOSW10, ISO10, SWFB10, FB10 for Isparta

As in the case of Izmir, floor acceleration values of fixed base systems are increased as the number of floors are decreased from 15 floors to 10 floors for Isparta. As it is previously mentioned in subsection 3.1.6, this is stemming from the increase in rigidity of the system while decrease in the flexibility. However, note that magnitude and distribution of floor accelerations in seismically isolated systems does not differ significantly since the seismic force to be transferred to the superstructure is governed by seismic isolation. Still, linear elastic response spectrum analysis is expected not to be assured to give the exact situation regarding accelerations being already irrespective of non-linear characteristics of the isolator units.

In Figures C.7 and C.8, increase in floor acceleration values can be investigated as compared to Figures C.3 and C.4, respectively.

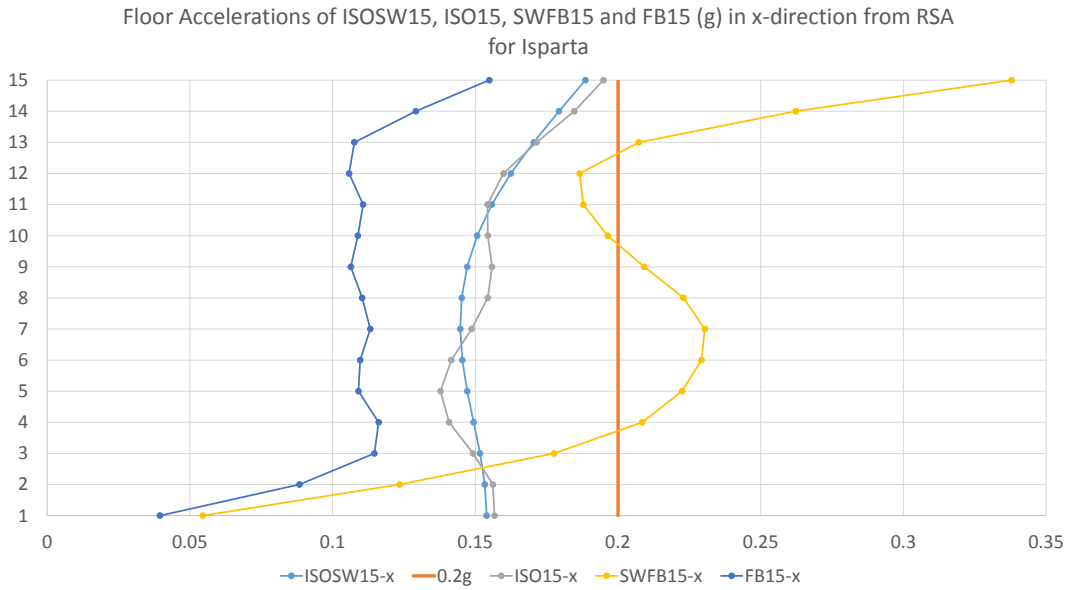


Figure C.3: PFA(g) (in x direction) through Floors of 15 Storey Systems for Isparta DBE Level from RSA

C.5 IDR(%) Results of ISOSW5, ISO5, SWFB5, FB5 for Isparta

Regarding the change in interstorey drift ratio through floors of 5 storey systems for Isparta, Figure C.9 shows the distribution in x direction and Figure C.10 in y direction.

As it can be seen from Figure C.9 and Figure C.10, drift values are decreasing for decreasing number of floors from 15 to 10 and finally, 5.

C.6 PFA(g) Results of ISOSW5, ISO5, SWFB5, FB5 for Isparta

In this subsection, final results from RSA are presented for Isparta. Similar distribution is achieved for floor accelerations in Figure C.11 and Figure C.12 with the ones in Figure 3.11 and Figure 3.12 which are obtained for Izmir.

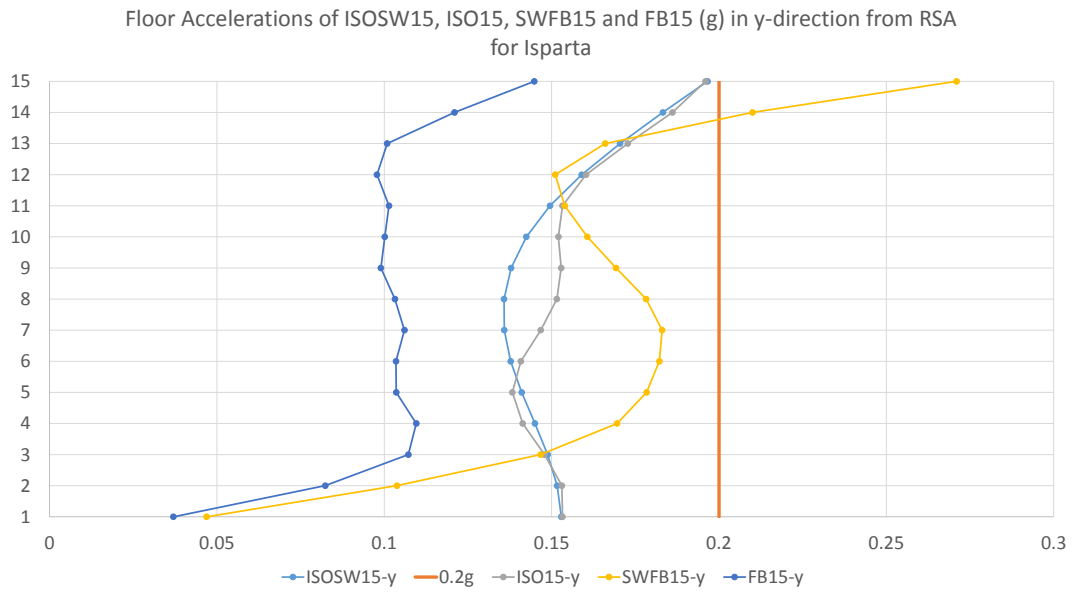


Figure C.4: PFA(g) (in y direction) through Floors of 15 Storey Systems for Isparta DBE Level from RSA

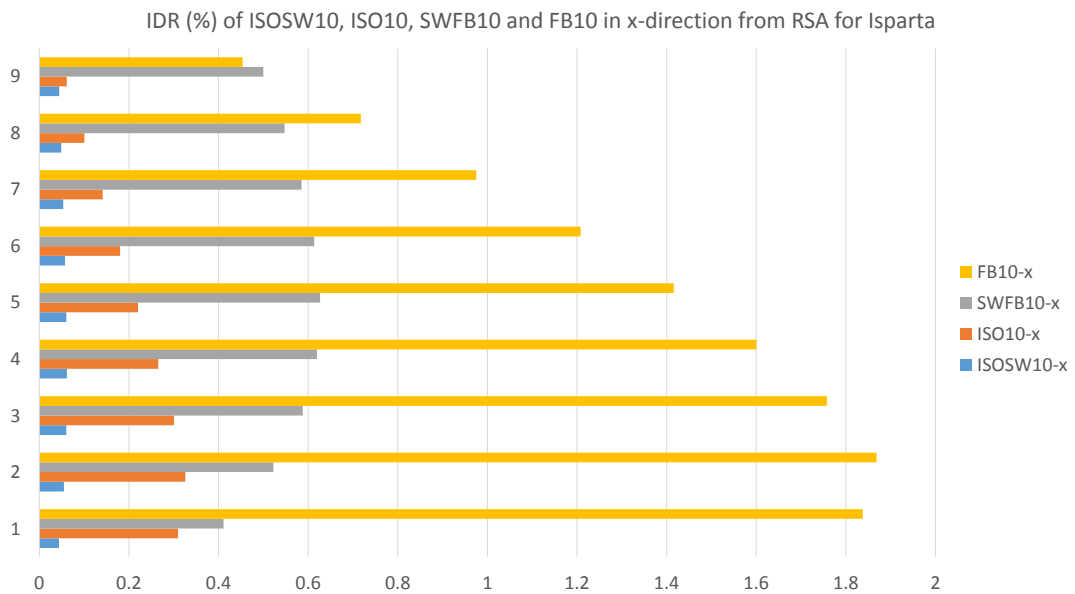


Figure C.5: IDR(%) (in x direction) through Floors of 10 Storey Systems for Isparta DBE Level from RSA

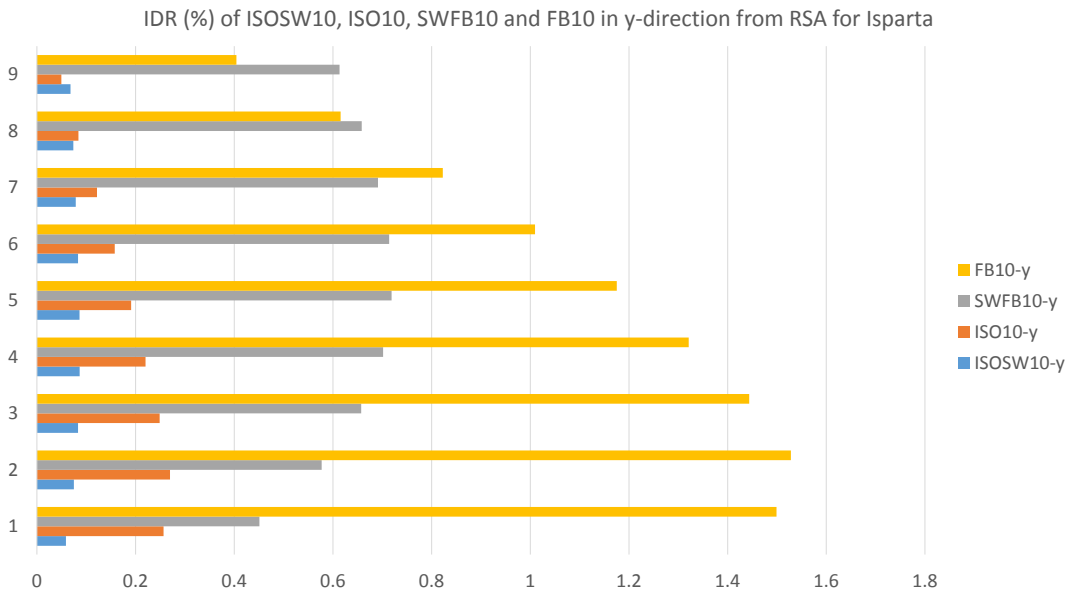


Figure C.6: IDR(%) (in y direction) through Floors of 10 Storey Systems for Isparta DBE Level from RSA

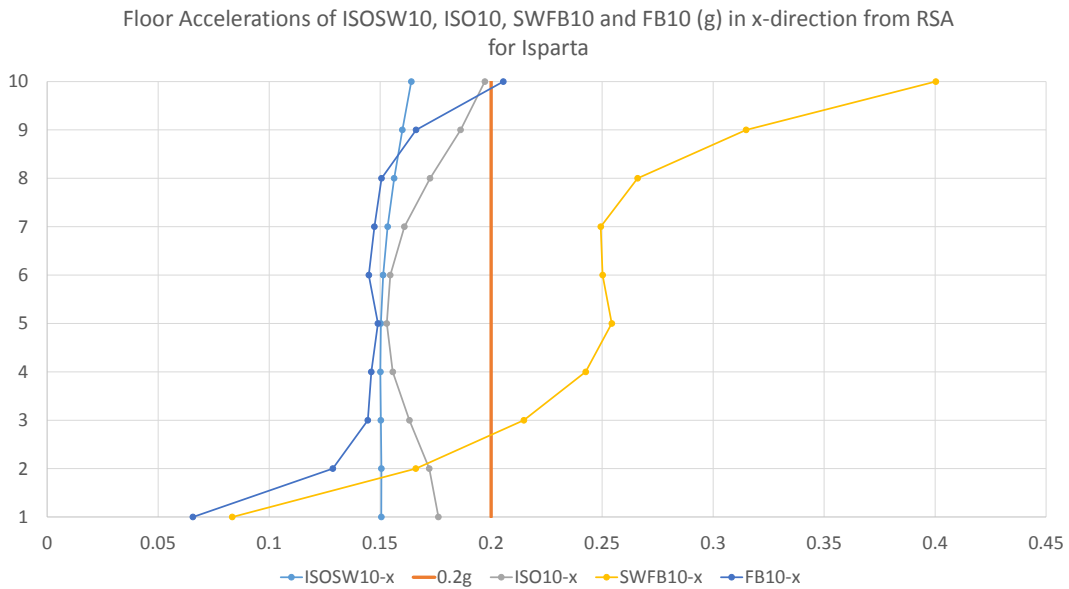


Figure C.7: PFA(g) (in x direction) through Floors of 10 Storey Systems for Isparta DBE Level from RSA

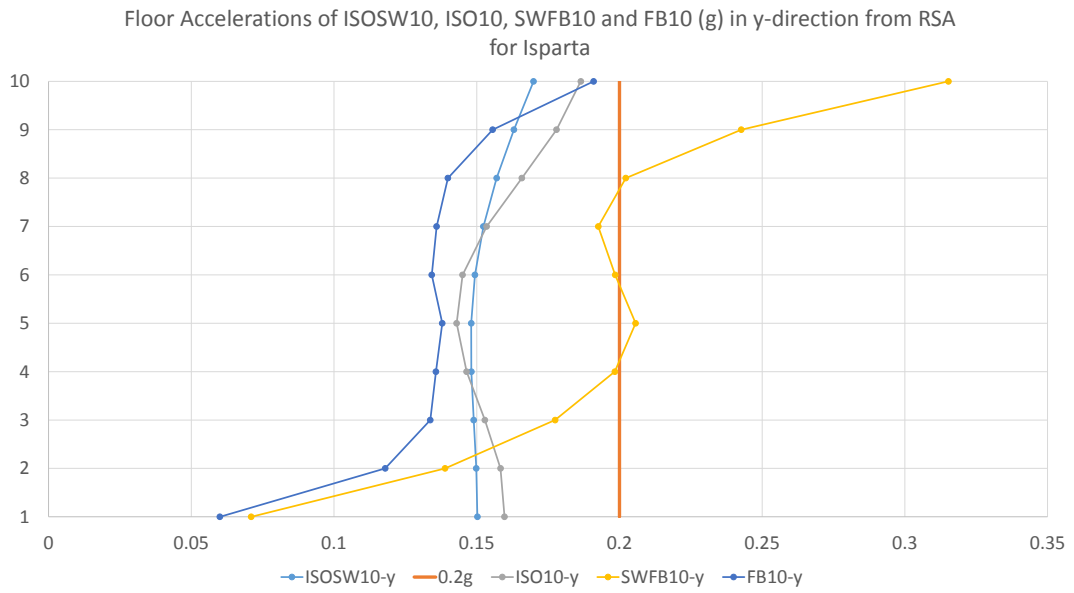


Figure C.8: PFA(g) (in y direction) through Floors of 10 Storey Systems for Isparta DBE Level from RSA

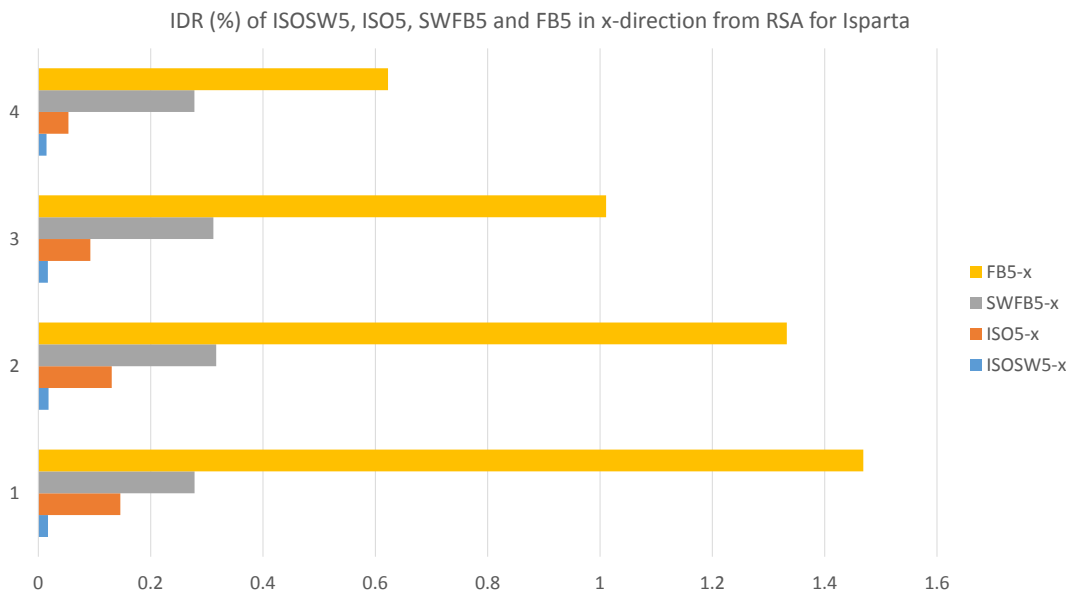


Figure C.9: IDR(%) (in x direction) through Floors of 5 Storey Systems for Isparta DBE Level from RSA

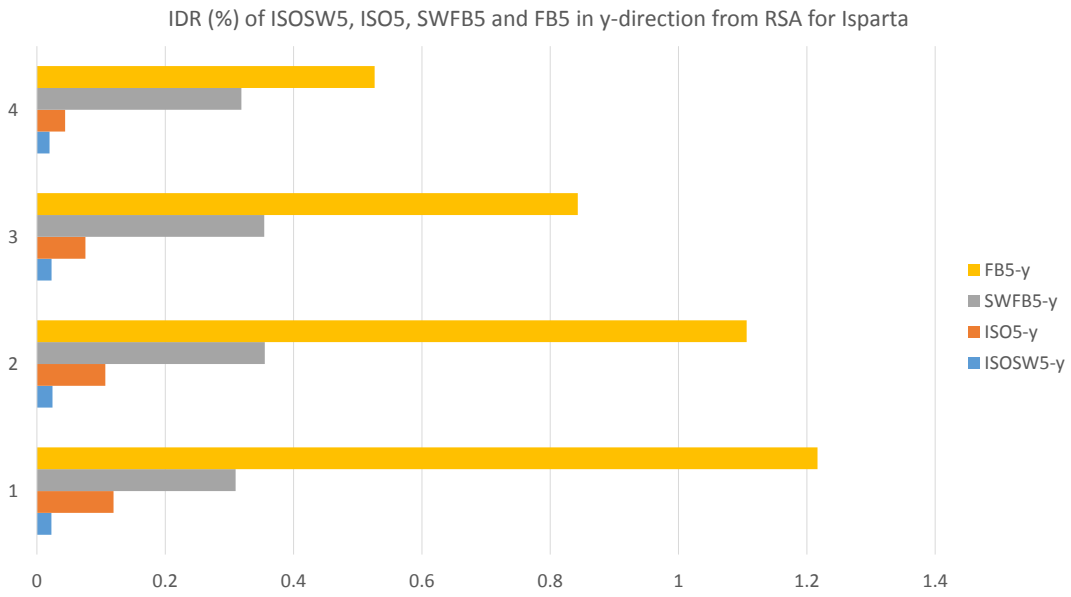


Figure C.10: IDR(%) (in y direction) through Floors of 5 Storey Systems for Isparta DBE Level from RSA

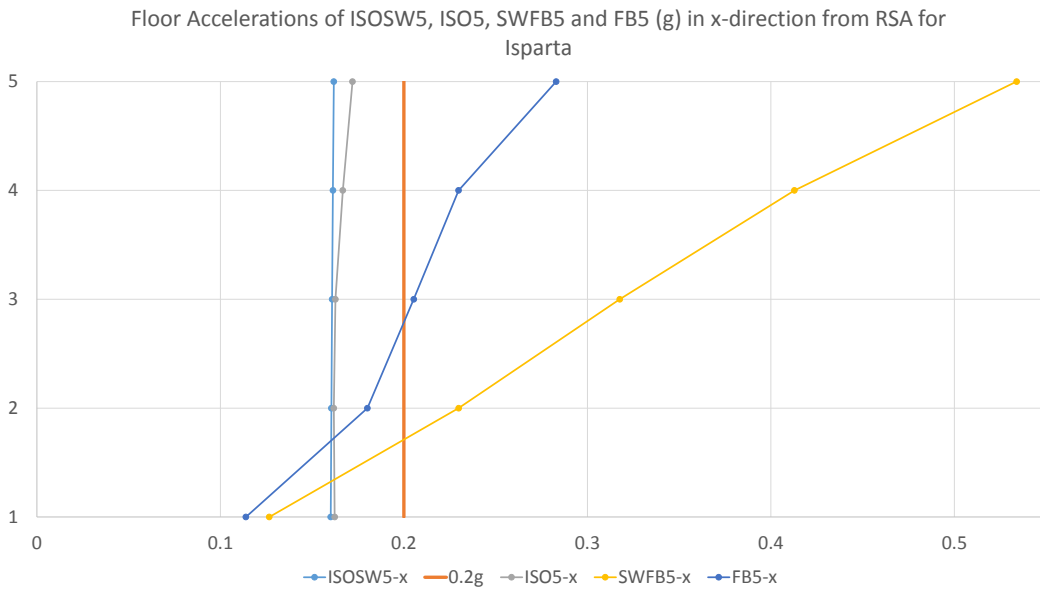


Figure C.11: PFA(g) (in x direction) through Floors of 5 Storey Systems for Isparta DBE Level from RSA

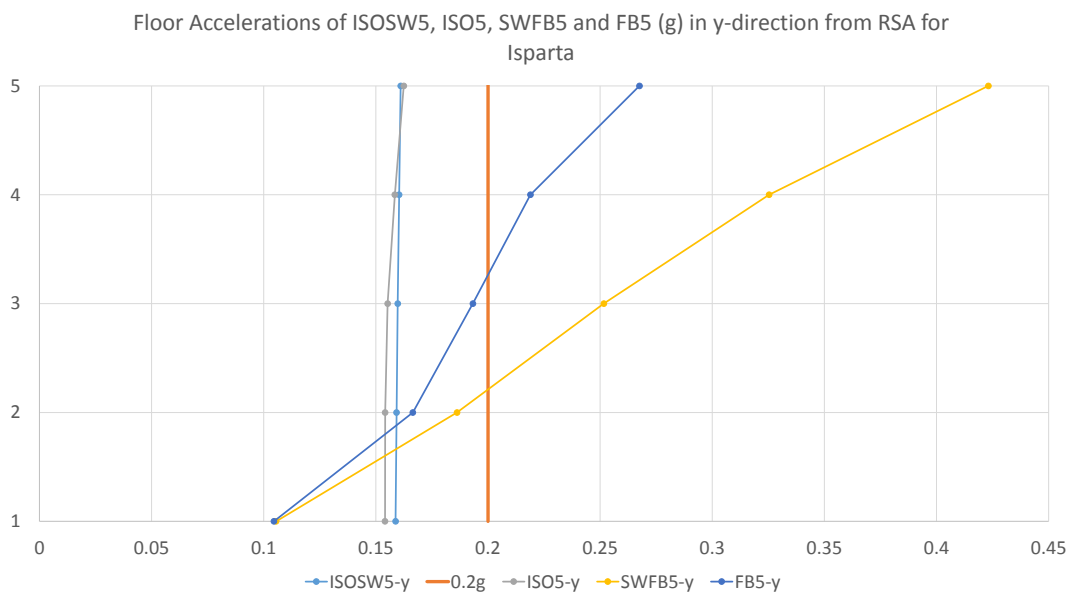


Figure C.12: PFA(g) (in y direction) through Floors of 5 Storey Systems for Isparta DBE Level from RSA

CURRICULUM VITAE

PERSONAL INFORMATION

Surname, Name: Ozdemir, Seda

Nationality: Turkish (TC)

Date and Place of Birth: 18.05.1989, Ankara

Marital Status: Single

Phone: +90 536 410 25 25

Fax: Fax Number

EDUCATION

Degree	Institution	Year of Graduation
B.S.	Dept. of Civil Engineering, METU	2014
High School	Fethiye Kemal Mumcu Anadolu Lisesi	2007

PROFESSIONAL EXPERIENCE

Year	Place	Enrollment
2013-2014	Prota Engineering & Consultancy	Structural Design Engineer
2014-	Sismolab	Structural Engineer

PUBLICATIONS

International Conference Publications

Remaining Service Life Assessment of River Bridges with Cracked Members. 8th International Conference on Bridge Maintenance, Safety and Management, 2016.